AD-A226 556

NPS 69-90-5

NAVAL POSTGRADUATE SCHOOL
Monterey, California

CONSTRAINED VISCOELASTIC LAYER DAMPING OF THICK ALUMINUM PLATES: DESIGN, ANALYSIS AND TESTING

by

LT Michael J. Bateman, USN
Professor K. Steven Kim
Professor Young S. Shin, Principal Investigator

Department of Mechanical Engineering

Period: 1 June, 1989 - 31 May 1990

UNCLASSIFIED

Prepared for: David Taylor Research Center
Bethesada, MD

NAVAL POSTGRADUATE SCHOOL
Monterey, California

Real Admiral R W. West, Jr.
Superintendent

Harrison Shull
Provost

This work was prepared in conjunction with research conducted for the David Taylor Research Center, Bethesda, MD, and funded by both the Naval Postgraduate School and the David Taylor Research Center.

This report was prepared by:

Michael J. Bateman
LT, USN

K. Steven Kim
Adjunct Research Professor
Dept. of Mechanical Engineering

Young S. Shin
Professor
Dept of Mechanical Engineering

Reviewed by:

Anthony J. Healey
Chairman
Dept. of Mechanical Engineering

Released by:

Gordon E. Schacher
Dean of Faculty and Graduate Studies

REPORT DOCUMENTATION PAGE

1a. REPORT SECURITY CLASSIFICATION UNCLASSIFIED	1b. RESTRICTIVE MARKINGS
2a. SECURITY CLASSIFICATION AUTHORITY	3. DISTRIBUTION/AVAILABILITY OF REPORT Approved for public release: Distribution is unlimited
2b. DECLASSIFICATION/DOWNGRADING SCHEDULE	
4. PERFORMING ORGANIZATION REPORT NUMBER(S) NPS-69-90-05	5. MONITORING ORGANIZATION REPORT NUMBER(S)
6a. NAME OF PERFORMING ORGANIZATION Naval Postgraduate School 6b. OFFICE SYMBOL (*If applicable*)	7a. NAME OF MONITORING ORGANIZATION David Taylor Research Center
6c. ADDRESS (*City, State, and ZIP Code*) Monterey, CA 93943-5000	7b. ADDRESS (*City, State, and ZIP Code*) Bethesda, MD 20084
8a. NAME OF FUNDING/SPONSORING ORGANIZATION David Taylor Research Center 8b. OFFICE SYMBOL (*If applicable*)	9. PROCUREMENT INSTRUMENT IDENTIFICATION NUMBER N0016790-WR-00300
8c. ADDRESS (*City, State, and ZIP Code*) Bethesda, MD 20084	10. SOURCE OF FUNDING NUMBERS PROGRAM ELEMENT NO: 64561N; PROJECT NO:; TASK NO:; WORK UNIT ACCESSION NO:

11. TITLE (*Include Security Classification*)
CONSTRAINED VISCOELASTIC LAYER DAMPING OF THICK ALUMINUM PLATES: DESIGN, ANALYSIS, AND TESTING

12. PERSONAL AUTHOR(S): Bateman, M. J., LT, USN, Kim, K. S., Adjunct Research Professor, and Shin, Y. S., Professor, Department of Mechanical Engineering

13a. TYPE OF REPORT	13b. TIME COVERED	14. DATE OF REPORT (*Year, Month, Day*)	15. PAGE COUNT
Progress Report	FROM 6-1-90 TO 5-31-90	May 1990	136

16. SUPPLEMENTARY NOTATION: The views expressed in this thesis are those of the author and do not reflect the official policy or position of the Department of Defence or the U.S. Government.

17. COSATI CODES			18. SUBJECT TERMS (*Continue on reverse if necessary and identify by block number*)
FIELD	GROUP	SUB-GROUP	Vibration, Damping, Viscoelastic Material, Constrained Layer Damping.

19. ABSTRACT (*Continue on reverse if necessary and identify by block number*)

Modern naval warfare has been increasingly dependent upon the acoustic silencing of the participants. Constrained viscoelastic layer damping of vibrating elements is one method which can be used to meet acoustic silencing goals. This paper considers constrained viscoelastic layer damping treatments applied to a thick aluminum plate, including single layer, double layer, a milled pocket plate, and a milled "floating element" configuration. High modal damping values were obtained for each damping configuration. The Modal Strain Energy method, using finite element analysis to estimate modal loss factors, was investigated for use as a tool in constrained viscoelastic layer damping design. A comparison of experimentally measured frequency response and modal loss factors with those predicted by the modal strain energy method is presented to confirm the possible use of the modal strain energy method as a design tool.

20. DISTRIBUTION/AVAILABILITY OF ABSTRACT ☒ UNCLASSIFIED/UNLIMITED ☐ SAME AS RPT ☐ DTIC USERS	21. ABSTRACT SECURITY CLASSIFICATION UNCLASSIFIED
22a. NAME OF RESPONSIBLE INDIVIDUAL Professor Y. S. Shin	22b. TELEPHONE (*Include Area Code*) (408) 646 - 2568 22c. OFFICE SYMBOL 69Sg

DD FORM 1473, 84 MAR — 83 APR edition may be used until exhausted; All other editions are obsolete

SECURITY CLASSIFICATION OF THIS PAGE

* U.S. Government Printing Office: 1986—606-24.

ABSTRACT

Modern naval warfare has been increasingly dependent upon the acoustic silencing of the participants. Constrained viscoelastic layer damping of vibrating elements is one method which can be used to meet acoustic silencing goals. This paper considers constrained viscoelastic layer damping treatments applied to a thick aluminum plate, including single layer, double layer, a milled pocket plate, and a milled "floating element" configuration. High modal damping values were obtained for each damping configuration. The Modal Strain Energy method, using finite element analysis to estimate modal loss factors, was investigated for use as a tool in constrained viscoelastic layer damping design. A comparison of experimentally measured frequency response and modal loss factors with those predicted by the modal strain energy method is presented to confirm the possible use of the modal strain energy method as a design tool.

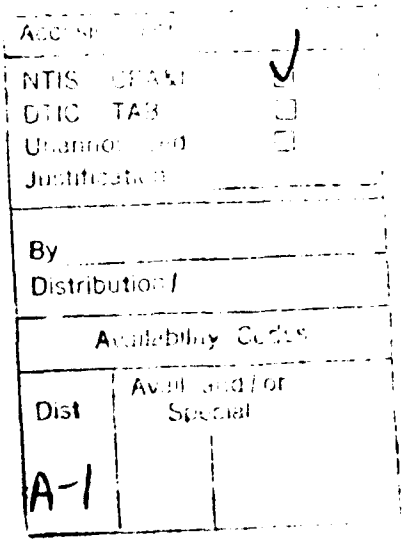

TABLE OF CONTENTS

LIST OF TABLES

LIST OF FIGURES

ACKNOWLEDGMENTS

The authors would like to thank Mr. David Marco for his invaluable assistance and support with the VAX computer. The authors would also like to acknowledge the fine laboratory support of Mr. Mardo Blanco, especially the fine job of welding the cover plates onto the pocket plate and floating element plate. This project was possible with funding from both the David Taylor Research Center and the Naval Postgraduate School. Many thanks to Dr. Lawrence Maga for his continued interest and support.

I. INTRODUCTION

Modern naval warfare, especially undersea warfare, depends heavily on the vessel being acoustically silent. A major source of radiated noise is the vibration of shipboard components. The reduction of these vibrations is of utmost importance if a ship is to accomplish its mission. One method of vibration damping that shows promise in damping over a broad spectrum of low frequency vibration is constrained viscoelastic layer damping. The constrained viscoelastic layer method uses the high energy dissipation characteristic of viscoelastic materials during periodic motion of shear deformation to absorb and dissipate the vibrational energy of the system in question. Unfortunately the design and analysis of such constrained viscoelastic layer systems is difficult, due in part to the following:

- The material properties of viscoelastic damping materials vary greatly with temperature and frequency.
- Closed form solutions to the equations of motion for constrained layer system exist only for beams and plates with simple boundary conditions.
- The exact complex valued eigenvalue analysis for constrained viscoelastic layer damping systems using the finite element method requires large amounts of computer storage and CPU time.

Johnson and Kienholz developed the Modal Strain Energy (MSE) method which uses the ratio of strain energy for each mode shape to approximate the modal damping of a structure for a given constrained viscoelastic damping system [Ref. 1]. This method is very attractive due to its simple concept and very useful because it can be applied to any general cases with arbitrary shape by using the finite element method. However, its effectiveness compared with experiments were reported for only a few cases. Maurer examined the effectiveness of the MSE method for two damped plate configurations: 1) a simple sandwich configuration, and 2) a plate with a milled pocket with damping material inserted and a welded cover plate acting as a constraining layer in a previous work [Ref.2]. However, he could not verify for the milled pocket plate case since the cover plate warped and delaminated itself from the damping material during welding, resulting in negligible damping [Ref. 2].

For certain naval applications the components to be damped will be thick in construction and may be exposed to an unfriendly environment. Therefore, in this research the pocket plate configuration and a second milled plate using a "floating element" in conjunction with constrained layer damping are investigated. These damping treatments are compared with the simple sandwich type treatments consisting of single and double constraining layers. Simple plate geometries were used to facilitate the experimental and computational effort. Therefore, this paper addresses the experimental testing and analysis of four thick aluminum plates, each with a different constrained viscoelastic layer damping treatment. The

effectiveness of the MSE method is investigated for each different damping treatment by evaluating its accuracy in modal damping value prediction compared with experimental results and usefulness as a possible design tool.

II. THEORY

A. VISCOELASTIC MATERIAL

Viscoelastic materials of interest for general naval applications are polymeric compounds made up of long molecular chains. These molecular chains can be strongly, or weakly, linked together, depending on their chemical composition and processing. The damping characteristics of viscoelastic arise from the deformation and recovery of the polymer network. Material properties of a viscoelastic material vary with temperature and frequency. As such, the damping characteristics of a system will vary as its operating environment changes. [Ref. 3]

Temperature will have the greatest effect on the material properties of damping materials [Ref. 3]. This effect is shown in Figure 2.1, where four distinct regions are observed. The lowest temperature region is the glassy region where the material's storage modulus is at its maximum value, and the loss factor is at a minimum. In the glassy region the modulus decreases slowly with temperature increase, whereas the loss factor increases rapidly with temperature. The second region is the transition region where the modulus decreases rapidly with increasing temperature and the loss factor reaches its peak value. The third region is the rubbery region where both the modulus and loss factor are at low values and show little variation with temperature. The fourth, and last, region is

the flow region and characterizes the behavior of some materials, mostly ceramics, at high temperatures. It should be noted that the transition region may vary in width from 20 °C up to a width of 200 °C. [Ref. 3]

The effect of frequency on viscoelastic materials is not as great as that of temperature. The modulus of the viscoelastic always increases with increasing frequency. The loss factor will initially increase with frequency, then peak, and subsequently decrease as frequency increases. A plot of storage modulus and loss factor versus frequency is shown in Figure 2.2. It should be noted that this plot is over a range of approximately ten decades, and hence it becomes obvious that a temperature change of a couple degrees will have a much greater effect on damping than a minor change in frequency. [Ref. 3]

Linear viscoelastic materials behave in a hysteretic manner under cyclic excitation. Therefore, the mechanical behavior of a viscoelastic material during steady state vibration is best described by using a complex stiffness, k* [Ref. 3].

$$k^* = k(1 + i\eta) \tag{2.1}$$

where,

η = material loss factor

The use of a complex stiffness then leads to the use of a complex Young's modulus and shear modulus [Ref. 3].

$$E^* = E(1 + i\eta) \tag{2.2}$$

$$G^* = G(1 + i\eta) \tag{2.3}$$

This concept of the complex modulus is used in subsequent analysis.

Viscoelastic material properties are commonly displayed using a "reduced frequency nomogram." The reduced frequency nomogram displays the variation of the viscoelastic material's loss factor and modulus with temperature and frequency. The "reduced frequency", $f_{\alpha t}$, is an empirically determined function that accounts for the viscoelastic's temperature and frequency dependence, and allows data for wide range of temperature and frequencies to be plotted on the same graph [Ref 4]. The reduced frequency nomogram for 3M ISD - 112 is shown in Figure 2.3. To find the loss factor and modulus using the nomogram, enter with the desired temperature and frequency. Follow the frequency line horizontally and the temperature line diagonally down the page until the two intersect. Then go vertically up or down to intersect the shear modulus or loss factor curves. Finally, read the value of the shear modulus or loss factor horizontally from the scale on the left [Ref. 4].

B. CONSTRAINED VISCOELASTIC LAYER DAMPING

A simple constrained layer damping treatment consists of a base layer (the structure to be damped), a damping layer, and the constraining

layer. This configuration is shown in Figure 2.4 with the thicknesses of the damping and constraining layers exaggerated for clarity.

The physical mechanism of damping can be explained by referring to Figure 2.4. When the base layer is deformed in a mode of vibration, the surface away from the neutral axis elongates, stretching the viscoelastic material. The top layer, being a stiff elastic material, tends not to elongate, and thereby "constrains" the viscoelastic material. Consequently, the cyclic motions of vibration induce a cyclic shearing strain in the viscoelastic. This cyclic shearing strain, together with its associated hysteresis loop cause the vibrational energy to be dissipated as heat. For the constraining layer to be effective, its stiffness should not exceed that of the base layer. [Ref. 4 & 5]

C. SYSTEM EQUATIONS OF MOTION

Continuous systems, such as plates, possess distributed characteristics of mass, damping, and stiffness. Classical vibration analysis of such systems involves the formation of a mathematical model that discretizes the system into a finite number of components in order to approximate the total system. Such a formulation results in the following equation:

$$[M]\{\ddot{x}(t)\} + [C]\{\dot{x}(t)\} + [K]\{x(t)\} = \{F(t)\} \tag{2.4}$$

where,

$[M]$ = system mass matrix

$[C]$ = system damping matrix

$[K]$ = system stiffness matrix

$\{F(t)\}$ = external excitation vector

$\{x(t)\}$ = displacement vector

For an undamped system without excitation, the above equation reduces to the eigenvalue problem.

$$[M]\{\ddot{x}(t)\} + [K]\{x(t)\} = 0 \tag{2.5}$$

This equation is then transformed to modal space using the linear transformation:

$$\{x(t)\} = [\phi]\{q(t)\} \tag{2.6}$$

where,

$[\phi]$ = modal matrix

$\{q(t)\}$ = modal response vector

Using this linear transformation the equation of motion can then be solved for the undamped modal frequencies and mode shapes.

To solve for the frequency response of a damped system, the linear transformation is applied to equation (2.4):

$$[M][\phi]\{\ddot{q}(t)\} + [C][\phi]\{\dot{q}(t)\} + [K][\phi]\{q(t)\} = \{F(t)\} \tag{2.7}$$

Assuming that the damping matrix [C] is proportional to a linear combination of the stiffness matrix [K] and mass matrix [M], the damping matrix can then be diagonalized using the same linear transformation used to diagonalize [K] and [M] in equation (2.5) above. The diagonal terms of the damping matrix then become $(\eta_i\omega_i)$, where η_i equals the modal loss factor and ω_i is the natural frequency of the i^{th} mode [Ref. 1] . Using this approximate diagonal damping matrix results in a system of uncoupled modal equations of motion:

$$\ddot{q}_i(t) + \eta_i\omega_i\dot{q}_i(t) + \omega_i^2 q_i(t) = f_i(t) \tag{2.8}$$

where,

$\ddot{q}_i(t)$ = modal acceleration of i^{th} mode

$\dot{q}_i(t)$ = modal velocity of i^{th} mode

$q_i(t)$ = modal displacement of i^{th} mode

η_i = modal loss factor of i^{th} mode

ω_i = i^{th} natural frequency

$f_i(t)$ = modal force in i^{th} mode

$j = \sqrt{-1}$

Assuming that a sinusoidal excitation produces a sinusoidal response,

$$\{f(t)\} = \{\tilde{f}\}e^{j\omega t} \qquad \{q(t)\} = \{Q\}e^{j\omega t} \tag{2.9}$$

the response for the i^{th} mode is then solved to be:

$$Q_i = \frac{\tilde{f}_i}{\omega_i^2 - \omega^2 + j\omega_i\eta_i\omega} \tag{2.10}$$

Subsequently, the response of the physical system can be found using:

$$\{x(t)\} = [\phi]\{Q\}e^{j\omega t} \tag{2.11}$$

D. MODAL STRAIN ENERGY METHOD

The equations of motion used to define the response of a system with viscoelastic materials need a complex eigenvalue analysis. However, the actual solution of these equations may be quite difficult. This is especially true when the system to be analyzed is comprised of materials whose properties vary with both temperature and frequency. Finite element techniques are generally used to compute the response of complicated systems. However, for the case of varying material properties many time consuming and costly runs must be made with the material properties changing at each frequency increment [Ref. 1]. In addition to the costly analysis of a single design configuration, changes in design options, design requirements, of the search for an optimum design can make the expense of finite element analysis too great. The development of the Modal Strain Energy (MSE) method by Johnson and Kienholz, however, makes the finite element analysis of complex viscoelastically damped structures a viable option [Ref. 1].

The MSE method assumes that a damped structure can be represented by the normal modes of the associated undamped system if appropriate damping terms are inserted into the uncoupled modal equations of motion (eqn 2.8) [Ref. 1]. The MSE method further assumes that the damping matrix of equation (2.4) can be diagonalized by the same real modal matrix that diagonalizes the system mass and stiffness matrices of equation (2.4).

The modal loss factors of equation (2.8) are calculated using the undamped mode shapes and material loss factors for each material. Since the material loss factors of the structure to be damped and the constraining layers are quite small compared to those of common viscoelastic cores, the modal loss factors can be estimated using the following equation [Ref. 1]:

$$\eta^{(r)} = \eta_v^{(r)} \frac{V_v^{(r)}}{V^{(r)}} \tag{2.12}$$

where,

$\eta^{(r)}$ = system loss factor in the r^{th} mode

$\eta_v^{(r)}$ = material loss factor of viscoelastic core at the r^{th} natural frequency

$V_v^{(r)}$ = strain energy in the viscoelastic core at r^{th} mode

$V^{(r)}$ = strain energy in the entire structure at r^{th} mode

The modal strain energies can be obtained for finite element analysis, and are a standard output option of the NASTRAN finite element code [Ref. 7].

The modal frequency response of the structure is then calculated using the modal loss factors found in equation (2.12). When computing the modal frequency response of a damped structure, the modal properties in the system matrices are assumed to be constant. However, viscoelastic materials have storage moduli which are frequency dependent. To account for this frequency dependence, Johnson and Kienholz devised the following correction factor to be applied to the modal loss factors calculated in equation (2.12) [Ref. 8].

$$\eta_c^{(r)} = \eta^{(r)} \sqrt{\frac{G_2(f_r)}{G_{2,ref}}} \tag{2.13}$$

where,

$\eta_c^{(r)}$ = corrected modal loss factor at the r^{th} mode

$G_2(f_r)$ = viscoelastic shear modulus at the r^{th} modal frequency

$G_{2,ref}$ = reference viscoelastic shear modulus used in the frequency response calculation

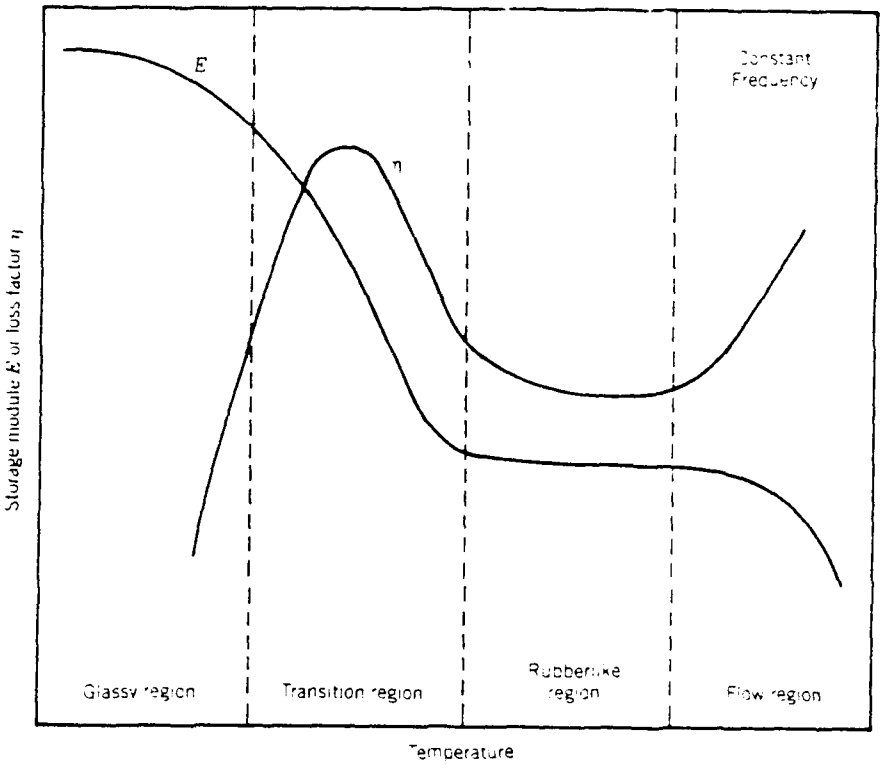

Figure 2.1. Variation of Viscoelastic Material Properties with Temperature [Ref. 3].

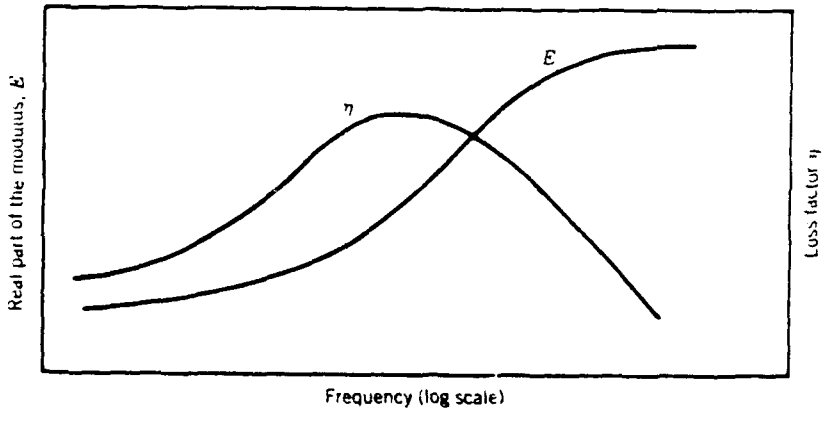

Figure 2.2. Variation of Viscoelastic Material Properties with Frequency [Ref. 3].

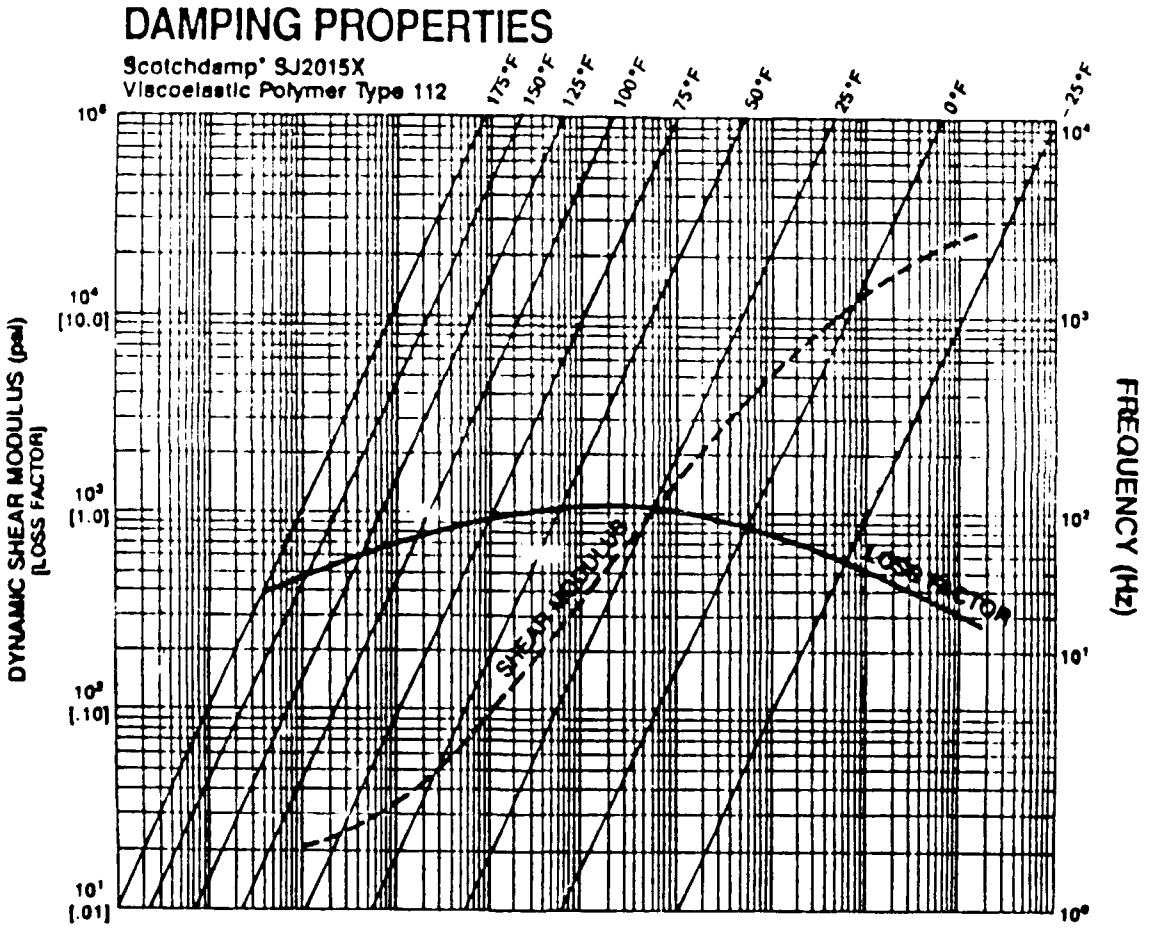

Figure 2.3. Temperature Frequency Nomogram for 3M ISD - 112.

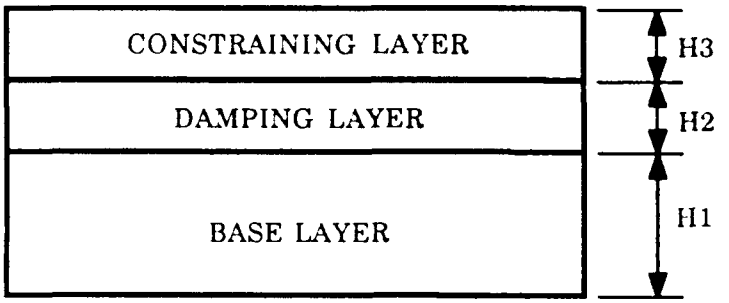

Figure 2.4. Single Constrained Layer Configuration.

III. DESIGN OF DAMPED PLATES

A. GENERAL SPECIMEN CONFIGURATIONS

For experimental testing and analysis purposes, four different, yet related, constrained layer damping treatments were selected in addition to an undamped "reference" plate. Two of the damping configurations were simple sandwich treatments consisting of one and two viscoelastic layers respectively. Another treatment was the "pocket plate" which was previously investigated by Maurer [Ref. 2]. The pocket plate was made from a solid plate which was then milled to accept damping material and a cover plate. The final damping treatment was a "floating element" configuration consisting of a solid plate milled to accept a double layer of damping material and a welded cover plate. Section views of these damping configurations are shown in Figure 3.1.

The purpose of the pocket plate is to protect the viscoelastic material from materials such as oil and salt water, which may harm the viscoelastic. Since previous attempts at using a welded cover plate were unsuccessful due to the heat of welding causing a delamination between the damping material and cover plate [Ref. 2], it was decided to move the viscoelastic material from the welding point by recessing it into a shallow pocket of its own as shown in Figure 3.1.

The "floating element" concept evolved because the welded cover plate of the pocket plate configuration does not produce the damping reaction that a true constraining layer would provide. If the cover plate is welded to the surrounding structure it cannot deform in bending as much as an unwelded constraining layer, thereby causing a reduction in the damping capability of the system. By using a piece of metal in the milled pocket with dimensions slightly smaller than the surrounding pocket, along with two layers of viscoelastic and a welded cover plate, a true constraining layer effect should be obtained. This configuration is shown in Figure 3.1.

In order to approximate a possible system to be damped, a plate with large dimensions was selected. The dimensions of the plates used for the damping treatments are 114.3 cm (45 in) in length and 38.1 cm (15 in) in width. In addition, possible naval applications for this type of damping would probably consist of thick plate members. For this reason it was also decided that thick plates would be used for the damping treatments. All the base plates and constraining layers were made of a standard 6061–T6 aluminum alloy. The design and selection of viscoelastic layer, base layer, and constraining layer thicknesses is discussed in the following sections.

B. DESIGN OF THE SINGLE DAMPING LAYER CONFIGURATION

In an attempt to approximate system loss factors and hence determine viscoelastic and constraining layer thicknesses for maximum

damping, a method developed by Nashif [Ref. 9] based on an analysis of simple sandwich damping systems by Ross, Kerwin, and Ungar [Ref. 10] was used. The Ross - Kerwin - Ungar (RKU) equations are base of the analysis of the simple sandwich system shown in Figure 3.2.

To find the loss factors of the damped system, the flexural rigidity of the system must first be determined. For the above system, the flexural rigidity, EI, is written as [Ref. 9]:

$$EI = \frac{E_1H_1^3}{12} + \frac{E_2H_2^3}{12} + \frac{E_3H_3^3}{12} + E_1H_1D^2 + E_2H_2(H_{21} - D)^2 + E_3H_3(H_{31} - D)^2 - \left[\frac{E_2H_2^2}{12} + \frac{E_2H_2}{2}(H_{21} - D) + E_3H_3(H_{31} - D)\right]\frac{H_{31} - D}{1 + g} \quad (3.1)$$

where,

$$D = \frac{E_2H_2\left(H_{21} - \frac{H_{31}}{2}\right) + g(E_2H_2H_{21} + E_3H_3H_{31})}{E_1H_1 + \frac{E_2H_2}{2} + g(E_1H_1 + E_2H_2 + E_3H_3)} \quad (3.2)$$

$$H_{31} = \frac{H_1 + H_3}{2} + H_2 \quad (3.3)$$

$$H_{21} = \frac{H_1 + H_2}{2} \quad (3.4)$$

$$g = \frac{G_2}{E_3H_3H_2K^2} \quad (3.5)$$

E = Young's modulus

G = Shear modulus

I = second moment of area

H = thickness of member

K = wave number

Subscripts refer to the layers labeled in Figure 3.1. No subscript refers to the composite system

For a simply supported plate the wave numbers and modal frequencies are found using [Ref.9]:

$$\omega_n = K_{nm}^2 \sqrt{\frac{EH^3 g_c}{12(1-\nu^2)H\rho}} \tag{3.6}$$

$$K_{nm}^2 = \left(\frac{n\pi}{a}\right)^2 + \left(\frac{m\pi}{b}\right)^2 \tag{3.7}$$

where,

a = semi–wave length of the plate

b = semi–wave width of the plate

ν = Poisson's ratio of the composite plate

ρ = density of the composite plate

g_c = gravitational constant

To introduce damping into the equations it is necessary to use the complex modulus concept expressed in Section II. Substituting the appropriate expressions for the complex shear and Young's modulus into equations (3.1), and assuming that damping in the base layer, (η_1), is small, and that the extensional stiffness of the damping layer is small

(since $E_2 << E_1$ and $E_2 << E_3$), the following expressions can be arrived at [Ref.9]:

$$EH^3 = E_1H_1^3 + E_3H_3^3 + \frac{12}{c^2 + d^2}(\alpha - \beta - \partial)_{RE} \tag{3.8}$$

$$EH^3\eta = E_3H_3\eta_3 + \frac{12}{c^2 + d^2}(\alpha - \beta - \partial)_{IM} \tag{3.9}$$

where,

$$\alpha = gE_1H_1E_3H_3H_{31}^2\{c(1 - \eta_2\eta_3) + d(\eta_2 + \eta_3) + j[c(\eta_2 + \eta_3)]\} \tag{3.10}$$

$$\beta = E_1H_1E_2H_2H_{31}[c + d\eta_2 + j(c\eta_2 - d)] \tag{3.11}$$

$$\partial = 2gE_2H_2E_3H_3H_{21}H_{31}\begin{Bmatrix} c(1 - 2\eta_2\eta_3 - \eta_2^2) + d(2\eta_2 + \eta_3 - \eta_2^2\eta_3) \\ + j[c(2\eta_2 + \eta_3 - \eta_2^2\eta_3) - d(1 - 2\eta_2\eta_3 - \eta_2^2)] \end{Bmatrix} \tag{3.12}$$

$$c = E_1H_1(1 + g) + gE_3H_3(1 - \eta_2\eta_3) \tag{3.13}$$

$$d = gE_1H_1\eta_2 + gE_3H_3(\eta_2 + \eta_3) \tag{3.14}$$

$$j = \sqrt{-1} \tag{3.15}$$

These equations were then applied to estimate the loss factors of the simple three–layer sandwich plate. The equations can be simplified by assuming that damping in the constraining layer (η_3) is negligible [Ref.9].

Since the boundary conditions for the plate used in this research (free-free-free-free) do not correspond to the simply supported conditions on

which equation (3.7) is based, modal frequencies for the free-free case were estimated using results from finite element analysis of a free-free plate and equation (3.6). The natural frequencies of an undamped plate with the dimensions previously given, and a thickness of 1.91 cm (0.75 in) were found using a normal mode extraction in NASTRAN. By substituting these modal frequencies into equation (3.6) and estimate of the wave parameter for each mode, K_{nm}^2, was obtained. Then, by using an iterative procedure outlined in Reference [9], modal loss factors were estimated for different layer thicknesses over a temperature range of 0.0 °C to 37.8 °C (30 °F to 100 °F).

The previous equations are easily programmed to compute loss factors for a wide variety of conditions. The variation of viscoelastic material properties with temperature and frequency was accounted for using a curve-fit to the reduced frequency nomogram developed by Drake [Ref. 11]. The material data for the following curve-fit equations is from the University of Dayton Research Institute [Ref. 12].

$$\log_{10}(M) = \log_{10}(ML) + \frac{\left[2\log_{10}\left(\frac{MROM}{ML}\right)\right]}{\left[1 + \left(\frac{FROM}{FR}\right)^n\right]} \tag{3.16}$$

$$\log_{10}(ETA) = \log_{10}(ETAFROL) + \frac{1}{2}C\left[A(SL + SH) + (SL - SH)\left(1 - \sqrt{1 + A^2}\right)\right] \tag{3.17}$$

$$\log_{10}(FR) = \log_{10}(F) - \frac{12(T - T\emptyset)}{(525 + T - T\emptyset)} \tag{3.18}$$

$$A = \frac{\log_{10}(FR) - \log_{10}(FROL)}{C} \tag{3.19}$$

where,

M = viscoelastic modulus

ETA = viscoelastic material loss factor

FR = reduced frequency (Hz)

F = frequency (Hz)

T = temperature (°F)

and,

TØ = 40 °C (104 °F)

FROM = 2.0×10^4 Hz

MROM = 4.75×10^6 Pa (688.94 psi)

n = 0.275

ML = 6.0×10^4 Pa (8.7 psi)

ETAFROL = 1.08

SL = 0.45

SH = –0.55

FROL = 5000 Hz

C = 2.5

In addition to the above constants, a Poisson's ratio of 0.49 and a density of 0.909 gram per cubic centimeter (0.035 lbm/in^3) was used for ISD–112 [Ref.12]. The following material properties were used for 6061–T6 aluminum [Ref.13].

$E = 70$ GPa (10×10^6 psi)

$\nu = 0.33$

$\rho = 2.7$ gm/cm^3 (0.0968 lbm/in^3)

Using the previous equations and material properties, a computer program was written to compute estimated modal loss factors and frequencies for a variety of base layer, viscoelastic layer, and constraining layer thicknesses. A listing of this program appears in Appendix A. Modal loss factors were computed for base layer thicknesses of 9.53 mm (0.375 in) to 19.05 mm (0.75 in) in 3.18 mm (0.125 in) increments. For each base layer thickness, the viscoelastic thickness was varied from 0.38 mm (0.015 in) to 1.52 mm (0.060 in) in 0.38 mm increments, and the constraining layer thickness was varied from 1.59 mm (0.0625 in) to 6.35 mm (0.25 in) in 1.59 mm increments. In addition, loss factors were also computed for a viscoelastic thickness of 0.127 mm (0.005 in). From the results of the analysis, a carpet plot [Ref. 3], was made for each of the base layer conditions. The carpet plot reflects, for the the first mode, the maximum loss factor and its corresponding temperature for each viscoelastic layer/constraining layer thickness configuration. The carpet plot for a base layer thickness of 12.7 mm (0.50 in) is shown in Figure 3.3. Based on the carpet plots and a desire for maximum damping, as well as a system which could be moved easily, a base layer thickness of 12.7 mm(0.50 in), a viscoelastic thickness of 0.38 mm (0.015 in), and a constraining layer thickness of 6.35 mm (0.25 in) was selected. The total system thickness was approximately 19.05 mm (0.75 in). This total system thickness would be maintained for all subsequent damping configurations.

To maintain continuity between damping systems, the milled "pocket plate" was given a viscoelastic thickness of 0.38 mm and a cover plate thickness of 6.35 mm for a total system thickness of 19.05 mm (0.75 in). In order to keep the heat of welding away from the viscoelastic material, the ISD–112 was recessed into a shallow pocket as indicated previously in Figure 3.1, and as shown in the pocket plate system arrangement in Figure 3.4. Detail drawings of the pocket plate are shown in Appendix C.

C. DESIGN OF THE DOUBLE DAMPING LAYER

The design of the double layer damping system was accomplished using a modification of the RKU analysis used in the previous section. The RKU equations are used by working from the top layer of the damping system down towards the base layer. As shown in Figure 3.5, the H3' constraining layer along with the H2' viscoelastic layer are combined with the H1' layer to form a three–layer system. Using the RKU equations, the stiffness of this system is computed and considered to be the equivalent stiffness of the top three layers of the total constrained layer damping system. The top three layers were then considered as a single layer with the equivalent stiffness previously calculated, and the RKU equations were again applied to compute estimated modal loss factors for the entire double layer damping system [Ref.3].

To maintain continuity among all the damping configurations, a base layer thickness of 12.77 mm (0.50 in) was chosen, and a total system thickness of 19.05 mm (0.75 in) was maintained. A design for high damping was then selected by computing modal loss factors for the constraining and damping layer thickness combinations shown in Table 3.1. The estimated modal loss factors for the first mode of vibration in each configuration are plotted as shown in Figure 3.6. A listing of the program used to compute the loss factors is in Appendix B.

From the data presented in Figure 3.6, viscoelastic thickness of 0.38 mm (0.015 in) and constraining layer thicknesses of 3.18 mm (0.125 in) were selected for the double layer configuration. This particular configuration estimates high damping over a wider temperature range than the other thickness combinations.

TABLE 3.1. THICKNESSES USED IN CALCULATION OF DOUBLE LAYER MODAL LOSS FACTORS.

Configuration	1	2	4	5	6
H2 (mm)	0.38	0.38	0.76	0.38	1.14
H1' (mm)	3.18	2.38	2.38	2.38	2.38
H2' (mm)	0.38	0.38	0.76	1.14	0.38
H3' (mm)	3.18	3.18	2.38	2.38	2.38

The milled "floating element" plate uses the same viscoelastic and constraining layer thicknesses as the simple two–layer configuration. In a

design similar to that of the pocket plate, the floating element and both layers of viscoelastic are recessed into a milled opening as shown previously in Figure 3.1 and further described in the floating element system configuration of Figure 3.7.

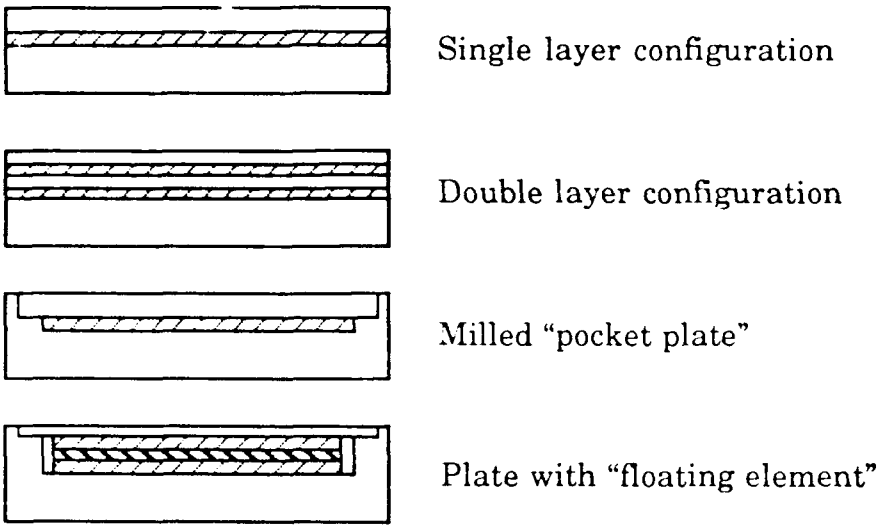

Figure 3.1. Four Damping Treatment Configurations.

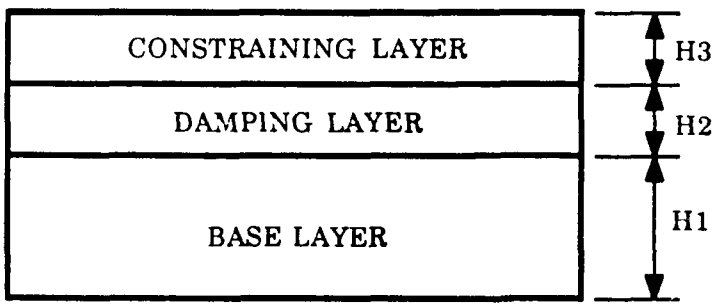

Figure 3.2. Elements of a Simple Sandwich Damping System.

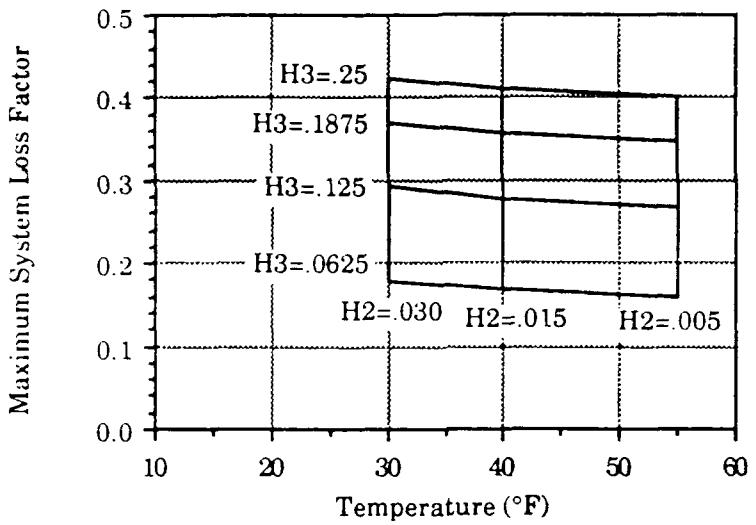

Figure 3.3. Carpet Plot of Maximum Loss Factors for a Base Layer with H1 = 12.7 mm.

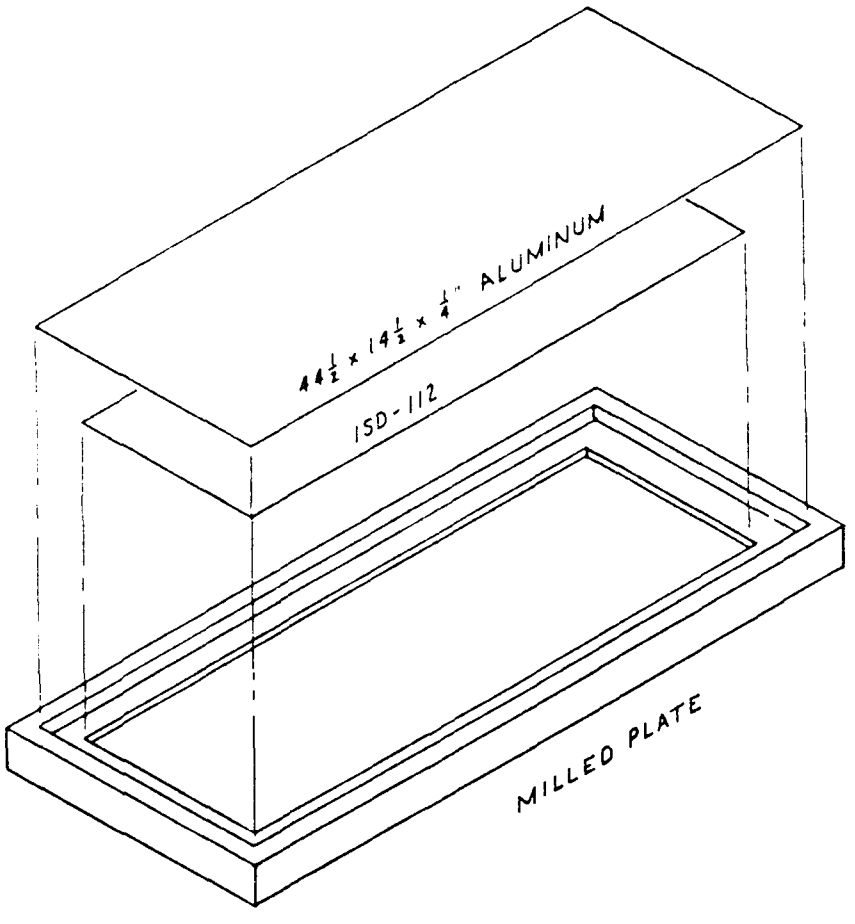

Figure 3.4. Arrangement of the Pocket Plate Configuration.

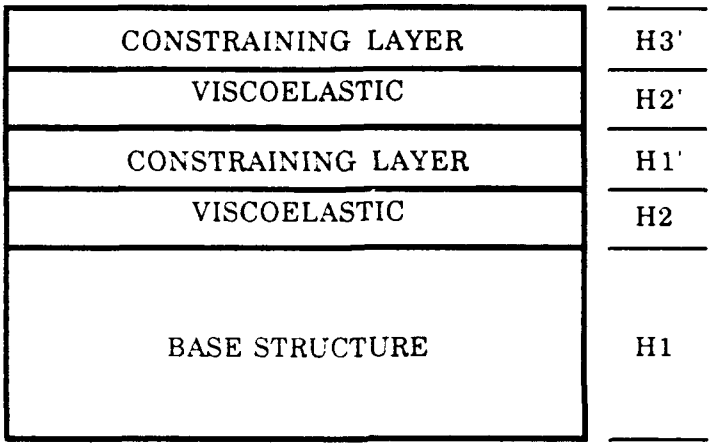

Figure 3.5. Configuration of the Double Constrained Layer System.

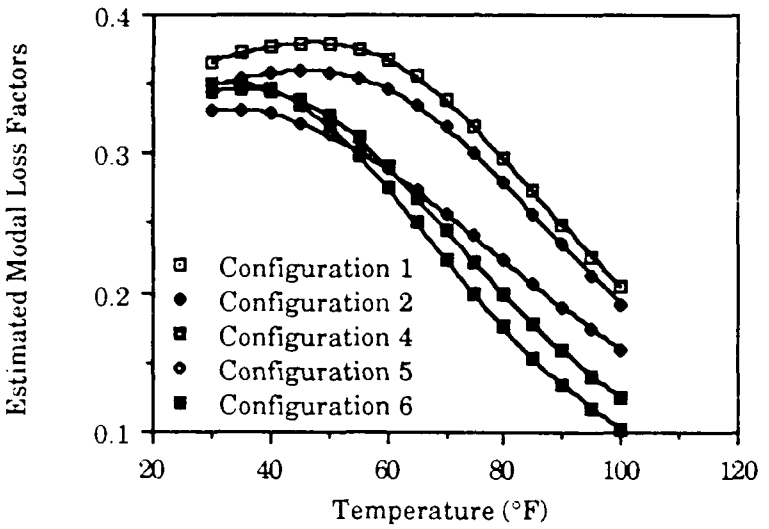

Figure 3.6. Modal Loss Factors for Double Constrained Layer Configurations.

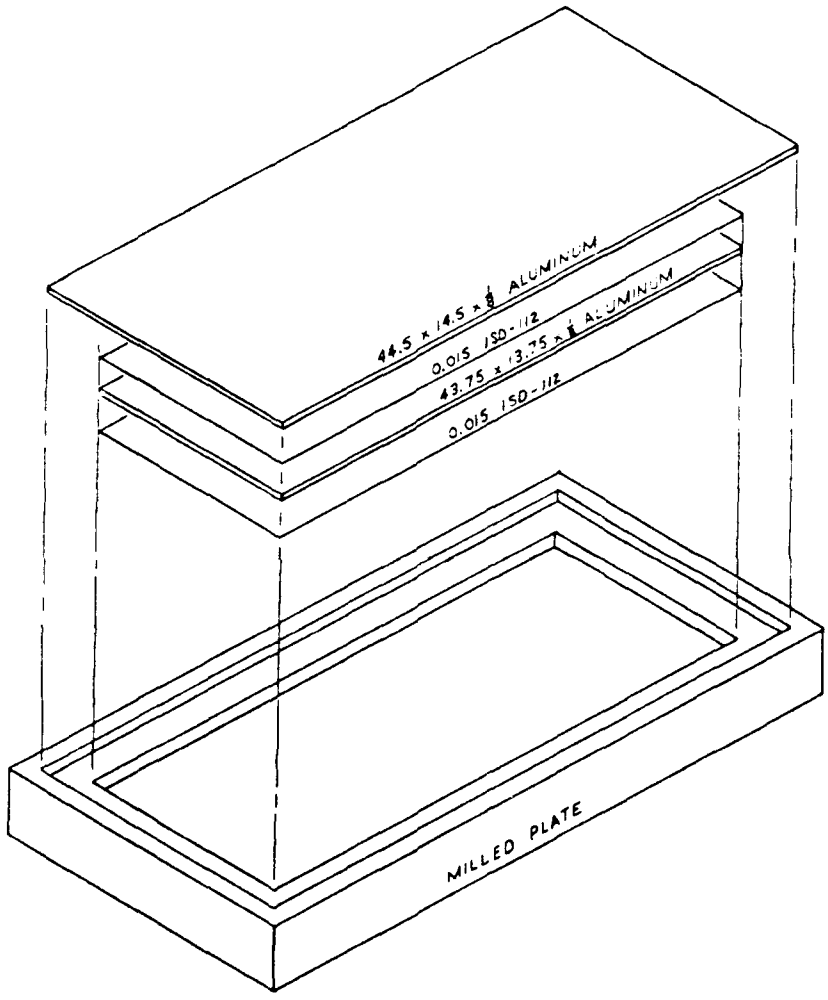

Figure 3.7. Floating Element System Configuration.

IV. EXPERIMENTAL RESULTS

A. TESTING ARRANGEMENT

Experimental testing was performed on each of the four damping configurations and the undamped reference plate. In order to approximate the free-free-free-free boundary condition, each plate was suspended from the roof of the testing chamber using elastic cords as shown in Figure 4.1. All of the tests were performed in a temperature controlled environmental chamber which enabled temperatures to be maintained within ±1 °C. The primary component and user interface was the Hewlett–Packard (HP) 3562A Dynamic Signal Analyzer (DSA). The HP-3562A was used to provide a swept sine signal to a vibration generator, and analyzed the returning data signals. The HP-3562A was used to compute the frequency response and coherence over a range of 50 Hz to 1050 Hz using the discrete Fourier Transform in the swept sine mode. Ten averages were performed at each data point using a frequency resolution of 625 mHz per step. The source level output to the vibration generator was set at 1.5 volts.

A schematic of the testing apparatus is shown in Figure 4.2. Swept sine source signals were fed from the output jack of the HP-3562A to a Wilcoxon F3 vibration generator via the piezoelectric output of a Wilcoxon PA7C power amplifier. The vibration generator was mounted 73.48 cm (28.93 in) from one end, and 12.7 cm (5.0 in) from the front edge of each

specimen as shown in Figure 4.3. An integral force transducer was mounted in the base of the vibration generator to measure the force input to the plate. This force signal was then fed to input channel one of the DSA via a PCB 462–A charge amplifier. Plate accelerations were recorded at various points using a PCB 303A–03 accelerometer as shown in Figure 4.3. Acceleration data was fed to input channel two of the DSA via a PCB 482A05 power supply. Frequency response and coherence data was then recorded on disk for further analysis.

Temperatures within the testing chamber were maintained using a NESLAB RTE–8 refrigerated circulating bath which pumped fluid through a small heat exchanger in the testing chamber as shown in Figure 4.2. In order to accurately monitor the temperature of the plates, a small thermocouple was inserted in the base of each plate.

B. TESTING PROCEDURE

1. Undamped reference plate

An undamped, reference, frequency response measurement was made at a temperature of 15.6 °C (60 °F) to set a standard response by which to measure the effectiveness of the damping treatments. The undamped frequency response was recorded over a frequency range of 50 – 1050 Hz using a resolution of 625 mHz per point in the DSA.

2. Damped plate measurements

Frequency response measurements of the damped plates were made at a temperature of 15.6 °C (60 °F) at several nodes on the plates in order to capture the damped response of as many modes as possible. A representation of these nodes is shown in Figure 4.3. Responses were recorded over a frequency range of 50 – 1050 Hz with a resolution of 625 mHz per point in the DSA. Zoom measurements were also made to capture better data for certain modes. Modal loss factors were then estimated from the frequency response and coherence measurements using a curve–fitting technique described in Reference [14].

C. SINGLE DAMPING LAYER RESULTS

The single damping layer treatment was tested at 4.44 °C (40 °F), 15.6 °C (60 °F), and 26.7 °C (80 °F) so that the effects of temperature on the damping treatment could be determined. A plot of the single damping layer frequency response at 15.6 °C is shown in Figure 4.4. The single layer damping treatment resulted in high damping with modal loss factors ranging from 0.223 at 53.4 Hz to 0.091 at 876.6 Hz. Due to the coupling of modes, loss factors for all modes were not measured. The frequency response of the damped plate is characterized by a frequency shift to the left and a smoothing of the frequency response when compared to the undamped reference plate. The single layer treatment was especially effective at reducing the frequency response of a mode cluster between 650

and 950 Hz. The frequency band of this cluster was shifted approximately 200 Hz with the amplitudes of the responses of the modes being dramatically reduced. The single layer treatment was also effective at reducing the amplitude of the response peaks over the entire spectrum of measurement. On average, the highest peaks of the frequency response in the undamped condition were reduced by 25 decibels, a reduction of 17.8 times.

The effect of temperature on the damping was quite pronounced as shown in Figure 4.5. As the testing temperature was decreased, the viscoelastic layer became stiffer and damping levels were increased. A comparative listing of the loss factors at different temperature is in Table 4.1 and a plot of the modal loss factors is shown in Figure 4.6. Figure 4.5 shows the trend of increased damping with temperature decrease, and a corresponding shift of modal frequencies to the right as the viscoelastic becomes stiffer. These changes are especially discernible at the lower frequencies.

TABLE 4.1. MEASURED MODAL LOSS FACTORS FOR THE SINGLE LAYER AT DIFFERENT TEMPERATURE.

4.44 °C (40 °F)		15.6 °C (60 °F)		26.7 °C (80 °F)	
f(Hz)	η	f(Hz)	η	f(Hz)	η
64.3	0.217	53.7	0.223	49.0	0.117
102.8	0.223	89.1	0.145	83.5	0.089
157.4	0.203	138.9	0.172	129.6	0.082
208.4	0.183	188.1	0.184	177.9	0.072
327.5	0.158	301.6	0.120	243.9	0.062
440.1	0.144	424.8	0.109	409.4	0.053
474.9	0.205	476.8	0.111	450.3	0.066
653.1	0.079	608.1	0.067	552.9	0.068
768.0	0.135	644.2	0.069	586.7	0.052
852.0	0.093	722.5	0.130	629.3	0.042
919.0	0.104	817.6	0.081	681.4	0.096
953.5	0.073	876.6	0.091	790.1	0.049
				858.2	0.056
				978.1	0.069

D. DOUBLE DAMPING LAYER RESULTS

The double layer damping configuration was also tested at 4.44 °C, 15.6 °C, and 26.7 °C. The frequency response of this configuration at 15.6 °C as compared to the undamped reference plate is shown in Figure 4.7. Damping in the double layer configuration is also high, with modal loss factors ranging form 0.301 at 53.3 Hz to 0.107 at 832.4 Hz. Due to modal coupling loss factors for all modes were not measured. The frequency response of the two–layer configuration is also characterized by a dramatic reduction in response amplitude and a frequency shift to the left. The peak undamped responses were reduced by an average of 27 decibels, or a reduction of 22.4 times from the reference condition.

The effect of temperature on the double layer damping treatment is shown in Figure 4.8. As with the single layer case, damping in the double layer configuration increased with a decrease in temperature. This configuration also shows the shift of modal frequencies to the right as temperature decreases and the viscoelastic becomes stiffer. Modal loss factors for the double layer configuration are listed in Table 4.2, and are plotted for comparison in Figure 4.9.

To compare the effectiveness of the single layer and double layer configurations their frequency responses at 15.6 °C are plotted in Figure 4.10 with a plot comparing modal loss factors in Figure 4.11. The two

responses are quite similar although the double layer configuration does show an increase of approximately 22 percent in modal loss factor.

TABLE 4.2. MEASURED MODAL LOSS FACTORS FOR THE DOUBLE LAYER AT DIFFERENT TEMPERATURE

4.44 °C (40 °F)		15.6 °C (60 °F)		26.7 °C (80 °F)	
f (Hz)	η	f (Hz)	η	f (Hz)	η
51.9	0.273	55.3	0.301	49.7	0.202
122.5	0.224	87.1	0.215	81.9	0.188
212.7	0.187	142.1	0.217	127.6	0.156
290.5	0.197	190.5	0.212	172.4	0.117
382.7	0.174	297.8	0.139	278.2	0.097
494.2	0.144	366.8	0.154	317.7	0.077
558.2	0.169	419.3	0.125	396.1	0.070
602.2	0.198	441.2	0.100	428.5	0.077
642.4	0.157	618.7	0.098	602.0	0.067
752.8	0.168	680.9	0.096	638.4	0.072
815.4	0.159	715.5	0.060	738.0	0.071
896.3	0.156	832.4	0.107	802.6	0.077
968.3	0.130			846.1	0.050

E. POCKET PLATE RESULTS

The milled pocket plate was constructed as previously shown in Figure 3.3. The constraining layer, or cover plate, was welded in place using tack welds in an attempt to keep the damping material away from the heat of welding, and the cover plate from warping, instead of using a continuous weld bead as was previously attempted [Ref. 2]. The cover plate was welded to the base at the corners, at the midpoint of the short side and at three equally spaced locations along the long dimension as shown in Figure 4.12. Following welding the plate was tested to ensure that the viscoelastic had not been damaged by the heat of welding.

The pocket plate was tested at 15.6 °C (60 °F) and the frequency response is shown in Figure 4.13. The response indicates that the viscoelastic layer was not damaged by welding and that good damping was attained. Modal loss factors ranged from 0.067 at 62.1 Hz to 0.090 at 923 Hz. Although damping is good, it is approximately half that of the single layer configuration. One reason for this is that the viscoelastic material does not completely cover the base structure. Another reason is the presence of the welded cover plate. Due to the welded conditions the cover plate cannot induce shear deformation in the viscoelastic layer as well as a true constraining layer, and therefore produces less damping than the single layer configuration. The effects of the welded cover plate are especially felt in modes below 300 Hz where the frequency response is quite peaked. The response curve becomes more rounded and the effects of the damping layer are seen as frequency increases.

The modal loss factors for the pocket plate are listed in Table 4.3 and are plotted in Figure 4.14. Even though the damping is less than the single layer, the plate is still adequately damped as shown in the frequency response plot in Figure 4.13. In this configuration the modal loss factors remained relatively constant throughout the testing spectrum. The increase in modal loss factor values above 800 Hz is due primarily to modal coupling, and the measured modal loss factors in this range are not reliable.

TABLE 4.3 MEASURED MODAL LOSS FACTORS FOR THE POCKET PLATE AT 15.6°C.

f(Hz)	η	f(Hz)	η
62.1	0.067	565.3	0.043
93.4	0.042	625.7	0.047
142.0	0.056	643.2	0.049
194.9	0.060	687.0	0.044
308.9	0.051	841.9	0.056
437.5	0.041	891.5	0.077
495.6	0.036	923.0	0.090

F. FLOATING ELEMENT RESULTS

The milled "floating element" configuration was constructed as previously shown in Figure 3.7. The cover plate was welded in a fashion similar to the pocket plate as shown in Figure 4.12. The center constraining layer, or floating element, was made slightly smaller than the surrounding structure thus allowing the floating element to act as a "true" constraining layer.

The frequency response of the floating element configuration at 15.6 °C (60 °F) is shown in Figure 4.15. The floating element is quite effective as the response shows a good reduction in peak modal response. Measured modal loss factors range from 0.089 at 66 Hz to 0.064 at 935 Hz. A listing of measured modal loss factors is in Table 4.4 and are plotted in Figure 4.16. As with the previous cases, the frequency response of the floating element configuration is characterized by a frequency shift to the left and a smoothing of the response as frequency increases.

In a comparison of the pocket plate and floating element configurations, the frequency responses are plotted in Figure 4.17. A comparison of modal loss factors for the two configurations is shown in Figure 4.18. The two frequency response plots are similar, however, the frequency response of the floating element configuration is more rounded than that of the pocket plate. The major difference between the two configurations is seen in Figure 4.18. Modal loss factors for the floating

element show an average increase of 25 percent over those of the pocket plate. Reasons for this increase are the added constraining effect of the floating element and additional layer of damping material present.

TABLE 4.4 MEASURED MODAL LOSS FACTORS FOR THE FLOATING ELEMENT AT 15.6°C.

f (Hz)	η	f (Hz)	η
66.0	0.089	508.1	0.089
104.9	0.040	540.6	0.115
154.0	0.094	618.7	0.121
211.4	0.058	656.7	0.100
272.8	0.063	708.6	0.088
323.5	0.075	857.6	0.089
435.8	0.090	935.4	0.064

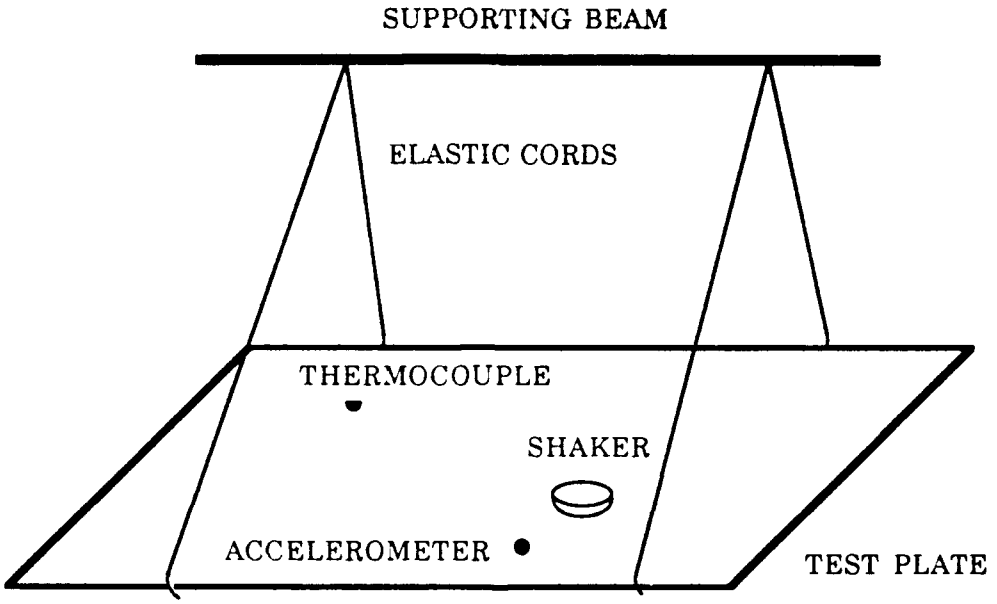

Figure 4.1. Testing Configuration in Testing Chamber.

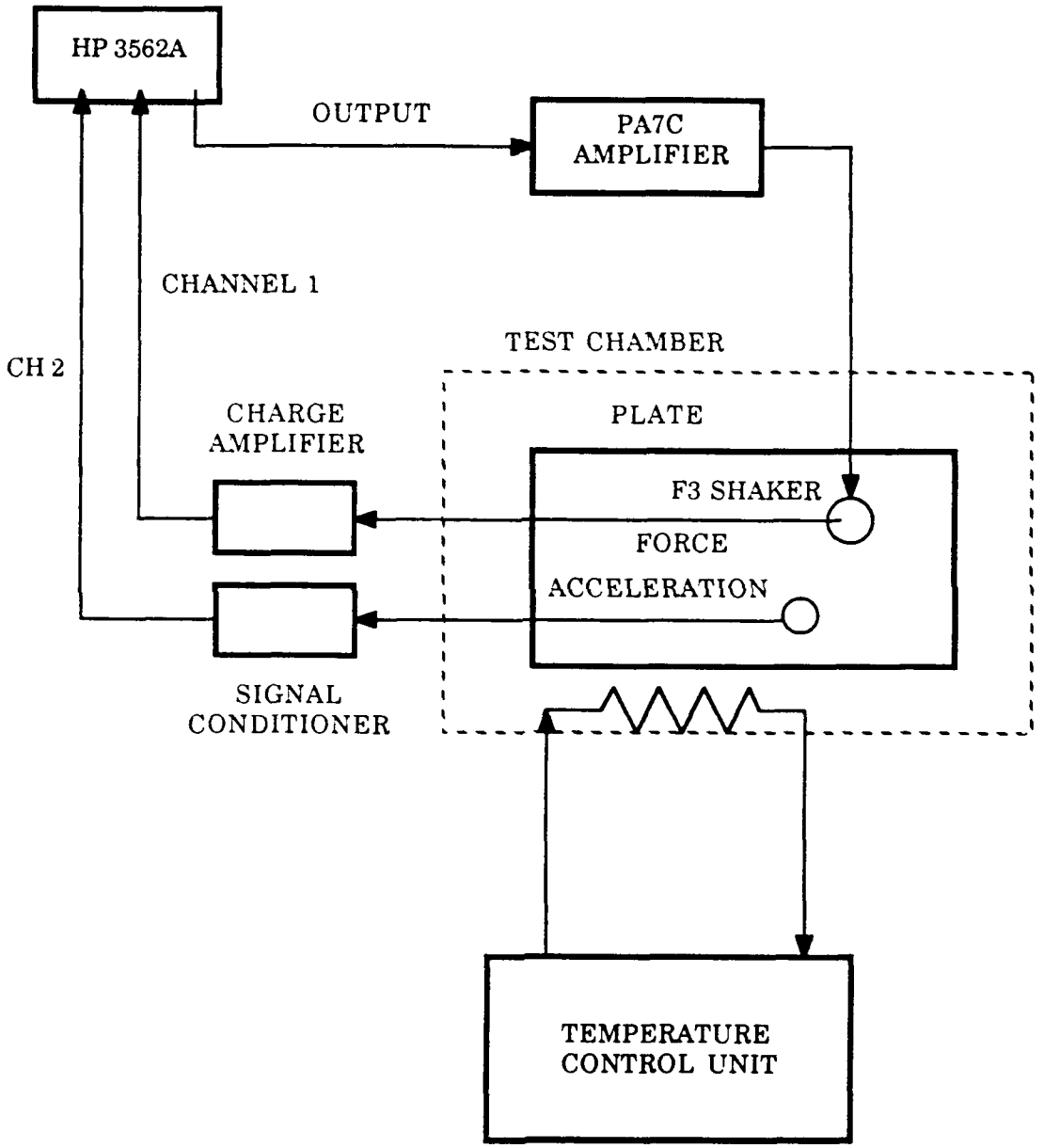

Figure 4.2. Schematic Diagram of Testing System.

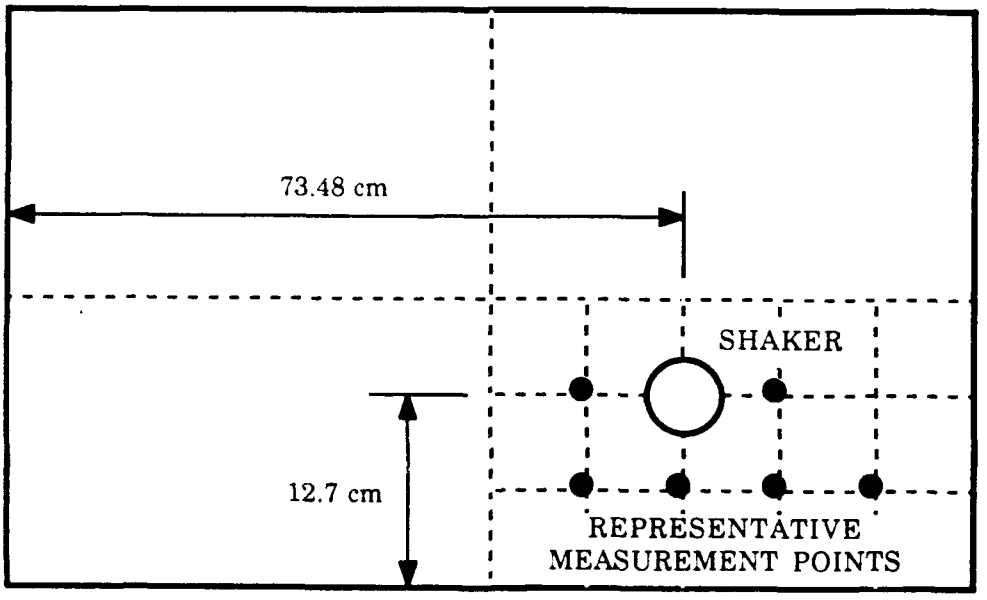

Figure 4.3. Shaker and Accelerometer Locations.

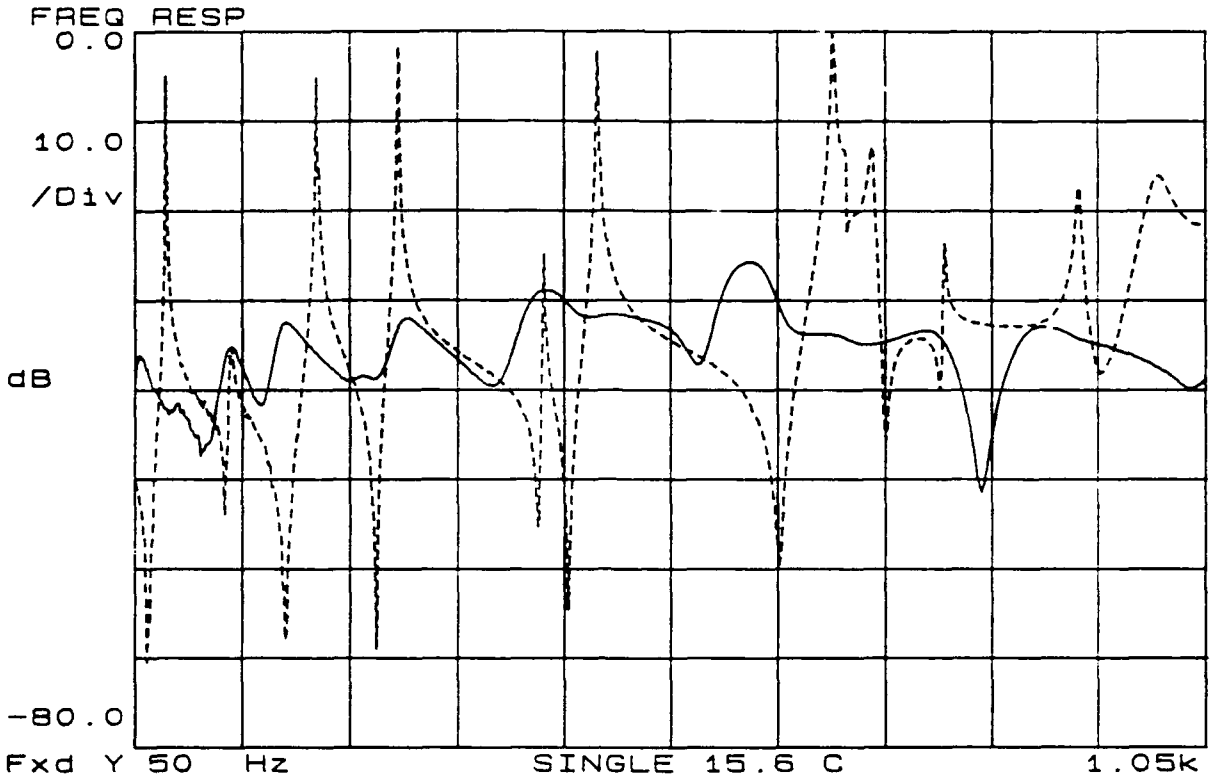

Figure 4.4. Frequency Response of the Single Layer Configuration at 15.6 °C.

[– – – –: undamped response; ———: damped response]

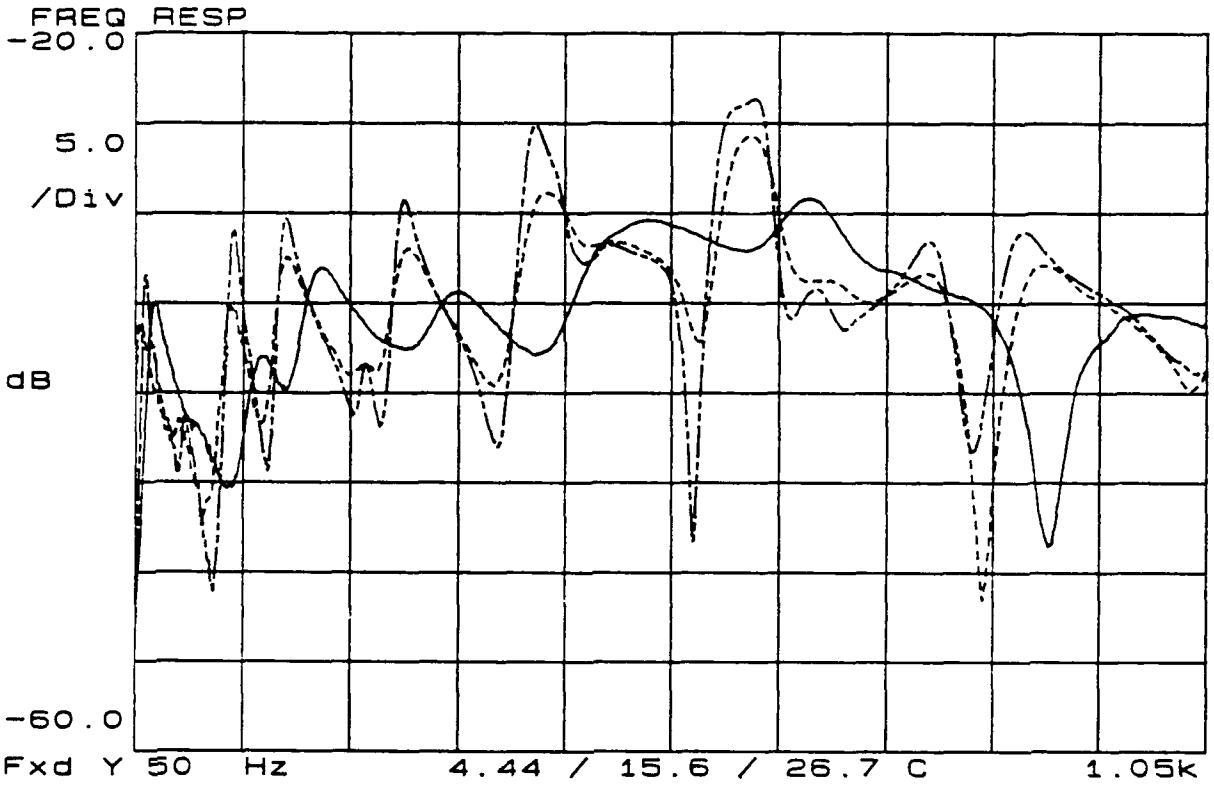

Figure 4.5. Frequency Response of the Single Layer Configuration at Different Temperatures.

[———: 4.44 °C, – – – –: 15.6 °C, ——– – ——: 26.7 °C]

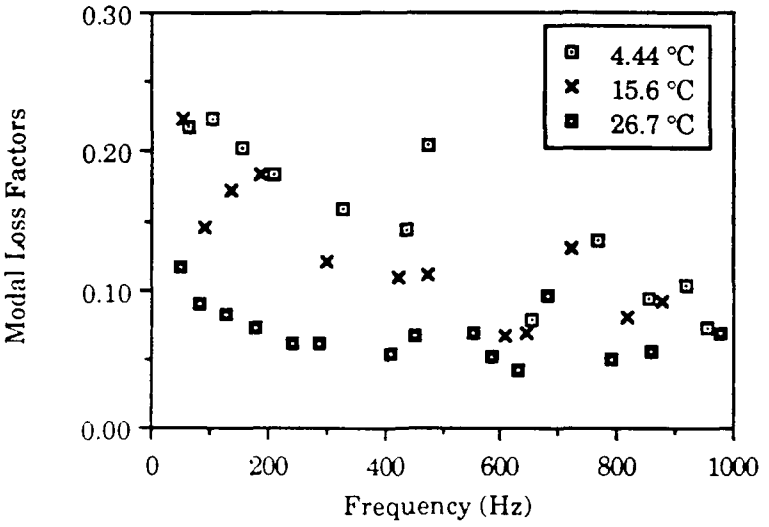

Figure 4.6. Comparison of Modal Loss Factors for the Single Layer Configuration at Different Temperatures.

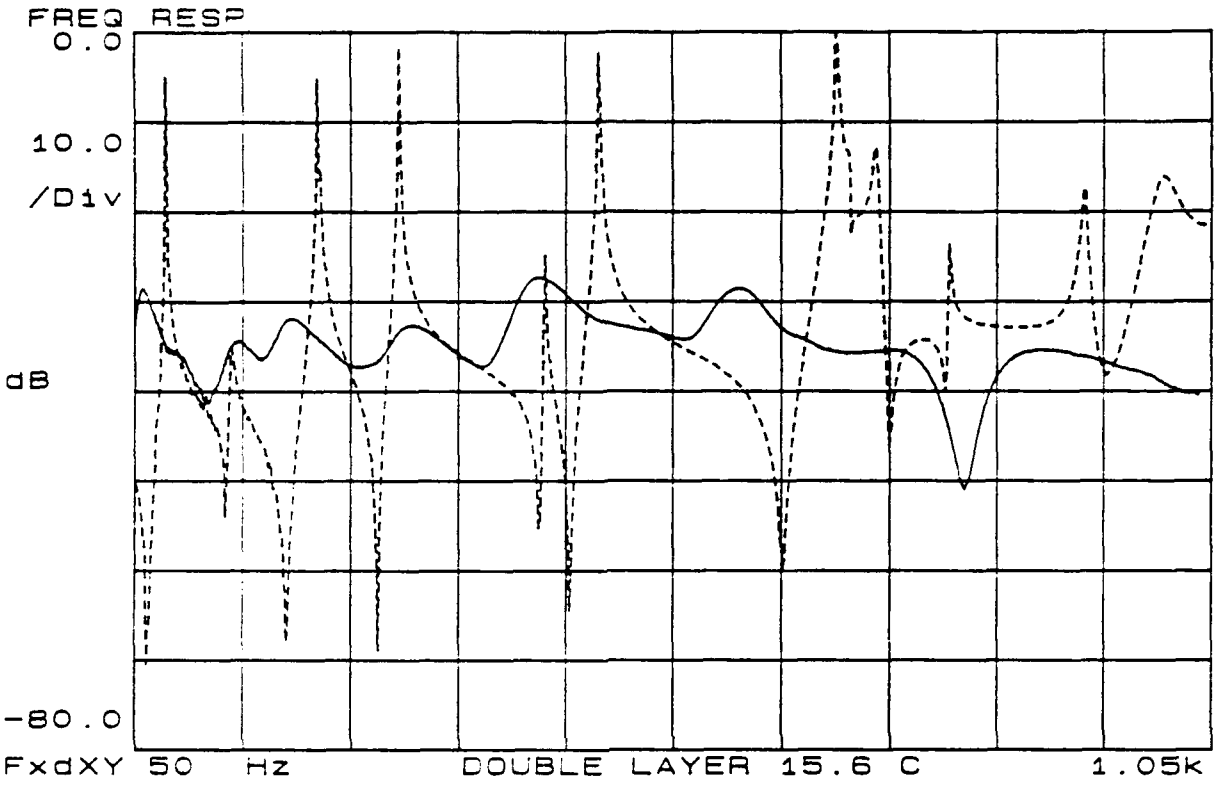

Figure 4.7. Frequency Response of the Double Layer at 15.6 °C.

[- - - - : undamped response , ——— : damped response]

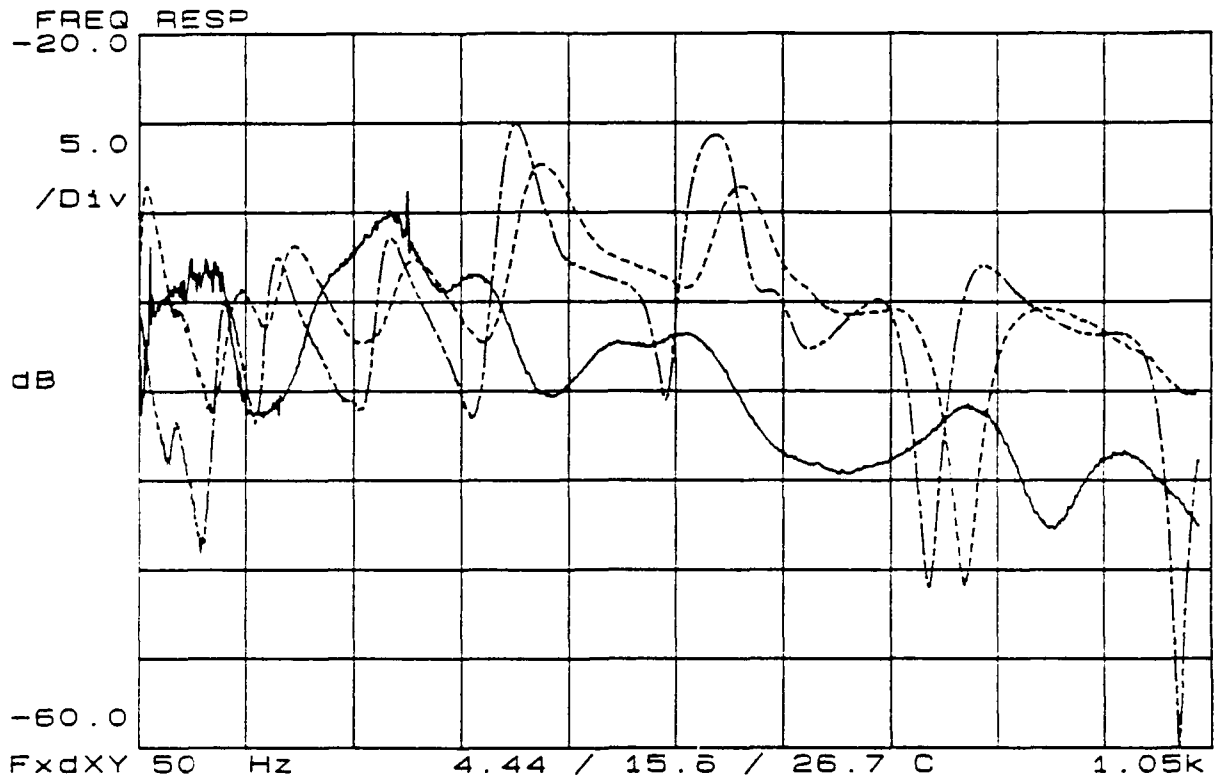

Figure 4.8. Frequency Response Comparison of the Double Layer Configuration at Different Temperatures.

[——— : 4.44 °C , - - - - : 15.6 °C , ——- - —— : 26.7 °C]

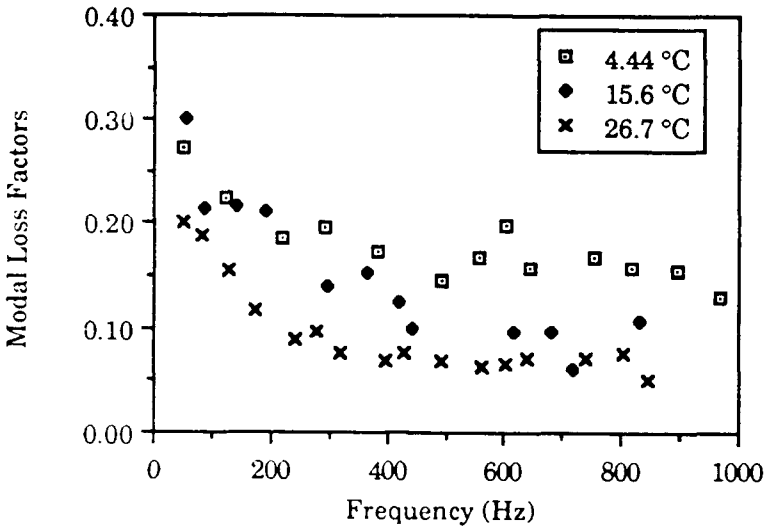

Figure 4.9. Comparison of Modal Loss Factors for the Double Layer at Different Temperatures.

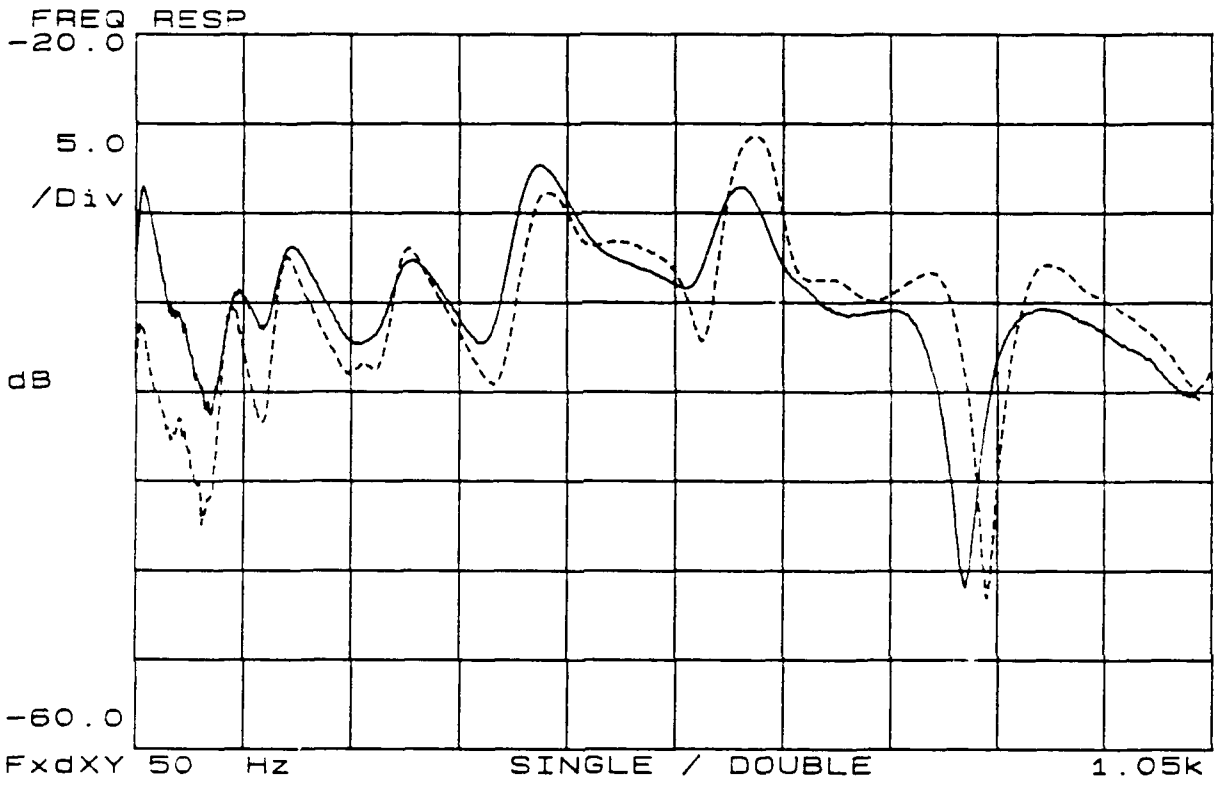

Figure 4.10. Frequency Response of the Double and Single Layer at 15.6 °C.

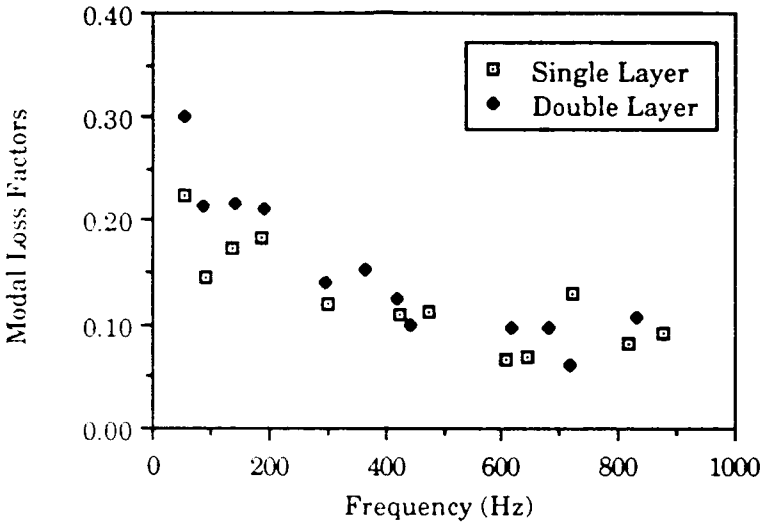

Figure 4.11. Modal Loss Factors for Single and double layer Configurations.

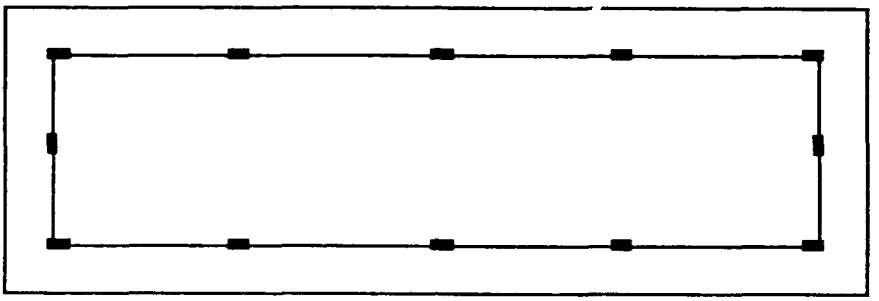

Figure 4.12. Location of Tack Welds on the Cover Plate of the Pocket Plate Configuration.

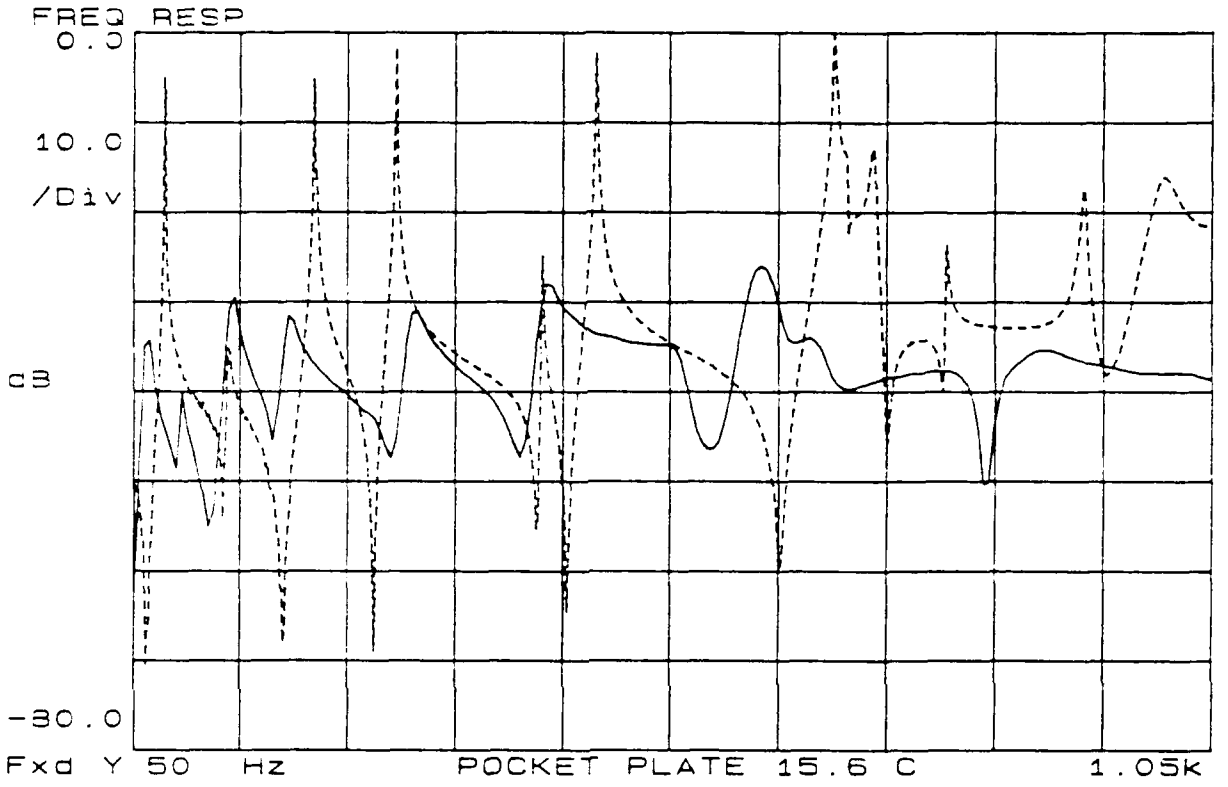

Figure 4.13. Frequency Response of the Pocket Plate Configuration at 15.6 °C.

[- - - - : reference plate , ——— : pocket plate]

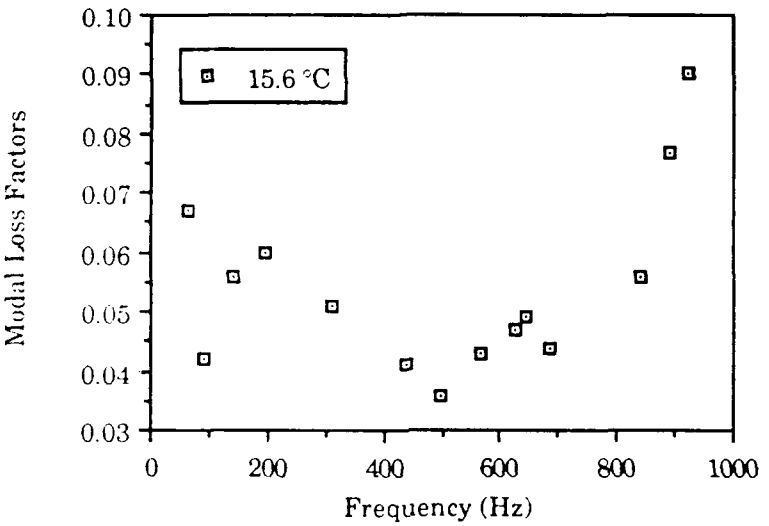

Figure 4.14. Modal Loss Factors for the Pocket Plate Configuration.

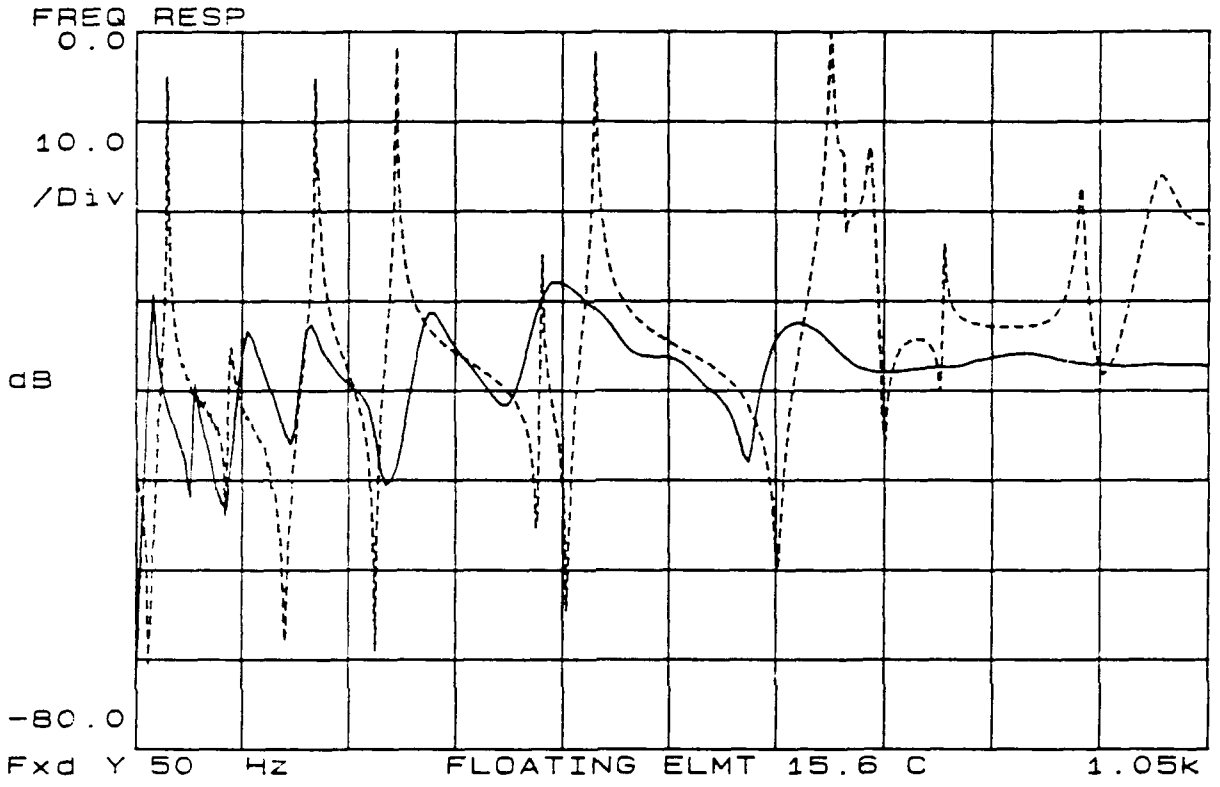

Figure 4.15. Frequency Response of the Floating Element at 15.6 °C .

[- - - - : undamped plate , ——— : floating element]

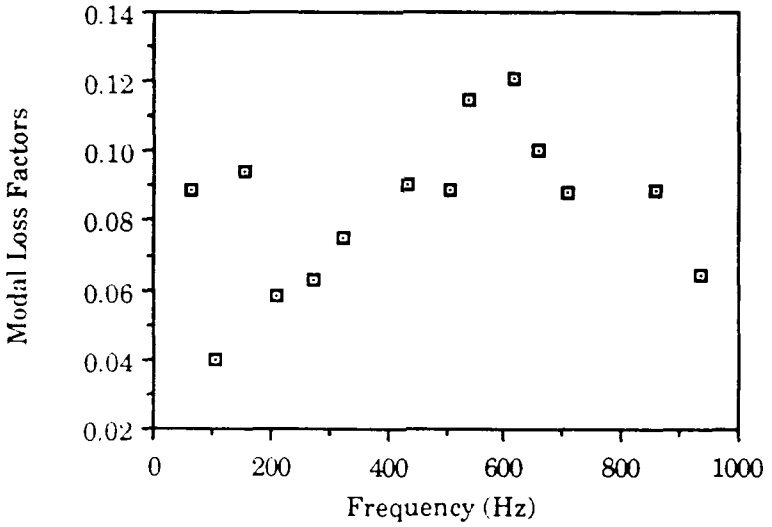

Figure 4.16. Modal Loss Factors for the Floating Element Configuration.

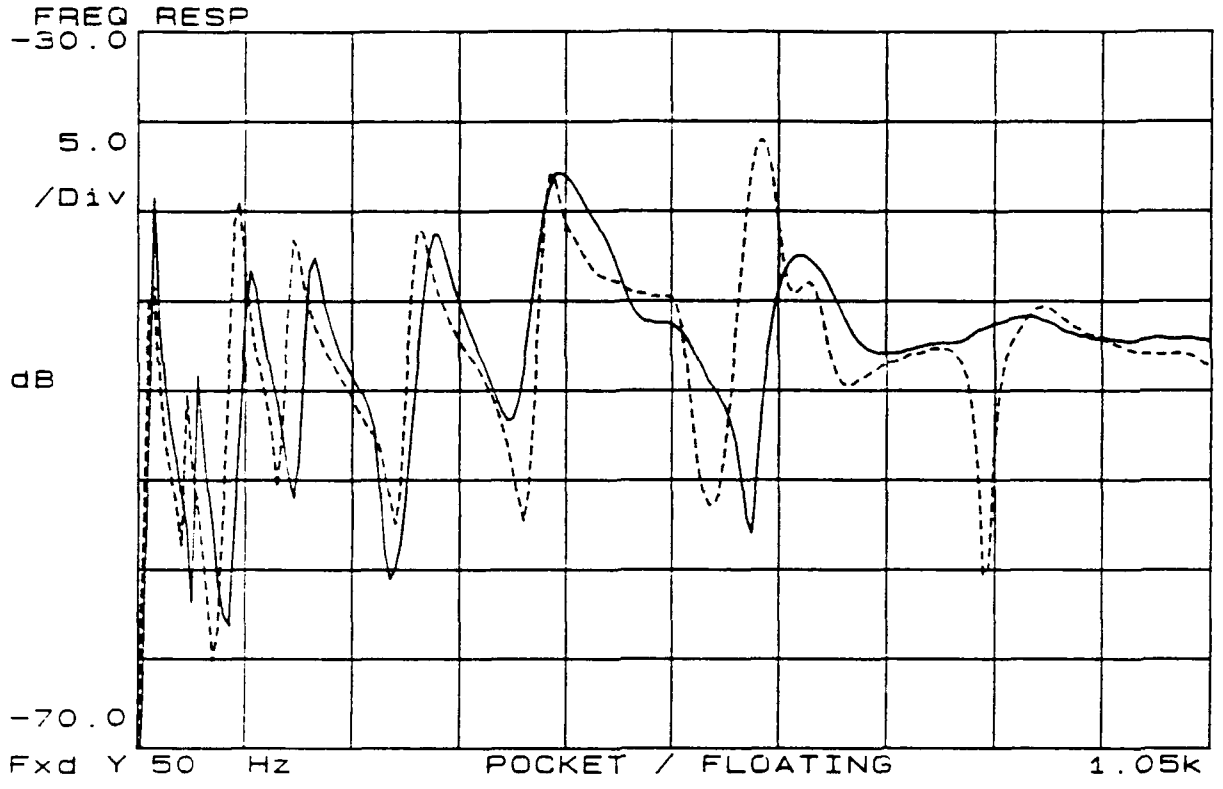

Figure 4.17. Comparison of Frequency Responses for the Pocket Plate and Floating Element Configurations.

[- - - - : pocket plate , ——— : floating element]

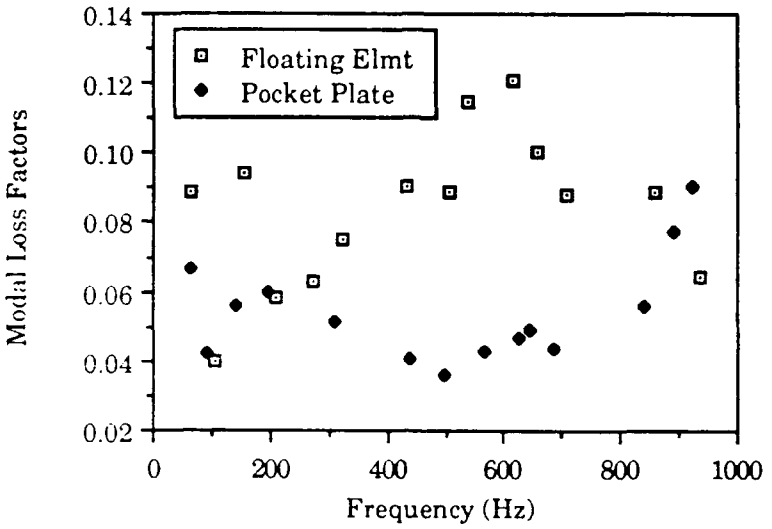

Figure 4.18. Modal Loss Factors for the Pocket Plate and Floating Element Configurations.

V. FINITE ELEMENT RESULTS

A. UNDAMPED REFERENCE PLATE

The first step in the finite element analysis procedure was to model and analyze the undamped reference plate for its modal frequencies and frequency response. The finite element model was generated using PATRAN, a computer aided interactive graphics program developed by PDA Engineering. PATRAN is widely used for conceptual, preliminary, and detailed design and analysis of complex systems. One of PATRAN's major advantages is in the interactive construction of finite element models for use by MSC/NASTRAN, and its ability to display MSC/NASTRAN results in an easily understood graphic format [Ref. 15].

The reference plate was modeled using 84 plate (QUAD4) elements as shown in Figure 5.1. The QUAD4 element is an isoparametric element with four nodes, one at each corner of the element [Ref. 7]. A normal mode extraction was then performed in order to compare numerical results with experimentally determined modal frequencies. Once satisfactory agreement between the modal frequencies calculated in NASTRAN and those obtained experimentally was attained, a direct frequency response calculation was performed in NASTRAN. This frequency response was then used as the reference response for further finite element models incorporating viscoelastic damping treatments. The excitation for the

frequency response calculation was a sinusoidal force with an amplitude of 1.0 applied at node 66. The response point was node 58 as shown in Figure 5.1. These two nodes correspond to the points on the plates used in the experimental portion of the research where the vibration generator and accelerometer were attached.

B. SINGLE DAMPING LAYER

The modeling of the single constrained layer damping system was done using techniques described by Johnson and Kienholz [Ref. 1]. As shown in Figure 5.2, the viscoelastic layer is modeled using solid (HEXA) elements, while the base layer and constraining layer were modeled using QUAD4 elements. The HEXA element is a solid, isoparametric element having eight nodes, one at each corner of the element with three translational degrees of freedom at each node [Ref. 7]. The use of solid elements for the viscoelastic layer allows the strain energy due to shearing to be adequately represented. Plate elements are used in the base layer and constraining layer because of their ability to account for stretching and bending deformations. The plate element allows its nodes to be offset from the plate's center to the surface of the plate, coincident with the corner nodes of the solid viscoelastic elements [Ref. 1]. Thus, the single constrained layer system was modeled using only two layers of nodes, a simple process in PATRAN. For the single layer configuration, a model

having 84 elements per layer, and an element meshing scheme shown in Figure 5.2 was used.

Once the damped plate had been modeled, normal mode extractions were made using MSC/NASTRAN. Five separate runs were conducted using the material properties of ISD–112 at 50, 200, 500, 800, and 1000 Hz and at a temperature of 15.6 °C (60 °F). In addition to the modal frequencies, the strain energy in the viscoelastic elements and the entire model were output from NASTRAN.

Since the shear modulus of a viscoelastic material changes with frequency, it was necessary to estimate the actual modal frequencies of the damped plate using an interpolation procedure outlined by Johnson and Kienholz [Ref. 16]. The first step of the interpolation process was to plot the shear modulus of ISD–112 versus frequency from 5 to 1000 Hz. Then, for the first mode, using NASTRAN results based on ISD–112 material properties a 50 Hz, the first modal frequency predicted by NASTRAN and the corresponding shear modulus were plotted. The same was then done using the first natural frequency predicted by normal mode extraction based on ISD–112 material properties at frequencies of 500 and 1000 Hz. A curve was then passed through these three points. The point where the NASTRAN modal frequencies for the first mode intersected the ISD–112 shear modulus curve was taken to be the interpolated modal frequency of the single damping layer configuration. A plot of the intersection of these

two curves for the first and second modes is shown in Figure 5.3. This interpolation process was then repeated for each mode through 1000 Hz.

Once the interpolated modal frequencies were found, the modal strain energy equations (2.12) and (2.13) were used to compute modal loss factors for the single layer configuration. A set of modal loss factors was computed based on the modal strain energies computed using viscoelastic properties at reference frequencies of 50 ,200, 500, and 800 Hz. A set of composite modal loss factors for the modal frequencies near these reference frequencies was then selected. The resulting modal loss factors are shown in Table 5.1 and are plotted versus frequency in Figure 5.4. As seen in Figure 5.4, the modal strain energy method is predicting high damping for this configuration with an average modal loss factor of 0.195.

TABLE 5.1. ESTIMATED MODAL LOSS FACTORS FOR THE SINGLE LAYER USING THE MODAL STRAIN ENERGY METHOD

f(Hz)	η	f(Hz)	η
63	0.249	517	0.237
95	0.181	586	0.217
153	0.234	632	0.164
202	0.212	663	0.155
285	0.229	712	0.180
322	0.214	827	0.134
447	0.200	869	0.152
463	0.108	883	0.115
483	0.258		

Using the set of composite modal loss factors, the modal frequency response of the damped plate was computed using MSC/NASTRAN. Modal damping was introduced to the model using the SDAMP option in the Case Control Deck and the TABDMP1 damping table in the Bulk Data Deck as described in the MSC/NASTRAN Handbook for Dynamic Analysis [Ref. 17]. Since NASTRAN uses a linear interpolation between points in the damping table to describe the modal damping in the model [Ref. 7], a simple curve fit was applied to the set of composite modal loss factors as shown in Figure 5.4. Points from this curve fit were then used in the NASTRAN damping table. To compute the modal frequency response, a unit excitation force was applied at the same node as the undamped plate, and the node used for the response was also the same as the undamped plate.

The results of the modal frequency response calculations are shown in Figure 5.5. The dashed line represents the undamped reference plate, and the solid line represents the modal frequency response of the single layer configuration. Material properties at 200 Hz were used for the ISD–112 damping material. The first thirty modes were used in the modal summation for the response. A listing of the MSC/NASTRAN data deck used to compute the modal frequency response is in Appendix D.

The modal loss factors estimated using the modal strain energy method are compared to those measured experimentally for the single layer configuration in Figure 5.6. The estimated loss factors are greater than the

experimentally determined loss factors throughout the spectrum of interest, and especially in the middle frequencies.

The modal frequency response of the single layer configuration is compared to the experimentally measured frequency response in Figure 5.7. The comparison was accomplished by normalizing both the experimentally determined frequency response and the frequency response computed in NASTRAN. Both responses were normalized using a value of $1.0 \frac{in/sec^2}{lb}$. The effects of the greater loss factors estimated by the modal strain energy method are obvious as the level of the predicted response is lower than the measured response. The shift in frequency between the two curves is due to the finite element model being inherently stiffer than the actual system. The correlation between the two curves is especially good below 250 Hz as this is where the differences between estimated and measured modal loss factors are the least.

C. DOUBLE DAMPING LAYER

The modeling of the double constrained layer damping system was accomplished as shown in Figure 5.8. The double layer configuration consists of a base layer modeled with offset QUAD4 elements, two viscoelastic layers consisting of HEXA elements, and the top constraining layer modeled with offset QUAD4 elements. The middle constraining layer

was modeled using three layers of HEXA elements in order to give this layer the stiffness necessary to act as a constraining layer. The model was meshed using 60 elements in each layer as shown in Figure 5.8.

Using this model, the modal strain energy method was applied to determine approximate modal frequencies and loss factors for the double layer configuration. To determine the loss factors, normal mode extractions were performed using reference frequencies of 50, 200, 500, 800, and 1000 Hz. A composite set of modal loss factors for the double layer system was then compiled based on the estimated modal frequency's relation to the reference frequency used to calculate modal strain energies. This composite set of modal loss factors is listed in Table 5.2, and is plotted in Figure 5.19 as a comparison to the experimentally determined modal loss factors for the double layer configuration. The estimated modal loss factors for the double layer show high damping, but they compare favorably with those measured experimentally.

The modal frequency response of the double layer configuration was computed in a manner similar to the single layer in that smoothed loss factor data was used in the MSC/NASTRAN damping table. Likewise, a unit excitation force was applied, and the first thirty modes were used in the modal summation. The results of the modal frequency response calculation are shown in Figure 5.10. The dashed line represents the undamped response, and the solid line represents the frequency response of the double layer configuration.

TABLE 5.2. ESTIMATED MODAL LOSS FACTORS FOR THE DOUBLE LAYER USING THE MODAL STRAIN ENERGY METHOD.

f(Hz)	η	f(Hz)	η
59	0.278	544	0.209
89.5	0.219	578	0.141
140	0.239	593	0.131
189	0.213	659	0.177
258	0.214	754	0.102
300	0.205	783	0.076
402	0.179	802	0.144
427	0.176	956	0.077
456	0.264	969	0.111
486	0.242	994	0.048

The frequency response calculated using NASTRAN was compared to the experimentally determined frequency response of the double layer configuration as shown in Figure 5.11. Comparison of the two frequency response curves shows similarity in form, but a much lower response level for the numerically determined response. Once again this could be due to the higher damping predicted by the modal strain energy method and the inherently higher stiffness of the finite element model.

D. POCKET PLATE RESULTS

The pocket plate configuration was modeled with the same offset plate elements and solid viscoelastic elements as the single layer configuration. However, the pocket plate required the modeling of the milled structure around the viscoelastic material and the welds between the cover plate and milled plate. A representation of the model is shown in Figure 5.12. The base structure, cover plate, and the structure immediately around the cover plate was modeled using offset plate elements. The viscoelastic material and the portion of the structure immediately adjacent to it were modeled using the solid HEXA elements. Since the viscoelastic material and cover plate are physically separated from the surrounding plate, except where the viscoelastic is adhered to the base structure, care was necessary in creating the finite element mesh.

The model was created in PATRAN using PATRAN's node editing and equivalencing capabilities [Ref. 18]. This allowed the generation of a finite element mesh with two nodes at the same geometric point in space. Using this node editing technique, a mesh was created which allowed the viscoelastic and cover plate to vibrate separately from the surrounding structure, yet at the same time, keep the number of elements and nodes in the model to a minimum. The welded points on the cover plate were also modeled using node editing techniques. At weld points the finite element node on the cover plate was equivalenced with its corresponding node on the base structure, resulting in a single node and a connection between an

otherwise separate base structure and cover plate. At non–welded points on the cover plate there were two nodes at the same geometric point; one to represent the cover plate, and the other to represent the base structure. The model was meshed using a 5x11 mesh resulting in 40 elements in the cover plate, viscoelastic and base layer as shown in Figure 5.12.

Using this modeling scheme, the modal strain energy method was employed to estimate the modal frequencies and loss factors. Normal mode extractions were made using viscoelastic material properties at 50, 200, 500, 800, and 1000 Hz. Using these reference frequencies a composite set of modal loss factors was obtained. These loss factors are listed in Table 5.3 and are plotted versus frequency in Figure 5.13. The estimated loss factors give good damping over the spectrum of interest with an average modal loss factor of 0.075. As with the previous cases, damping values used for the modal frequency response calculation came from a curve–fit to the set of composite modal loss factors.

The modal frequency response of the pocket plate was computed using the first 30 modes and viscoelastic material properties at 200 Hz. The resulting estimated frequency response is shown in Figure 5.14. The response shows a definite frequency shift to the left along with good damping of the frequency response when compared to the undamped response.

The estimated modal loss factors and modal frequency response for the pocket plate were compared to those measured experimentally. The loss factor comparison is shown is Figure 5.15 and the frequency response comparison is shown in Figure 5.16. The estimated modal loss factors are higher than those measured experimentally, however, the frequency responses compare quite favorably with each other. The frequency response curve calculated through finite element analysis has a lower response level and a frequency shift to the right of the measured frequency response. This is expected due to the increase in damping predicted by the modal strain energy method and by the fact that the finite element model is inherently stiffer than the physical system

TABLE 5.3. ESTIMATED MODAL LOSS FACTORS FOR THE POCKET PLATE USING THE MODAL STRAIN ENERGY METHOD.

f (Hz)	η	f (Hz)	η
67	0.046	511	0.113
109	0.034	588	0.104
162	0.091	625	0.086
217.5	0.063	668	0.089
295	0.091	713	0.077
333	0.047	831	0.077
453	0.07	834	0.065
477	0.093	868	0.051

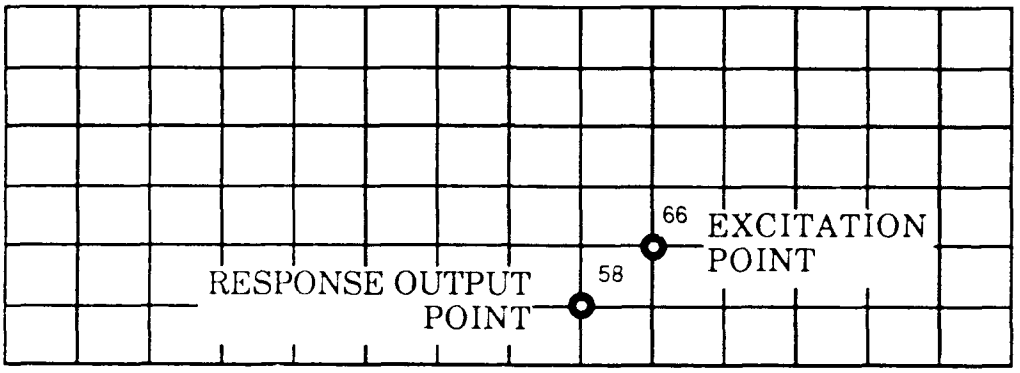

Figure 5.1. Finite Element Model of the Undamped Reference Plate.

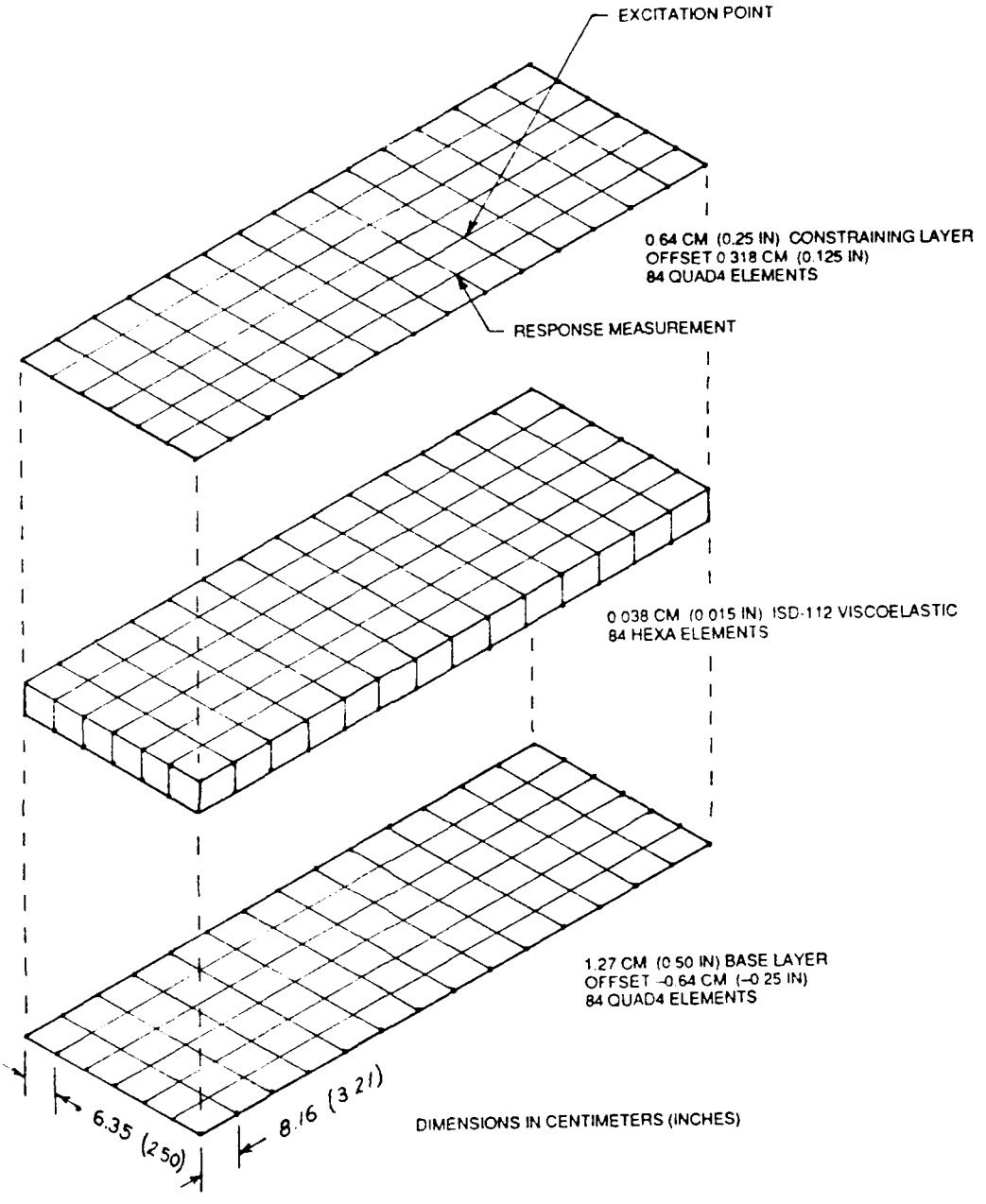

Figure 5.2. Finite Element Representation of the Single Constrained Layer Configuration.

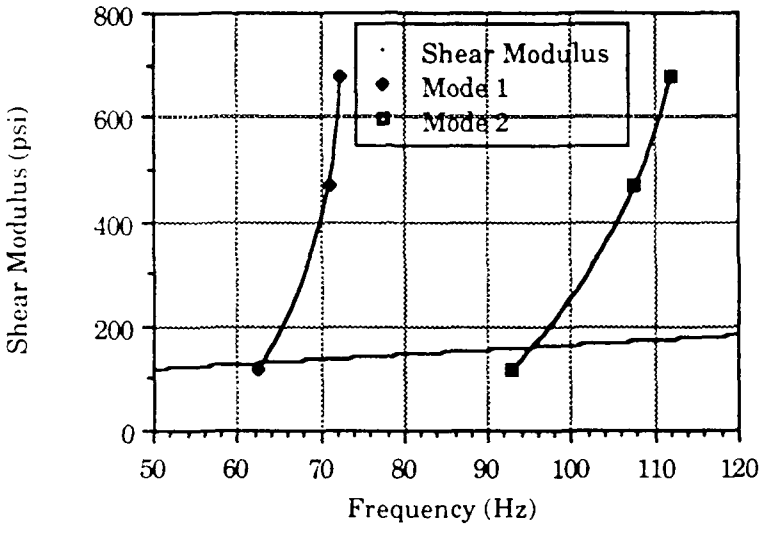

Figure 5.3. Interpolation of the First and Second Modal Frequencies for the Single Constrained Layer Configuration.

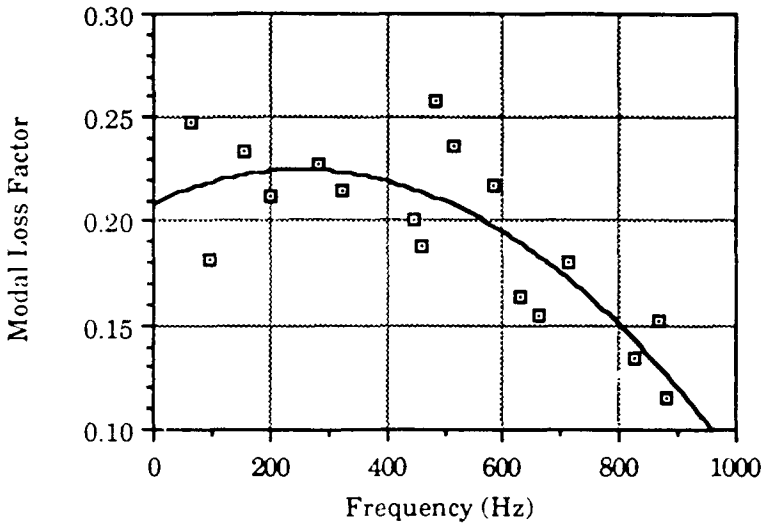

Figure 5.4. Estimated Modal Loss Factors for the Single Layer Configuration with the Curve Fit Used for the MSC/NASTRAN Damping Table.

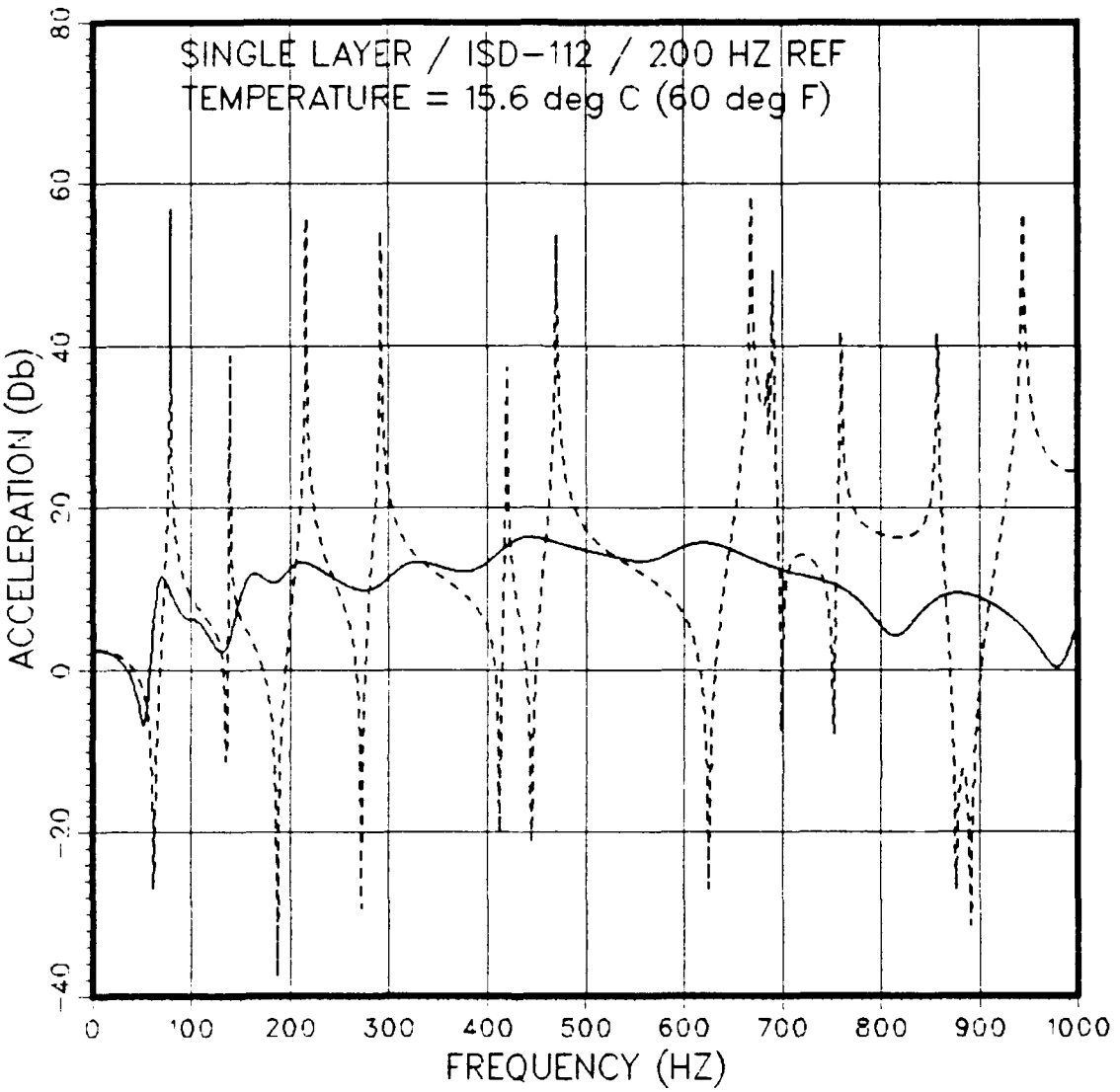

Figure 5.5. Calculated Modal Frequency Response of the Single Layer Configuration Using NASTRAN.

[– – – – : reference plate , ——— : single layer]

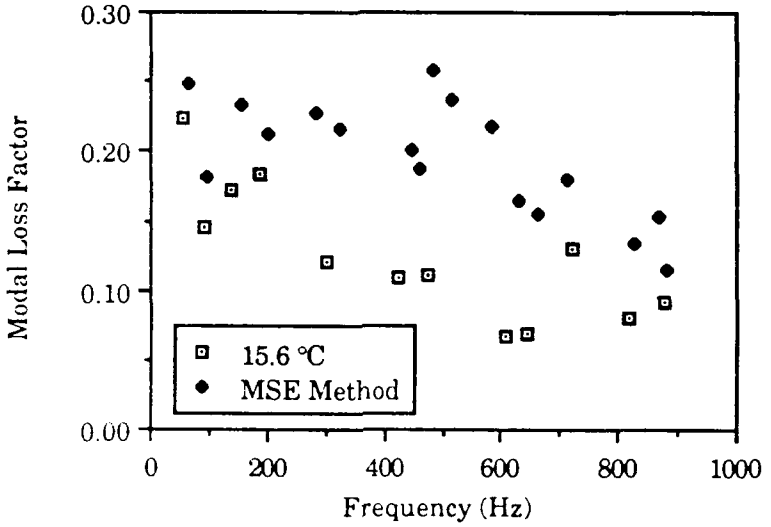

Figure 5.6. Comparison of Estimated and Measured Modal Loss Factors for the Single Layer Configuration.

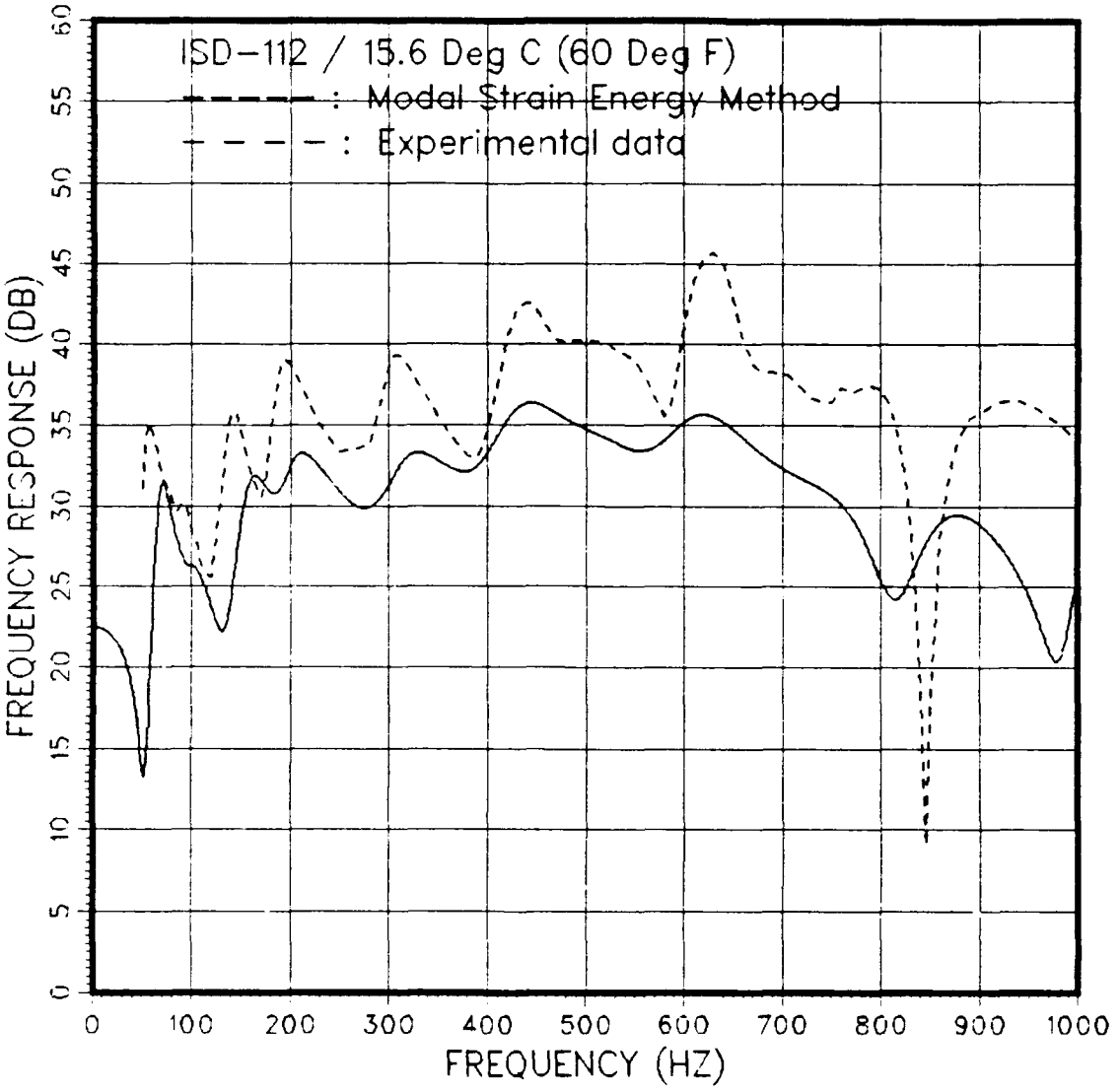

Figure 5.7. Comparison of Estimated and Measured Frequency Response for the Single Layer Configuration.

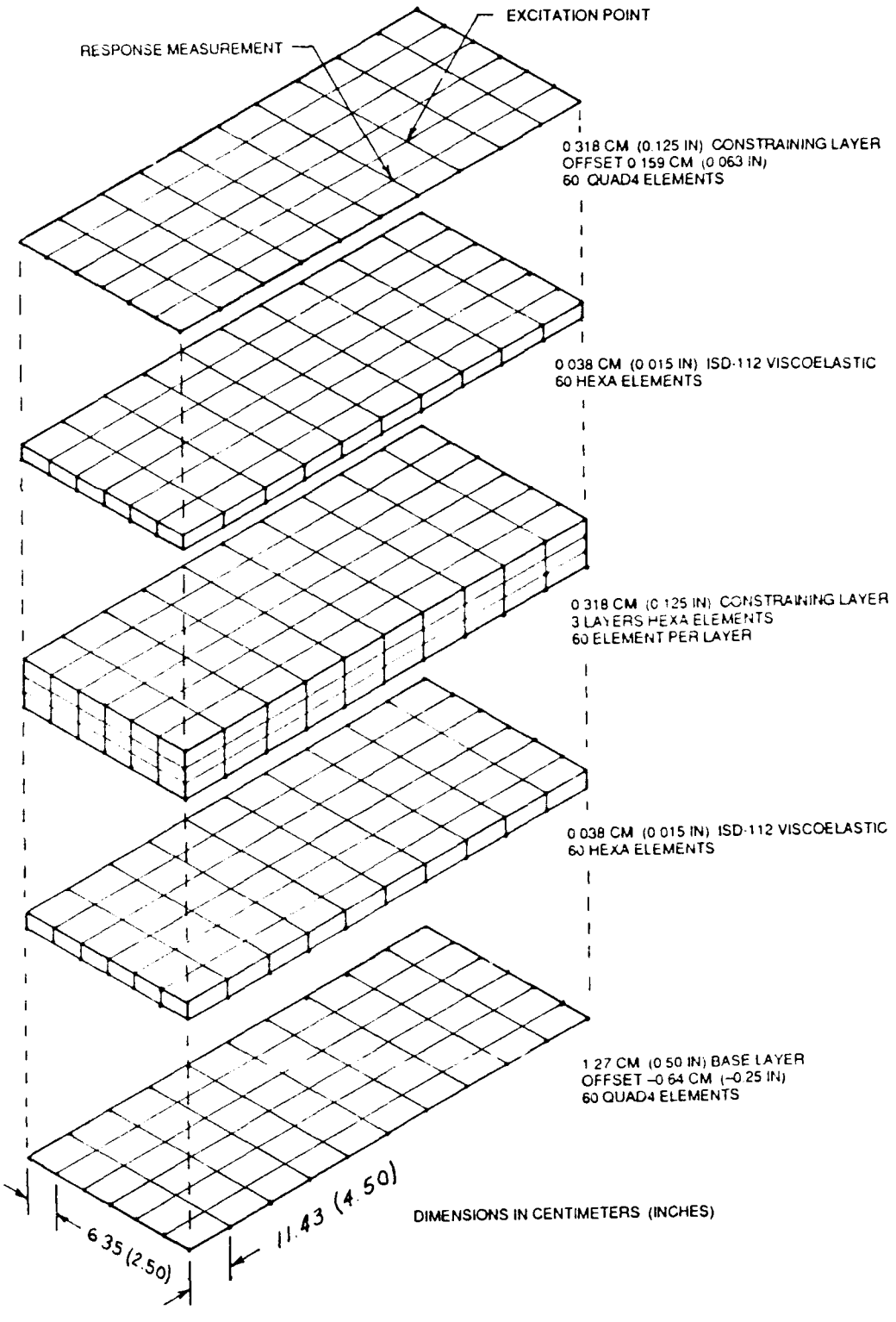

Figure 5.8. Finite Element Representation of the Double Layer Configuration.

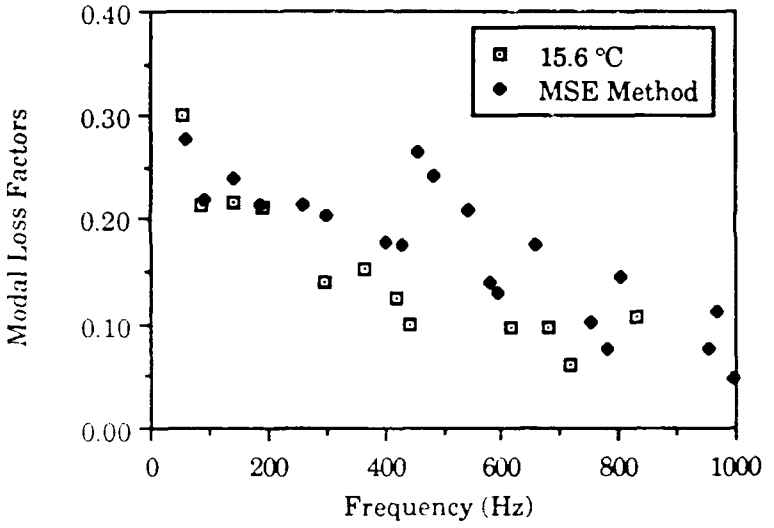

Figure 5.9. Modal Loss Factors for the Double Layer Configuration as Determined from the Modal Strain Energy Method and Determined Experimentally.

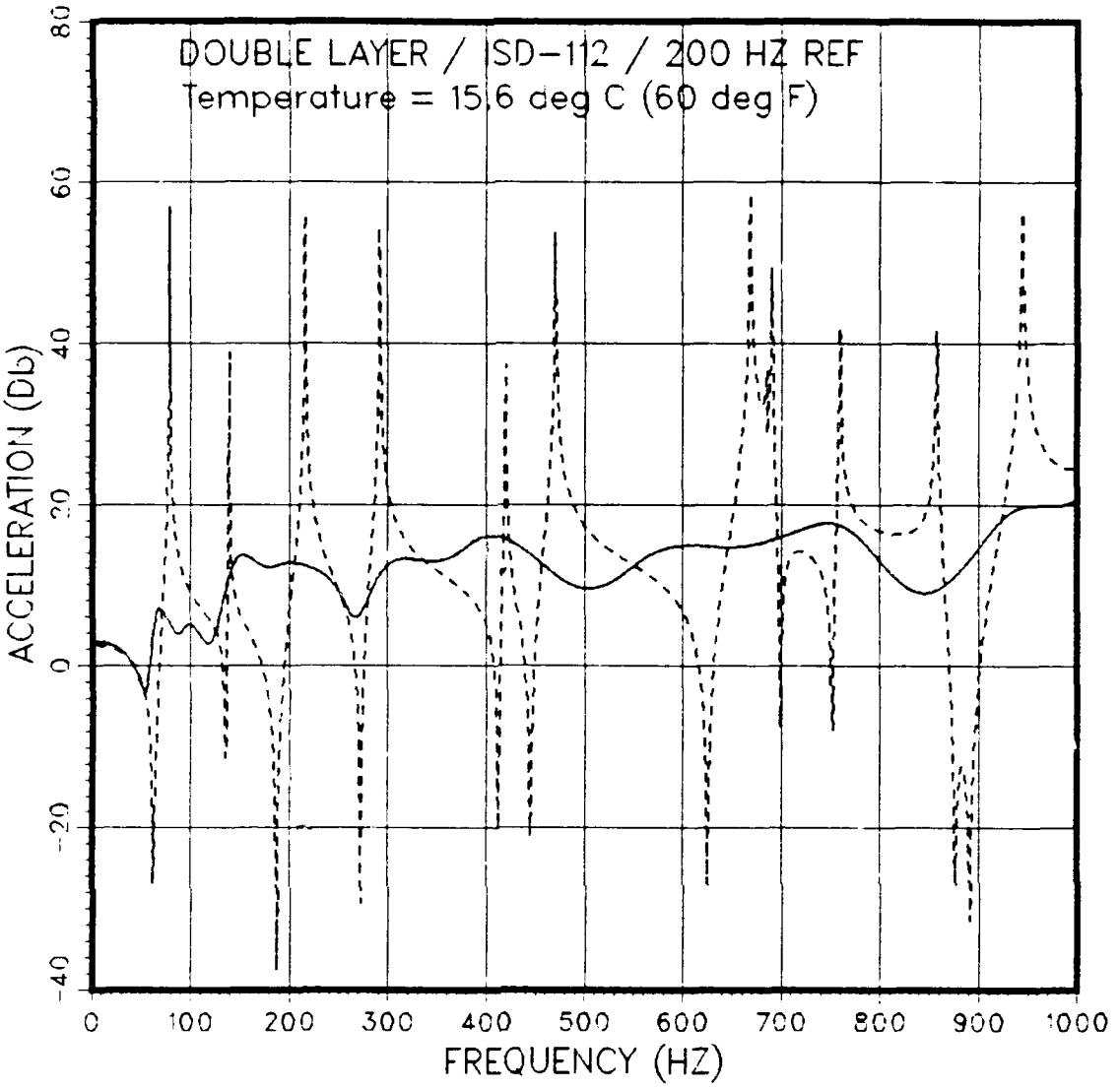

Figure 5.10. Calculated Modal Frequency Response for the Double Layer Configuration Using NASTRAN.

[– – – – : reference plate , ——— : double layer]

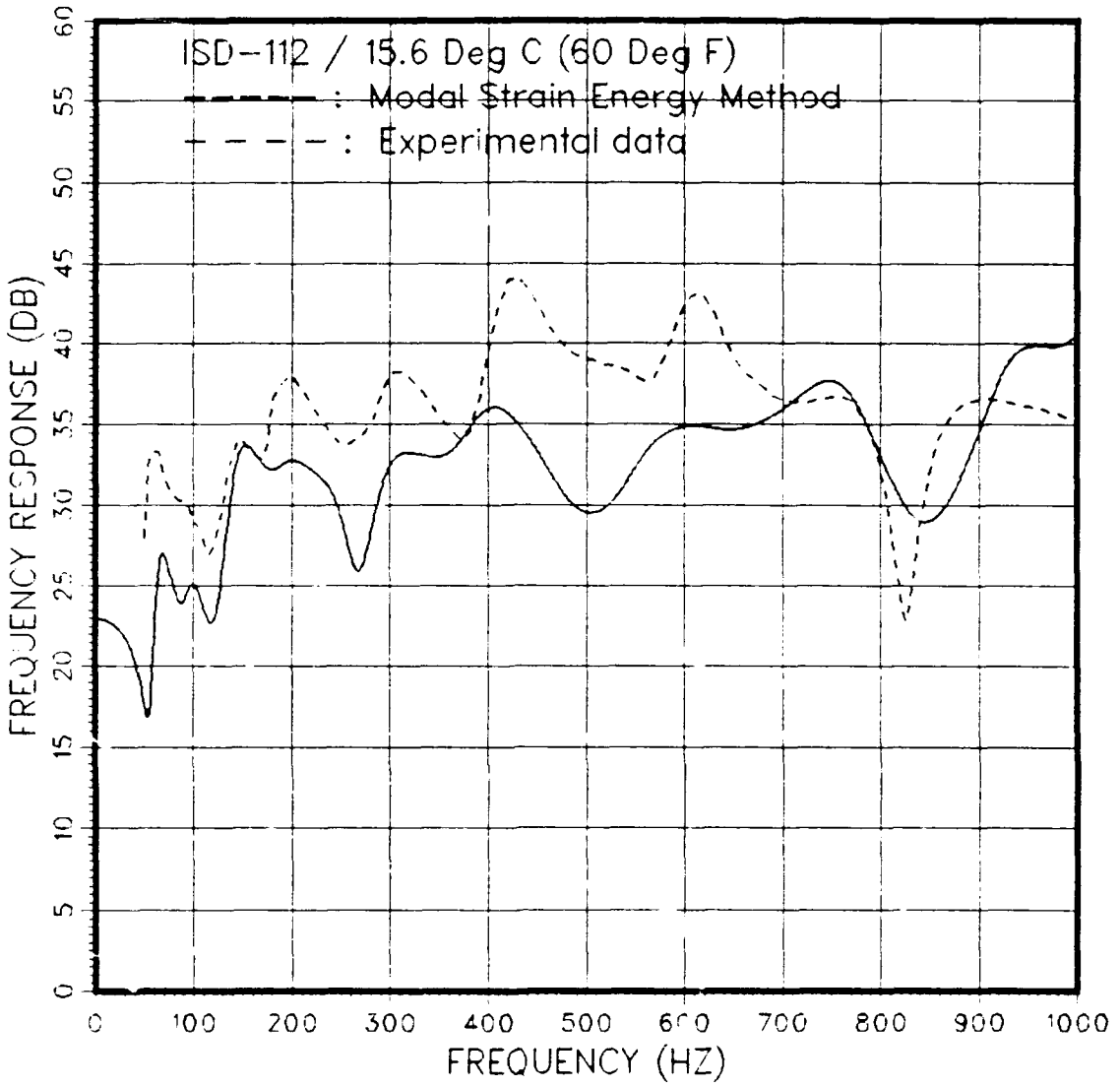

Figure 5.11. Comparison of the Experimentally Determined and Numerically Predicted Frequency Responses for the Double Layer Configuration.

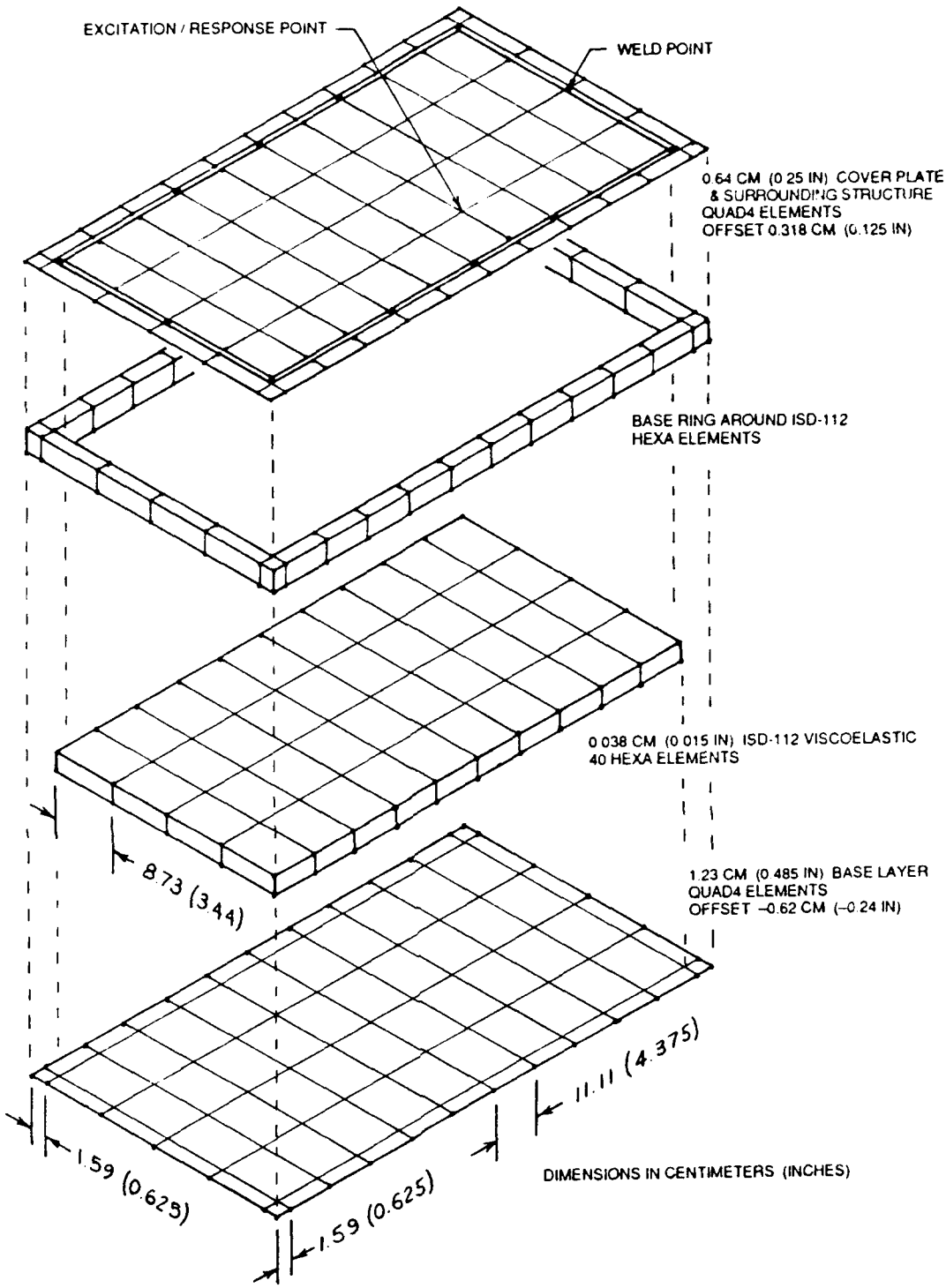

Figure 5.12. Finite Element Representation of the Pocket Plate Configuration.

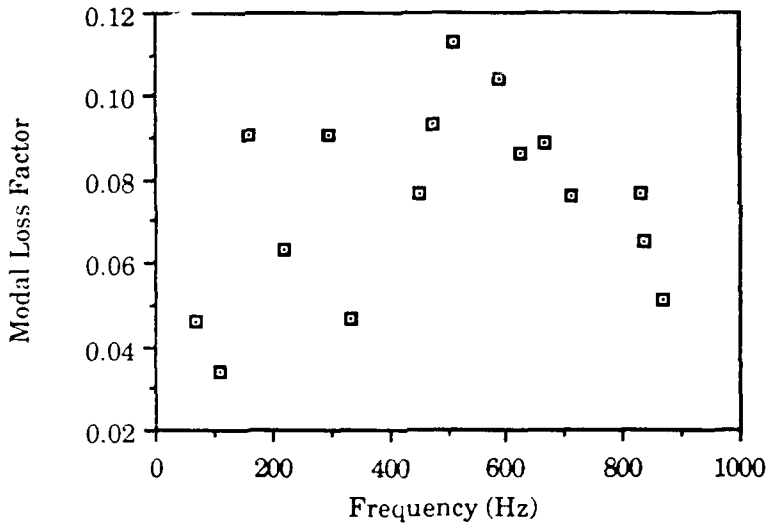

Figure 5.13. Estimated Modal Loss Factors for the Pocket Plate.

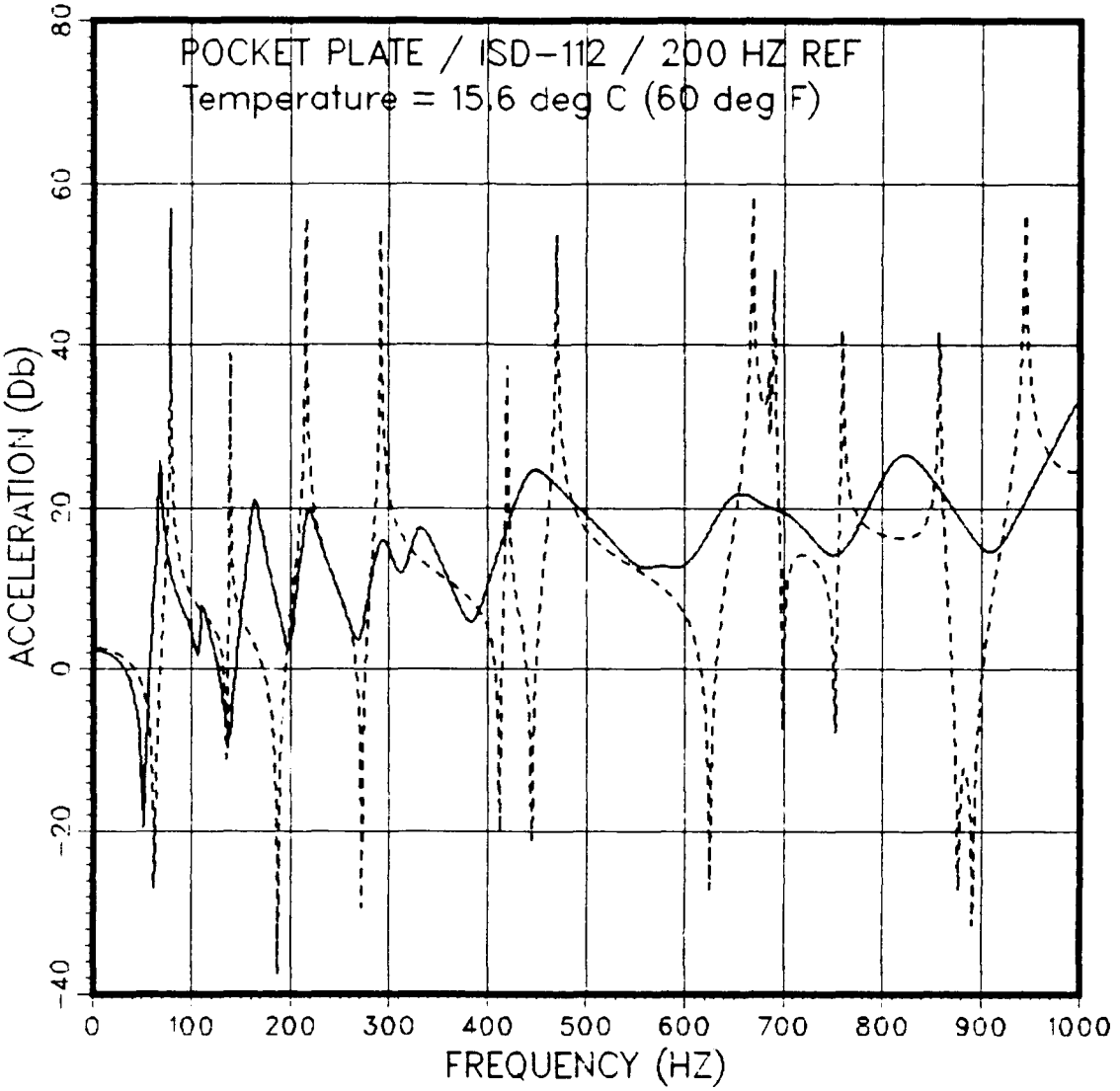

Figure 5.14. Estimated Frequency Response

for the Pocket Plate Configuration.

[– – – –: reference plate , ——— : pocket plate]

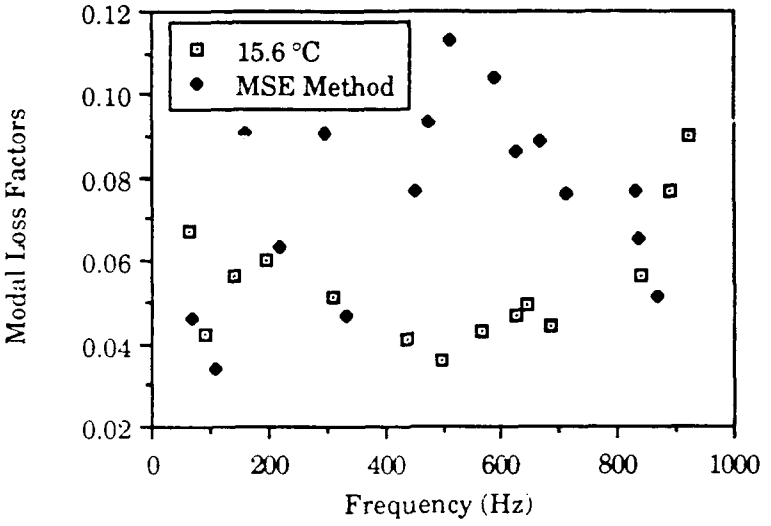

Figure 5.15 Comparison of Experimentally Measured and Estimated Modal Loss Factors for the Pocket Plate Configuration.

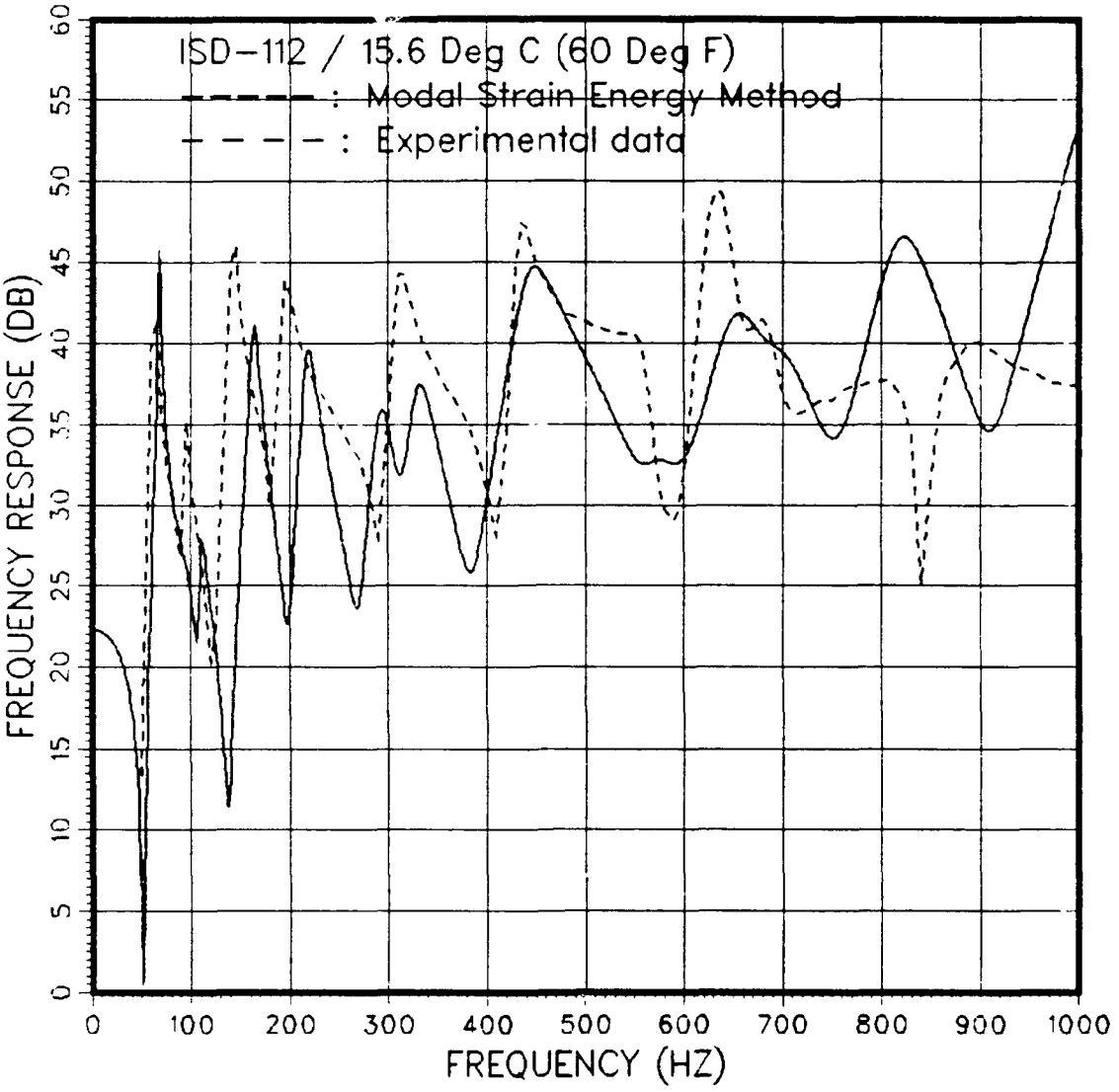

Figure 5.16. Comparison of Experimental and Predicted Frequency Responses for the Pocket Plate Configuration.

VI. CONCLUSIONS

Constrained viscoelastic layer damping is an extremely effective method for reducing broadband vibration. In each of the experimental cases the peak amplitudes of frequency response were reduced by approximately 25 decibels, a reduction of 18 times below the undamped reference plate.

In a comparison of experimentally determined modal loss factors for the four treatments, the double layer configuration yields the largest damping and the pocket plate the least as shown in Figure 6.1. Of particular note are the performance of the pocket plate and floating element configurations. Although they are not ideal configurations in terms of "true" constrained viscoelastic layer damping, the damping levels achieved are quite satisfactory. As was previously reported in Section IV, the floating element configuration yielded an average increase of 25 percent over the modal loss factors of the pocket plate. It is also noted that the average modal loss factor for the pocket plate is approximately 50 percent of the average modal loss factor of the single layer configuration. Similarly, the average modal loss factor for the floating element configuration is approximately 50 percent that of the double layer treatment.

The modal strain energy method tends to overpredict the modal loss factors by as much as 50 percent for these highly damped, thick plates.

Figure 6.2 shows that, although the modal strain energy method predicted modal loss factors greater than those measured, the same relative differences in modal loss factor between damping configurations are maintained. The estimated modal loss factors for the pocket plate are approximately 60 percent less than those of the single layer configuration. This indicates that there is a consistency between the damping values predicted by the modal strain energy method and those of the actual physical system.

There are several possible reasons for the differences between the experimentally determined modal loss factors and those estimated by the modal strain energy method. The first is that the material properties of ISD–112 as reported by the 3M Corporation on the reduced frequency nomogram may not be consistent with the material properties actually present in the material used. Since the numerical analysis was based on the reported material properties this is a possible source of uncertainty in the results.

The second source of uncertainty is in the adhesion of the ISD–112 to the aluminum plates. Although the plates were clean when the ISD–112 was applied, it was noted that the adhesive qualities of the ISD–112 were not uniform throughout the material. A lack of adhesion may cause a reduction in the damping capability of the system.

Another source for the difference between the experimental results and numerical results lies within the finite element model. The number of elements used in the model greatly affects its "stiffness." As the number of elements is increased the model should become less stiff and results are expected to approach those that are measured. Also, the type of element used to model the base layer and constraining layer may have an effect. In this research plate elements were used to model both the base and constraining layers. It is possible that one or more layers of solid elements may produce results that agree better with experimental results.

One drawback to the modal strain energy method in design is the large amount of CPU time required for normal mode extraction and modal frequency response; especially in complex structures with a large number of elements. Therefore, although the modal strain energy method is good for analyzing a design, it may face a big difficulty to be used for design optimization due to the large amount of CPU time required for normal mode extraction and modal frequency response calculations.

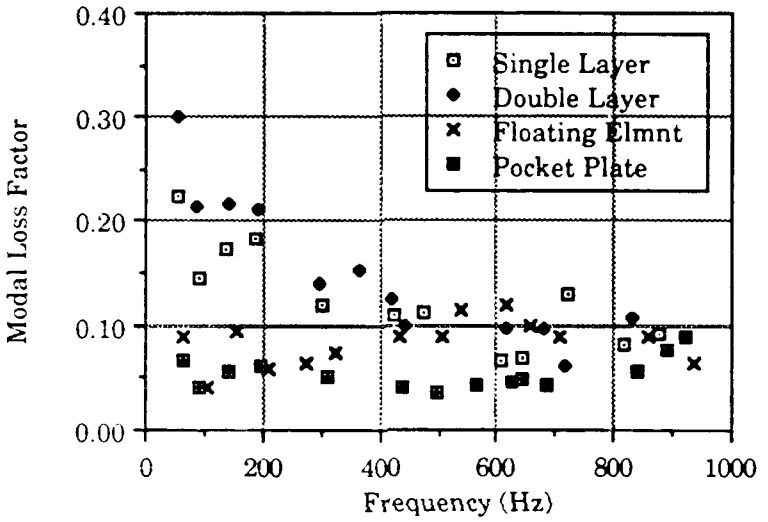

Figure 6.1. Comparison of Experimentally Measured Modal Loss Factors for the Four Damping Configurations.

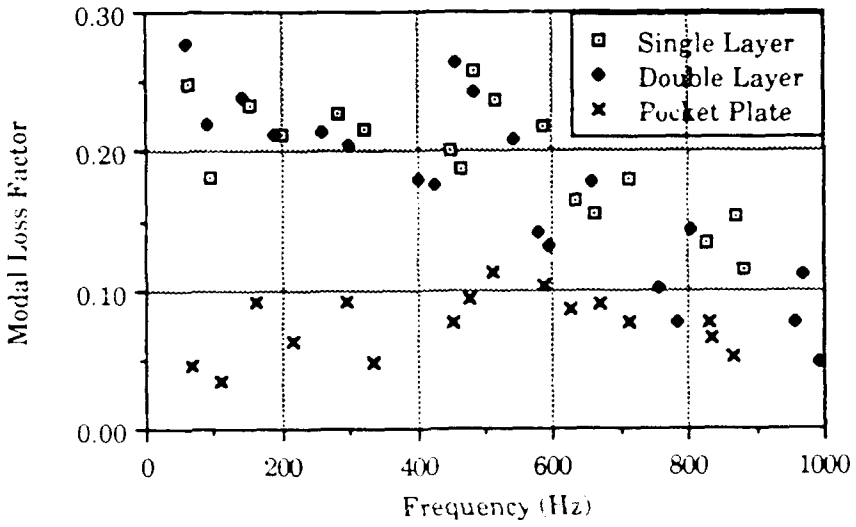

Figure 6.2. Comparison of Estimated Modal Loss Factors for the Single Layer, Double Layer, and Pocket Plate Configurations.

VII. RECOMMENDATIONS

The thick plate used in this research is a generic model of many physical systems that may see use in naval application. There are several areas which deserve more research and clarification, including the following:

- Model the floating element configuration in finite elements and check the effectiveness of the modal strain energy method in predicting modal loss factors for this configuration.
- Investigate the relationship between mode shapes and damping values. It seems some modal damping values are very low due to their twisting mode shapes.
- For pocket plate and floating element configurations, weld the whole cover plate (continuous weld) and investigate the damping characteristics to compare the vibration reduction capabilities of the two different milled plate damping treatments.
- Investigate methods for improving the adhesion of ISD–112 to the base structure and constraining layer.

APPENDIX A

FORTRAN PROGRAM USED TO COMPUTE MODAL LOSS FACTORS FOR THE SINGLE DAMPING LAYER DESIGN

This program used the Ross–Kerwin–Ungar equations of Section III to compute estimated modal frequencies and loss factors for the single layer configuration. Modal frequencies for an undamped plate are read from a data file and estimated modal frequencies and loss factors for various layer thicknesses are output to another file. Material properties of ISD–112 are computed using University of Dayton data and curve-fitting equations to the reduced frequency nomogram [Ref. 9,12]. The units used in this program are pounds, inches, and seconds.

```
      PROGRAM CARPET
C ***********************************************************************
C  THIS PROGRAM IS TO CALCULATE SYSTEM LOSS FACTORS FOR VARIOUS
C  TEMPERATURES AND MODES OF A CONSTRAINED LAYER VISCOELASTIC
C  DAMPING SYSTEM USING THE ROSS KERWIN UNGAR EQUATIONS.  SYSTEM LOSS
C  FACTORS ARE COMPUTED FOR A TEMPERATURE RANGE OF 30 100 DEGREES
C  FAHRENHEIT.  BASE PLATE THICKNESSES VARY FROM 0.375 TO 0.75 INCHES
C  IN 0.125 INCREMENTS.  FOR EACH BASE PLATE THICKNESS, THE VISCOELASTIC
C  THICKNESS IS VARIED FROM 0.015 TO 0.060 INCHES IN 0.015 INCH
C  INCREMENTS.  FOR EACH VISCOELASTIC THICKNESS THE CONSTRAINING
C  LAYER THICKNESS IS VARIED FROM 0.0625 TO 0.25 INCHES IN
C  0 0625 INCH INCREMENTS.
C  THIS PROGRAM APLIES TO A FREE-FREE-FREE-FREE PLATE.
C
C  THE VISCOELASTIC MATERIAL IS 3M ISD-112.
C
C  THE FOLLOWING COEFFICIENTS ARE DEFINED:
C       E1 = YOUNG'S MODULUS OF BASE PLATE (PSI)
C       E2 = YOUNG'S MODULUS OF VISCOELASTIC LAYER (PSI)
C       E3 = YOUNG'S MODULUS OF CONSTRAINING LAYER (PSI)
C       G2 = SHEAR MODULUS OF VISCOELASTIC MATERIAL (PSI)
C       NU1 = POISSON'S RATIO OF BASE PLATE
C       NU2 = POISSON'S RATIO OF VISCOELASTIC MATERIAL
C       H1 = THICKNESS OF BASE PLATE (IN)
C       H2 = THICKNESS OF VISCOELASTIC LAYER (IN)
C       H3 = THICKNESS OF CONSTRAINING LAYER (IN)
C       HTOT = TOTAL PLATE THICKNESS (IN)
C       RHO1 = DENSITY OF BASE PLATE (LBF-SEC**2/IN**4)
C       RHO2 = DENSITY OF VISCOELASTIC MATERIAL
C       RHO3 = DENSITY OF CONSTRAINING LAYER
C       T0,FROM,NROM,N,ML,ETFROL,SL,SH,FROL, & C ARE COEFFICIENTS
C        FOR THE REDUCED FREQUENCY NOMOGRAM EQUATIONS
C       FP = MODAL FREQUENCY OF THE UNDAMPED BASE PLATE (HZ)
C       FCP = MODAL FREQUENCY OF THE COMPOSITE PLATE (HZ)
C       ETA2 = LOSS FACTOR OF VISCOELASTIC MATERIAL
C       ETAS = SYSTEM LOSS FACTOR
C       KQR = WAVE NUMBER OF PLATE
C       GC = GRAVITATIONAL CONSTANT (IN/SEC**2)
C       T = TEMPERATURE OF VISCOELASTIC MATERIAL (DEG F)
C       WP = MODAL FREQUENCY OF UNDAMPED PLATE (RAD/SEC)
C       FP = MODAL FREQUENCY OF UNDAMPED PLATE (HZ)
C       WCP = MODAL FREQUENCY OF DAMPED PLATE (RAD/SEC)
C       FCP = MODAL FREQUENCY OF DAMPED PLATE (HZ)
C
C  THE UNITS USED IN THIS PROGRAM ARE LB, INCH, SEC, DEGREES F
C
C  UNDAMPED MODAL FREQUENCIES ARE FROM A FINITE ELEMENT ANALYSIS
C  OF THE FREE-FREE-FREE-FREE PLATE.
C
C  RESULTS ARE OUTPUT TO DATA FILE "LOSFCTR DATA"
C  PRIOR TO RUNNING THE PROGRAM TYPE THE COMMAND
C        "FILEDEF LOSFCTR DISK LOSFCTR DATA"
C
C  FINITE ELEMENT MODAL FREQUENCIES ARE INPUT FROM FILE:
C        "PLTFRQ DATA"
C
C ***********************************************************************
C
      REAL E1,E2,E3,NU1,NU2,H1,H2,H3,RHO1,RHO2,RHO3,HTOT
      REAL T0,FROM,NROM,N,ML,ETFROL,SL,SH,FROL,C
      REAL FP,FCP,ETA2,ETAS,KQR,PI,GC,T
      REAL FR10,ETA210,SUB1,SUB2,SUB3,H10
      REAL H21,H31,G,C1,ALPHRE,ALPHIM,BRE,BIM,DELRE
      REAL DELIM,ENCUBE,SUB4,SUB5,WP,WCP,DEN3,SUB6,SUB7,SUB8
      INTEGER V
      DIMENSION WP(8)
      PI=4.*ATAN(1.)
C
      OPEN(UNIT=10,FILE='LOSFCTR',STATUS='OLD')
      OPEN(UNIT=11,FILE='PLTFRQ',STATUS='OLD')
C
C  ASSIGN MATERIAL CONSTANTS FOR BASE PLATE,CONSTRAINING LAYER
```

```
C  AND VISCOELASTIC
C
      E1=1.0E7
      MU1=0.750
      RHO1=.0968
      NU1=.33
      RHO2=.035
      E3=1.0E7
      RHO3=.0968
      GC=386.
      NU2=.5
C
C  DEFINE CONSTANTS FOR NOMOGRAM EQUATIONS
C
      T0=104.0
      FROM=2.0E4
      MROM=688.94
      M=.275
      ML=8.7
      ETAROL=1.08
      SL=0.45
      SH=-.55
      FROL=5000.0
      C=2.5
C
C  BASE PLATE THICKNESS LOOP
C
      H1=0.375
      DO 100 J=1,4
      WRITE(10,703) 'BASE PLATE THICKNESS, H1=',H1
703   FORMAT(A27,F4.3)
      WRITE(10,*)
C
C  VISCOELASTIC THICKNESS LOOP
C
      H2=0.015
      DO 150 V=1,4
C
C  CONSTRAINING LAYER THICKNESS LOOP
C
      H3=0.0625
      DO 200 L=1,4
      WRITE(10,702) 'VISCOELASTIC LAYER THICKNESS, H2=',H2
      WRITE(10,*)
      WRITE(10,702) 'CONSTRAINING LAYER THICKNESS, H3=',H3
702   FORMAT(A35,F6.4)
      WRITE(10,*)
      WRITE(10,700) 'TEMP','MODE','FCP','ETA2','ETAS','G2'
700   FORMAT(A8,3X,A5,4A15)
C
C  PLATE MODE LOOP, READ MODAL FREQUENCY AND COMPUTE WAVE NUMBER
C
      HTOT=H1+H2+H3
      DO 300 I=1,8
      READ(11,*) WP(I)
C
C  CALCULATE MODAL FREQUENCY AND WAVE NUMBER OF BASE PLATE
C
      SUB7 = SQRT((E1*(HTOT**3)*GC)/(12.*(1.-NU1**2)*RHO1*H1))
      KQR=WP(I)/SUB7
      FP=WP(I)/(2.*PI)
C
C  TEMPERATURE LOOP
C
      T=30.0
      DO 400 K=1,15
C
C  CALCULATE PROPERTIES OF VISCOELASTIC FOR GIVEN TEMPERATURE AND
C  MODE
C
501   FR10=LOG10(FP)-(12.*(T-T0))/(525.+T-T0)
      FR=10.**(FR10)
```

```
      A=(FR10-LOG10(FROL))/C
      SUB1=C*((SL+SH)*A+(SL-SH)*(1.-SQRT(1.+A**2.)))/2.
      ETA210=LOG10(ETAROL)+SUB1
C
C  VISCOELASTIC LOSS FACTOR
C
      ETA2=10.**(ETA210)
      SUB2=2.*LOG10(FROM/ML)
      SUB3=1.+(FROM/FR)**N
      M10=LOG10(ML)+SUB2/SUB3
C
C  VISCOELASTIC SHEAR MODULUS
C
      G2=10.**(M10)
C
C  VISCOELASTIC YOUNG'S MODULUS
C
      E2=G2*2.*(1.+NU2)
C
C  CALCULATIONS FOR DAMPED PLATE AT TEMPERATURE T USING ROSS-
C  KERWIN-UNGAR EQUATIONS
C
      G=G2/(E3*H3*H2*KQR)
      H21=(H1+H2)/2.
      H31=H2+(H1+H3)/2.
      C1=C1*H1*(1.+G)+G*E3*H3
      D=G*ETA2*(E1*H1+E3*H3)
      ALPHRE=G*E1*H1*E3*H3*(H31**2.)*(C1+D*ETA2)
      ALPHIM=G*E1*H1*E3*H3*(H31**2.)*C1*ETA2
      BRE=E1*H1*E2*H2*H31*(C1+D*ETA2)
      BIM=E1*H1*E2*H2*H31*(C1*ETA2-D)
      SUB8=2.*G*E2*H2*E3*H3*H21*H31*C
      DELRE=SUB8*((1.-(ETA2**2.))+(D*(2.*ETA2)))
      DELIM=SUB8*(C1*(2.*ETA2)-(D*(1.-(ETA2**2.))))
      SUB6=(12./(C1**2.+D**2.))*(ALPHRE-BRE-DELRE)
      EHCUBE=(E1*(H1**3.))+E3*(H3**3.)+SUB6
C
C  MODAL FREQUENCY OF DAMPED PLATE
C
      DENS=RHO1*H1+RHO2*H2+H3*RHO3
      SUB5=(EHCUBE*GC)/(12.*(1.-NU1**2.)*DENS)
      WCP=KQR*SQRT(SUB5)
      FCP=WCP/(2.*PI)
C
C  COMPARISON OF FP AND FCP
C
      IF (ABS(1.-FP/FCP).LE. 0.1) THEN
         GOTO 500
      ELSE
         FP=FCP
         GOTO 501
      ENDIF
C
C  COMPUTE SYSTEM LOSS FACTOR
C
500   SUB6=(12./(C1**2.+D**2.))*(ALPHIM-BIM-DELIM)
      ETAS=(1./EHCUBE)*SUB6
C
C  PRINT RESULTS
C
      WRITE(10,701) T,I,FCP,ETA2,ETAS,G2
701   FORMAT(5X,F7.3,2X,I2,3X,4E15.4)
C
C  NEXT TEMPERATURE
C
      T=T+5.0
400   CONTINUE
C
C  NEXT MODE
C
      WRITE(10,*)
300   CONTINUE
```

```
      REWIND(UNIT=11)
C
C  NEXT CONSTRAINING LAYER THICKNESS
C
      H3=H3+0.0625
200   CONTINUE
C
C  NEXT VISCOELASTIC LAYER THICKNESS
C
      H2=H2+0.015
150   CONTINUE
C
C  NEXT BASE PLATE THICKNESS
C
      H1=H1+0.125
100   CONTINUE
      CLOSE(UNIT=10)
      CLOSE(UNIT=11)
      END
```

APPENDIX B

FORTRAN PROGRAM USED TO COMPUTE MODAL LOSS FACTORS FOR THE DOUBLE DAMPING LAYER CONFIGURATION DESIGN

This program uses the Ross–Kerwin–Ungar equations of Chapter 3 to compute estimated modal frequencies and loss factors for the double layer configuration. Modal frequencies for an undamped plate are read from a data file and estimated modal frequencies and loss factors for various layer thickness combinations in the double layer configuration are output to another data file. Material properties of ISD–112 are computed using University of Dayton data and curve-fitting equations to the reduced frequency nomogram [Ref. 9,12]. The units used in this program are pounds, inches, and seconds.

```
      PROGRAM THOLYR
C
C ***********************************************************************
C
C   THIS PROGRAM COMPUTES THE SYSTEM LOSS FACTOR AND MODAL FREQUENCY OF
C   A DOUBLE CONSTRAINED LAYER VISCOELASTICALLY DAMPED PLATE.  THE LOSS
C   FACTORS ARE COMPUTED FOR A SPECIFIC PLATE/DAMPING LAYER
C   CONFIGURATION AND OVER A TEMPERATURE RANGE OF 30-100 DEGREES
C   FARENHEIT.
C
C   THIS PROGRAM APPLIES TO A FREE-FREE-FREE-FREE PLATE AND THE UNDAMPED
C   MODAL FREQUENCIES ARE DETERMINED FROM FINITE ELEMENT ANALYSIS AND
C   ARE READ INTO THIS PROGRAM FROM FILE 'PLTFRQ'.
C
C   THE VISCOELASTIC MATERIAL IS 3M ISD-112.  VISCOELASTIC MATERIAL
C   DATA IS FROM UNIVERSITY OF DAYTON RESEARCH INSTITUTE
C
C   THE UNITS USED IN THIS PROGRAM ARE LB, INCH, SEC, AND DEGREES F.
C
C   LOSS FACTORS, DAMPED PLATE MODAL FREQUENCIES, AND ISD-112 PROPERTIES
C   ARE COMPUTED IN SUBROUTINE 'RKU' FOR EACH N-TH CONSTRAINED LAYER
C   SYSTEM.  UPON COMPLETION OF EACH TEMPERATURE COMPUTATION THE SYSTEM
C   LOSS FACTOR AND CORRESPONDING DAMPED PLATE FREQUENCY ARE WRITTEN TO
C   FILE 'THOLYR DATA'.
C
C   THE FOLLOWING COEFFICIENTS ARE DEFINED:
C       E1 = YOUNG'S MODULUS OF BASE PLATE (PSI)
C       E3 = EQUIVALENT YOUNG'S MODULUS OF N-TH CONSTRAINED LAYER SYSTEM
C       E3PRM = YOUNG'S MODULUS OF THE CONSTRAINING LAYER IN N-TH LAYER
C       ENCUBE = EQUIVALENT STIFFNESS OF CONSTRAINED LAYER SYSTEM
C       ETAS = SYSTEM LOSS FACTOR
C       ETA3 = LOSS FACTOR OF N-TH CONSTRAINED LAYER SYSTEM
C       ETA3PM = LOSS FACTOR OF CONSTRAINING LAYER IN THE N-TH LAYER (=0
C       FCP = FREQUENCY OF THE DAMPED PLATE  (HZ)
C       FP = FREQUENCY OF UNDAMPED PLATE  (HZ)
C       GC = GRAVITATIONAL CONSTANT
C       H1 = THICKNESS OF BASE PLATE
C       H2 = THICKNESS OF 1ST VISCOELASTIC LAYER
C       H3 = THICKNESS OF N-TH CONSTRAINED LAYER SYSTEM
C       H4 = TOTAL DAMPED PLATE THICKNESS
C       H1PRM = THICKNESS OF BASE LAYER IN N-TH LAYER
C       H2PRM = THICKNESS OF VEM IN N-TH LAYER
C       H3PRM = THICKNESS OF CONSTRAINING LAYER IN N-TH LAYER
C       KQR = WAVE NUMBER OF UNDAMPED PLATE
C       NU1 = POISSON'S RATIO OF BASE PLATE AND CONSTRAINING LAYERS
C       NU2 = POISSON'S RATIO OF VISCOELASTIC MATERIAL
C       NU2PRM = POISSON'S RATIO OF VEM IN N-TH LAYER
C       RHO1 = DENSITY OF BASE PLATE AND CONSTRAINING LAYERS
C       RHO2 = DENSITY OF VISCOELASTIC MATERIAL
C       RHO2PM = DENSITY OF VEM IN N-TH LAYER
C       RHO3 = DENSITY OF N-TH LAYER (= RHO1)
C       RHO3PM = DENSITY OF N-TH LAYER CONSTRAINING LAYER
C       T = TEMPERATURE VARIABLE
C       WP = FREQUENCY OF UNDAMPED PLATE  (RAD/SEC)
C
C       C,ETFROL,FROL,FROM,ML,MROM,N,SH,SL,TO = COEFFICIENTS FOR THE
C           REDUCED FREQUENCY NOMOGRAM EQUATIONS
C
C ***********************************************************************
C
      REAL C,E1,E3,E3PRM,ENCUBE,ETAS,ETA3,ETA3PM,ETFROL,FCP,FP,FROL
      REAL FROM,GC,H1,H2,H3,H4,H1PRM,H2PRM,H3PRM,KQR,ML,MROM,N,NU1
      REAL NU2,NU2PM,PI,RHO1,RHO2,RHO2PM,SH,SL,SUB1,T,TO,WP
      REAL RHO3,RHO3PM
C
      DIMENSION WP(17)
      PI=4.0*ATAN(1.0)
C
      OPEN(UNIT=10,FILE='PLTFRQ',STATUS='OLD')
      OPEN(UNIT=11,FILE='THOLYR',STATUS='OLD')
C
C  ASSIGN LAYER THICKNESSES
```

```
C
      H1=0.5
      H2=0.045
      H1PRM=0.09375
      H2PRM=0.015
      H3PRM=0.09375
      H3=H1PRM+H2PRM+H3PRM
      H4=H1+H2+H3
C
C   ASSIGN MATERIAL CONSTANTS
C
      E1=1.0E7
      RHO1=0.0968
      NU1=0.33
      RHO2=0.035
      NU2=0.49
      RHO2PM=0.035
      NU2PM=0.5
      RHO3=0.0968
      E3PRM=1.0E7
      RHO3PM=0.0968
      ETA3PM=0.0
      ETA3 = 0.0
C
      GC=386.0
C
C   DEFINE VISCOELASTIC CONSTANTS FOR NOMOGRAM EQUATIONS
C
      T0= 104.0
      FROM=2.0E4
      GROM=688.94
      N=0.275
      ML=8.7
      ETFROL=1.08
      SL=0.45
      SH=-0.55
      FROL=5000.0
      C=2.5
C
C   WRITE PLATE CHARACTERISTICS
C
      WRITE(11,700) 'H1 =',H1
      WRITE(11,700) 'H2 =',H2
      WRITE(11,700) 'H1PRIME =',H1PRM
      WRITE(11,700) 'H2PRIME =',H2PRM
      WRITE(11,700) 'H3PRIME =',H3PRM
      WRITE(11,*)
      WRITE(11,*)
700   FORMAT(A12,F6.5)
      WRITE(11,701) 'TEMP','MODE','FCP','ETAS'
701   FORMAT(A8,3X,A5,2A15)
      WRITE(11,*)
C
C   PLATE MODE LOOP
C
      DO 100 I=1,17
      READ(10,*) WP(I)
C
C   CALCULATE MODAL FREQUENCY AND WAVE NUMBER OF UNDAMPED PLATE
C
      SUB1=SQRT((E1*(H4**3)*GC)/(12.*(1.-NU1**2)*RHO1*H4))
      KQR=WP(I)/SUB1
      FP=WP(I)/(2.*PI)
C
C   TEMPERATURE LOOP
C
      T=30.0
      DO 200 K=1,15
C
C   COMPUTE SYSTEM LOSS FACTOR AND STIFFNESS FOR N-TH LAYER
C
      CALL RKU(H1PRM,H2PRM,H3PRM,E1,RHO1,NU1,NU2PM,RHO2PM,E3PRM,RHO3PM,
```

```
     ETA3PH,T,FP,KQR,ETAS,EHCUBE,FCP,TO,FROM,NROM,N,ML,ETFROL,SL,SH,
     ETROL,C)
C
C  CONVERT RESULTS FROM N-TH LAYER CALCULATION TO TOTAL PLATE
C
      ETA3= 0.0
      FP = WP(I)/(2.*PI)
C     FP=FCP
      E3=EHCUBE/(H3**3)
C
C  COMPUTE SYSTEM LOSS FACTOR AND FREQUENCY FOR TOTAL PLATE
C
      CALL RKU(H1,H2,H3,E1,RHO1,NU1,NU2,RHO2,E3,RHO3,ETA3,T,FP,KQR,ETAS,
     EHCUBE,FCP,TO,FROM,NROM,N,ML,ETFROL,SL,SH,FROL,C)
C
C  PRINT RESULTS
C
      WRITE(11,702) T,I,FCP,ETAS
702   FORMAT(5X,F7.3,2X,I2,3X,2E15.4)
C
C  NEXT TEMPERATURE
C
      T=T+5.0
200   CONTINUE
C
C  NEXT MODE
C
      WRITE(11,*)
100   CONTINUE
C
      CLOSE(UNIT=11)
      CLOSE(UNIT=10)
      END
C
C ***********************************************************************
C ***********************************************************************
C
      SUBROUTINE RKU(H1,H2,H3,E1,RHO1,NU1,NU2,RHO2,E3,RHO3,ETA3,T,FP,
     CKQR,ETAS,EHCUBE,FCP,TO,FROM,NROM,N,ML,ETFROL,SL,SH,FROL,C)
C
C ***********************************************************************
C
C   THIS SUBROUTINE CALCULATES VISCOELASTIC PROPERTIES BASED ON THE
C   UNIVERSITY OF DAYTON REDUCED FREQUENCY NOMOGRAM EQUATIONS, AND THEN
C   CALCULATES PLATE STIFFNESSES AND LOSS FACTORS BASED ON THE ROSS-
C   KERWIN-UNGAR EQUATIONS.
C
C   THE FOLLOWING ADDITIONAL VARIABLES ARE DEFINED FOR USE IN THIS
C   SUBROUTINE:
C
C       A = COEFFICIENT FOR NOMOGRAM EQUATIONS
C       ALPHIM,ALPHRE = IMAGINARY AND REAL COMPONENTS OF COEFFICIENT
C           ALPHA IN THE RKU EQUATIONS
C       BIM,BRE = IMAGINARY AND REAL COMPONENTS OF COEFFICIENT 'B' IN
C           THE RKU EQUATIONS
C       C1,D = COEFFICIENTS FOR RKU EQUATIONS
C       DELIM,DELRE = IMAGINARY AND REAL COMPONENTS OF COEFFICIENT
C           DELTA IN THE RKU EQUATIONS
C       DENS = COMBINATION OF MATERIAL DENSITIES USED TO COMPUTE THE
C           FREQUENCY OF THE DAMPED PLATE AND DAMPING LAYERS
C       EHCUBE = EQUIVALENT STIFFNESS OF DAMPED PLATE AS COMPUTED
C           USING RKU EQUATIONS
C       ETA2 = LOSS FACTOR OF VEM COMPUTED IN NOMOGRAM EQUATIONS
C       ETA210 = LOG10(ETA2)
C       ETAS = SYSTEM LOSS FACTOR COMPUTED BY RKU EQUATIONS
C       FCP = MODAL FREQUENCY OF DAMPED PLATE (HZ)
C       FP = MODAL FREQUENCY OF UNDAMPED PLATE (HZ)
C       FR = REDUCED FREQUENCY OF VEM
C       FR10 = LOG10(FR)
C       G2 = SHEAR MODULUS OF VEM
C       H21,H31 = RKU EQUATION COEFFICIENTS
C       H10 = LOG10(G2) AS COMPUTED BY NOMOGRAM EQUATIONS
```

```
C       WCP = FREQUENCY OF DAMPED PLATE (RAD/SEC)
C
C ***********************************************************************
C
      REAL A,ALPHIM,ALPHRE,BIM,BRE,C,C1,D,DELIM,DELRE,DENS,E1,E2,E3
      REAL EHCUBE,ETA2,ETA3,ETA210,ETAS,ETAROL,FCP,FP,FR,FR10,FROL,FROM
      REAL G,G2,GC,H1,H2,H3,H21,H31,KQR,M10,ML,MROM,N,NU1,NU2,PI,RHO1
      REAL RHO2,RHO3,SH,SL,SUB1,SUB2,SUB3,SUB4,SUB5,SUB6,SUB7,SUB8
      REAL SUB9,SUB10,SUB11,T,T0,WCP
C
      PI=4.0*ATAN(1.0)
      GC=386.0
C
C  CALCULATE PROPERTIES OF VEM FOR GIVEN TEMPERATURE AND MODE
C
501   FR10=LOG10(FP)-(12.*(T-T0))/(525.+T-T0)
      FR=10.**(FR10)
      A=(FR10-LOG10(FROL))/C
      SUB1=C*((SL+SH)*A+(SL-SH)*(1.-SQRT(1.+A**2)))/2.
      ETA210=LOG10(ETAROL)+SUB1
C
C  VISCOELASTIC LOSS FACTOR
C
      ETA2=10.**(ETA210)
C
C  VISCOELASTIC SHEAR MODULUS
C
      SUB2=2.*LOG10(MROM/ML)
      SUB3=1.+(FROM/FR)**N
      M10=LOG10(ML)+SUB2/SUB3
      G2=10.**(M10)
C
C  VISCOELASTIC YOUNG'S MODULUS
C
      E2=G2*2.*(1.+NU2)
C
C  CALCULATIONS FOR DAMPED PLATE USING RKU EQUATIONS
C
      G=G2/(E3*H3*H2*KQR)
      H21=(H1+H2)/2.
      H31=H2+(H1+H3)/2.
      C1=E1*H1*(1.+G)+G*E3*H3*(1.-ETA2*ETA3)
      D=G*E1*H1*ETA2+G*E3*H3*(ETA2+ETA3)
      SUB4=G*E1*H1*E3*H3*(H31**2)
      ALPHRE=SUB4*(C1*(1.-ETA2*ETA3)+D*(ETA2+ETA3))
      ALPHIM=SUB4*(C1*(ETA2+ETA3))
      SUB5=E1*H1*E2*H2*H31
      BRE=SUB5*(C1+D*ETA2)
      BIM=SUB5*(C1*ETA2-D)
      SUB6=2.*G*E2*H2*E3*H3*H21*H31
      SUB7=1.-2.*ETA2*ETA3-(ETA2**2)
      SUB8=2.*ETA2+ETA3-(ETA2**2)*ETA3
      DELRE=SUB6*(C1*SUB7+D*SUB8)
      DELIM=SUB6*(C1*SUB8-D*SUB7)
C
      SUB9=(12./(C1**2+D**2))*(ALPHRE-BRE-DELRE)
      EHCUBE=E1*(H1**3)+E3*(H3**3)+SUB9
C
C  MODAL FREQUENCY OF DAMPED PLATE
C
      DENS=RHO1*H1+RHO2*H2+RHO3*H3
      SUB10=(EHCUBE*GC)/(12.*(NU1**2)*DENS)
      WCP=KQR*SQRT(SUB10)
      FCP=WCP/(2.*PI)
C
C  COMPARISON OF FP AND FCP
C
      IF(ABS(1.-FP/FCP) .LE. 0.10) THEN
          GOTO 500
      ELSE
          FP=FCP
          GOTO 501
```

```
      ENDIF
C
C  COMPUTE SYSTEM LOSS FACTOR
C
500   SUB11=(12./(C1**2*D**2))*(ALPHIM-DIM-DELIM)
      ETAS=(1./ENCUBE)*((E3*N3*ETA3)+SUB11)
C
      END
```

APPENDIX C

DESIGN DRAWINGS FOR THE MACHINING OF THE FLOATING ELEMENT AND POCKET PLATE CONFIGURATIONS

The drawings shown in Figures C.1 and C.2 were used to machine the pocket plate and floating element plate used in the experiments. These drawings are included to show the relation of the pocket for the ISD–112 to the cover plate and how the viscoelastic was protected from the heat of welding.

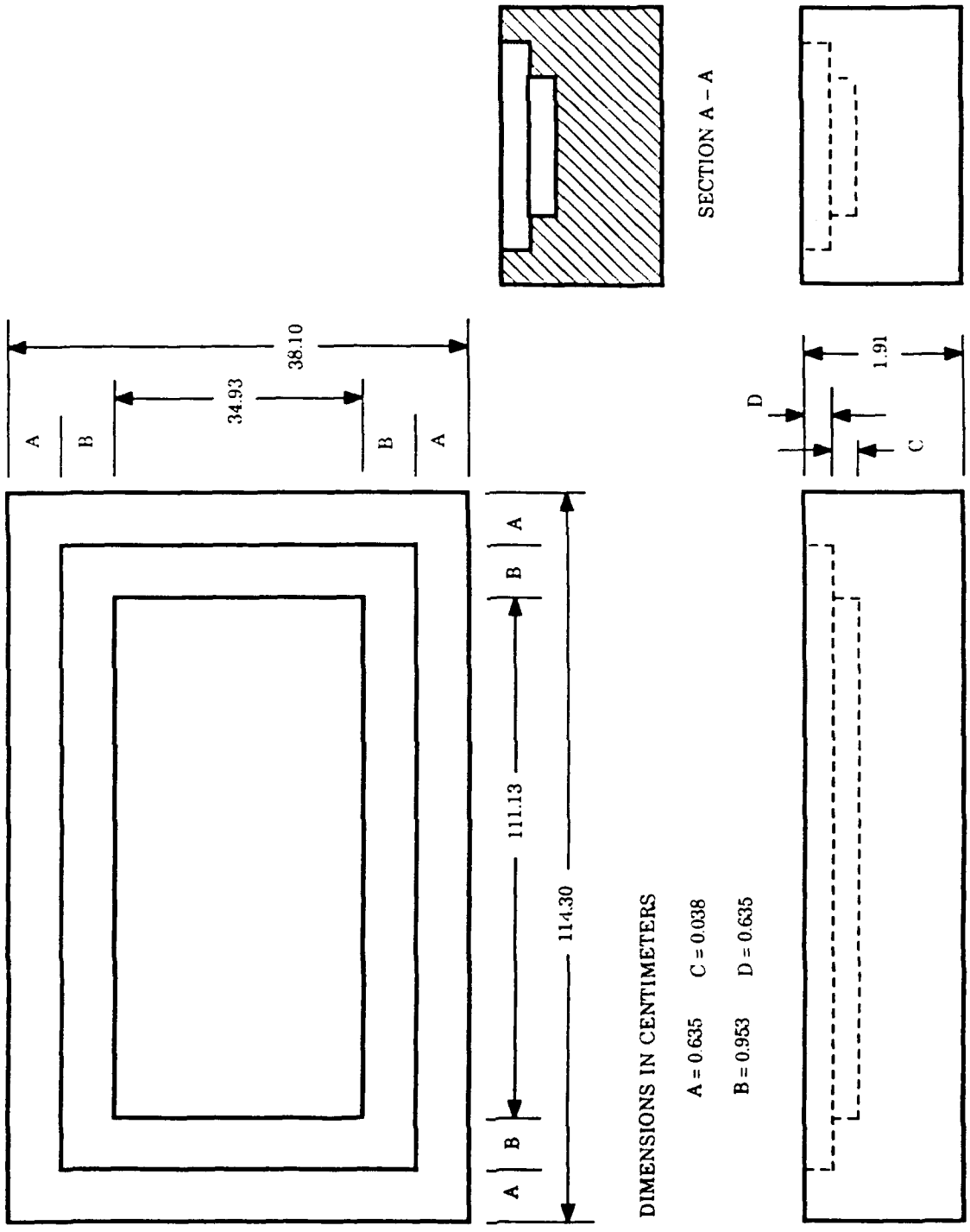

Figure C.1. Design Drawing of the Pocket Plate Configuration.

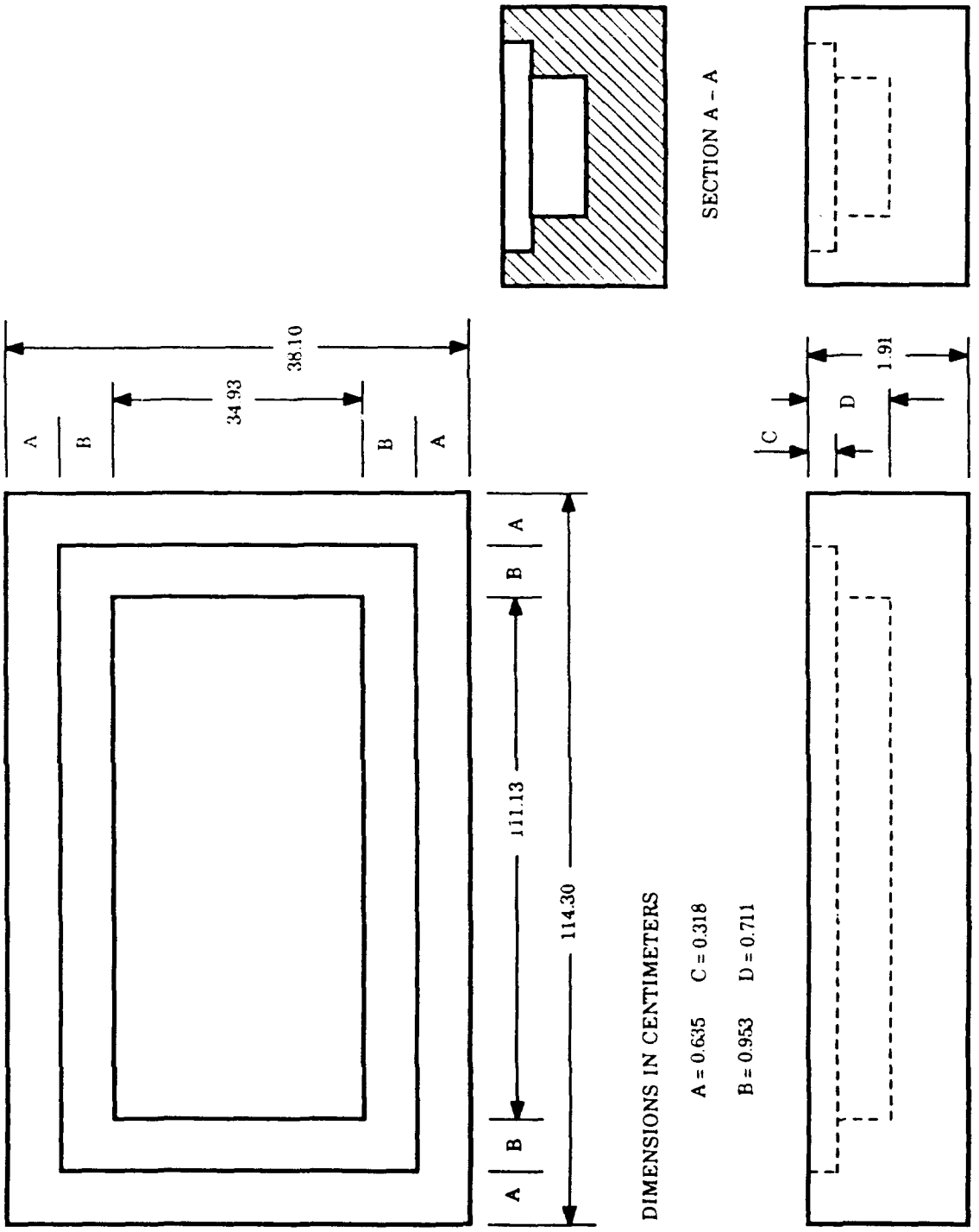

Figure C.2. Design Drawing of the Floating Element Configuration.

APPENDIX D

REPRESENTATIVE MSC/NASTRAN DATA DECK FOR THE DAMPING CONFIGURATIONS

This data deck was used to compute the modal frequency response of the single layer damping configuration and is a representative sample of the NASTRAN decks used for the other finite element models. The values in the damping table are from a curve fit to the modal loss factors estimated from the modal strain energy method. Since the data deck for the normal mode and modal strain energy extraction is virtually identical to this deck, the Case Control deck commands for the normal mode analysis are included, but are commented out.

The OUTPUT request provides data for an x–y plot of the modal frequency response.

The units used in this deck are pounds, inches, and seconds.

```
id single,mfr
sol 30
$
$ ************************************************************************
$       THIS DECK IS TO COMPUTE THE MODAL FREQUENCY RESPONSE OF A 15x45
$  INCH ALUMINUM PLATE WITH A CONSTRAINED VISCOELASTIC DAMPING LAYER.
$  THE MODEL HAS 252 ELEMENTS WITH 84 ELEMENTS IN EACH LAYER.  THE QUAD
$  ELEMENTS ARE OFFSET FROM THE HEX ELEMENTS AS SUGGESTED BY THE
$  LITERATURE.
$
$       THE MATERIAL PROPERTIES OF ISD-112 ARE FROM THE 3M CORPORATION.
$
$       THE MODAL LOSS FACTORS IN THE DAMPING TABLE ARE FROM A CURVE-FIT
$  TO THE SET OF MODAL LOSS FACTORS COMPUTED FROM THE MODAL STRAIN ENERGY
$  METHOD.
$
$       THE UNITS USED IN THIS DECK ARE POUNDS,INCHES, AND SECONDS
$ ************************************************************************
time 3000
cend
title = MODAL FREQUENCY RESPONSE / 200 HZ / 3M
method = 1
spc = 1
dload = 10
frequency = 10
sdamping = 101
set 111 = 95
svector = all
acceleration(plot,phase) = 111
output(xyplot)
xyprint acce / 95(t3)
$
$ ***************
$       THE FOLLOWING LINES ARE THE CASE CONTROL DECK CARDS FOR THE
$  NORMAL MODE EXTRACTION AND STRAIN ENERGY REQUEST
$ method = 1
$ spc = 1
$ set 10 = all
$ set 11 = 169,thru,252
$ ese = 11
$
$ ****************
BEGIN BULK
$ TITLE = SINGLE LAYER WITH QUAD OFFSET
$ DATA DECK PRODUCED BY PATRAS VERSION 2.0: 24-NOV-89 08:31:48
GRID            1       45.0000 15.0000 0.51500
GRID            2       45.0000 15.0000 0.50000
GRID            3       45.0000 12.5000 0.51500
GRID            4       45.0000 12.5000 0.50000
GRID            5       45.0000 10.0000 0.51500
GRID            6       45.0000 10.0000 0.50000
```

```
GRID            7       45.0000 7.50000 0.51500
GRID            8       45.0000 7.50000 0.50000
GRID            9       45.0000 5.00000 0.51500
GRID           10       45.0000 5.00000 0.50000
GRID           11       45.0000 2.50000 0.51500
GRID           12       45.0000 2.50000 0.50000
GRID           13       45.0000 0.      0.51500
GRID           14       45.0000 0.      0.50000
GRID           15       41.7857 15.0000 0.51500
GRID           16       41.7857 15.0000 0.50000
GRID           17       41.7857 12.5000 0.51500
GRID           18       41.7857 12.5000 0.50000
GRID           19       41.7857 10.0000 0.51500
GRID           20       41.7857 10.0000 0.50000
GRID           21       41.7857 7.50000 0.51500
GRID           22       41.7857 7.50000 0.50000
GRID           23       41.7857 5.00000 0.51500
GRID           24       41.7857 5.00000 0.50000
GRID           25       41.7857 2.50000 0.51500
GRID           26       41.7857 2.50000 0.50000
GRID           27       41.7857 0.      0.51500
GRID           28       41.7857 0.      0.50000
GRID           29       38.5714 15.0000 0.51500
GRID           30       38.5714 15.0000 0.50000
GRID           31       38.5714 12.5000 0.51500
GRID           32       38.5714 12.5000 0.50000
GRID           33       38.5714 10.0000 0.51500
GRID           34       38.5714 10.0000 0.50000
GRID           35       38.5714 7.50000 0.51500
GRID           36       38.5714 7.50000 0.50000
GRID           37       38.5714 5.00000 0.51500
GRID           38       38.5714 5.00000 0.50000
GRID           39       38.5714 2.50000 0.51500
GRID           40       38.5714 2.50000 0.50000
GRID           41       38.5714 0.      0.51500
GRID           42       38.5714 0.      0.50000
GRID           43       35.3571 15.0000 0.51500
GRID           44       35.3571 15.0000 0.50000
GRID           45       35.3571 12.5000 0.51500
GRID           46       35.3571 12.5000 0.50000
GRID           47       35.3571 10.0000 0.51500
GRID           48       35.3571 10.0000 0.50000
GRID           49       35.3571 7.50000 0.51500
GRID           50       35.3571 7.50000 0.50000
GRID           51       35.3571 5.00000 0.51500
GRID           52       35.3571 5.00000 0.50000
GRID           53       35.3571 2.50000 0.51500
GRID           54       35.3571 2.50000 0.50000
GRID           55       35.3571 0.      0.51500
GRID           56       35.3571 0.      0.50000
GRID           57       32.1429 15.0000 0.51500
```

```
GRID       58      32.1429 15.0000 0.50000
GRID       59      32.1429 12.5000 0.51500
GRID       60      32.1429 12.5000 0.50000
GRID       61      32.1429 10.0000 0.51500
GRID       62      32.1429 10.0000 0.50000
GRID       63      32.1429 7.50000 0.51500
GRID       64      32.1429 7.50000 0.50000
GRID       65      32.1429 5.00000 0.51500
GRID       66      32.1429 5.00000 0.50000
GRID       67      32.1429 2.50000 0.51500
GRID       68      32.1429 2.50000 0.50000
GRID       69      32.1429 0.      0.51500
GRID       70      32.1429 0.      0.50000
GRID       71      28.9286 15.0000 0.51500
GRID       72      28.9286 15.0000 0.50000
GRID       73      28.9286 12.5000 0.51500
GRID       74      28.9286 12.5000 0.50000
GRID       75      28.9286 10.0000 0.51500
GRID       76      28.9286 10.0000 0.50000
GRID       77      28.9286 7.50000 0.51500
GRID       78      28.9286 7.50000 0.50000
GRID       79      28.9286 5.00000 0.51500
GRID       80      28.9286 5.00000 0.50000
GRID       81      28.9286 2.50000 0.51500
GRID       82      28.9286 2.50000 0.50000
GRID       83      28.9286 0.      0.51500
GRID       84      28.9286 0.      0.50000
GRID       85      25.7143 15.0000 0.51500
GRID       86      25.7143 15.0000 0.50000
GRID       87      25.7143 12.5000 0.51500
GRID       88      25.7143 12.5000 0.50000
GRID       89      25.7143 10.0000 0.51500
GRID       90      25.7143 10.0000 0.50000
GRID       91      25.7143 7.50000 0.51500
GRID       92      25.7143 7.50000 0.50000
GRID       93      25.7143 5.00000 0.51500
GRID       94      25.7143 5.00000 0.50000
GRID       95      25.7143 2.50000 0.51500
GRID       96      25.7143 2.50000 0.50000
GRID       97      25.7143 0.      0.51500
GRID       98      25.7143 0.      0.50000
GRID       99      22.5000 15.0000 0.51500
GRID       100     22.5000 15.0000 0.50000
GRID       101     22.5000 12.5000 0.51500
GRID       102     22.5000 12.5000 0.50000
GRID       103     22.5000 10.0000 0.51500
GRID       104     22.5000 10.0000 0.50000
GRID       105     22.5000 7.50000 0.51500
GRID       106     22.5000 7.50000 0.50000
GRID       107     22.5000 5.00000 0.51500
GRID       108     22.5000 5.00000 0.50000
```

```
GRID        109         22.5000 2.50000 0.51500
GRID        110         22.5000 2.50000 0.50000
GRID        111         22.5000 0.      0.51500
GRID        112         22.5000 0.      0.50000
GRID        113         19.2857 15.0000 0.51500
GRID        114         19.2857 15.0000 0.50000
GRID        115         19.2857 12.5000 0.51500
GRID        116         19.2857 12.5000 0.50000
GRID        117         19.2857 10.0000 0.51500
GRID        118         19.2857 10.0000 0.50000
GRID        119         19.2857 7.50000 0.51500
GRID        120         19.2857 7.50000 0.50000
GRID        121         19.2857 5.00000 0.51500
GRID        122         19.2857 5.00000 0.50000
GRID        123         19.2857 2.50000 0.51500
GRID        124         19.2857 2.50000 0.50000
GRID        125         19.2857 0.      0.51500
GRID        126         19.2857 0.      0.50000
GRID        127         16.0714 15.0000 0.51500
GRID        128         16.0714 15.0000 0.50000
GRID        129         16.0714 12.5000 0.51500
GRID        130         16.0714 12.5000 0.50000
GRID        131         16.0714 10.0000 0.51500
GRID        132         16.0714 10.0000 0.50000
GRID        133         16.0714 7.50000 0.51500
GRID        134         16.0714 7.50000 0.50000
GRID        135         16.0714 5.00000 0.51500
GRID        136         16.0714 5.00000 0.50000
GRID        137         16.0714 2.50000 0.51500
GRID        138         16.0714 2.50000 0.50000
GRID        139         16.0714 0.      0.51500
GRID        140         16.0714 0.      0.50000
GRID        141         12.8571 15.0000 0.51500
GRID        142         12.8571 15.0000 0.50000
GRID        143         12.8571 12.5000 0.51500
GRID        144         12.8571 12.5000 0.50000
GRID        145         12.8571 10.0000 0.51500
GRID        146         12.8571 10.0000 0.50000
GRID        147         12.8571 7.50000 0.51500
GRID        148         12.8571 7.50000 0.50000
GRID        149         12.8571 5.00000 0.51500
GRID        150         12.8571 5.00000 0.50000
GRID        151         12.8571 2.50000 0.51500
GRID        152         12.8571 2.50000 0.50000
GRID        153         12.8571 0.      0.51500
GRID        154         12.8571 0.      0.50000
GRID        155         9.64286 15.0000 0.51500
GRID        156         9.64286 15.0000 0.50000
GRID        157         6.42857 15.0000 0.51500
GRID        158         6.42857 15.0000 0.50000
GRID        159         3.21429 15.0000 0.51500
```

```
GRID    160     3.21429 15.0000 0.50000
GRID    161     0.      15.0000 0.51500
GRID    162     0.      15.0000 0.50000
GRID    163     9.64286 12.5000 0.51500
GRID    164     9.64286 12.5000 0.50000
GRID    165     9.64286 10.0000 0.51500
GRID    166     9.64286 10.0000 0.50000
GRID    167     9.64286 7.50000 0.51500
GRID    168     9.64286 7.50000 0.50000
GRID    169     9.64286 5.00000 0.51500
GRID    170     9.64286 5.00000 0.50000
GRID    171     9.64286 2.50000 0.51500
GRID    172     9.64286 2.50000 0.50000
GRID    173     9.64286 0.      0.51500
GRID    174     9.64286 0.      0.50000
GRID    175     6.42857 12.5000 0.51500
GRID    176     6.42857 12.5000 0.50000
GRID    177     3.21429 12.5000 0.51500
GRID    178     3.21429 12.5000 0.50000
GRID    179     0.      12.5000 0.51500
GRID    180     0.      12.5000 0.50000
GRID    181     6.42857 10.0000 0.51500
GRID    182     6.42857 10.0000 0.50000
GRID    183     6.42857 7.50000 0.51500
GRID    184     6.42857 7.50000 0.50000
GRID    185     6.42857 5.00000 0.51500
GRID    186     6.42857 2.50000 0.51500
GRID    187     6.42857 5.00000 0.50000
GRID    188     6.42857 2.50000 0.50000
GRID    189     6.42857 0.      0.51500
GRID    190     6.42857 0.      0.50000
GRID    191     3.21429 10.0000 0.51500
GRID    192     3.21429 10.0000 0.50000
GRID    193     0.      10.0000 0.51500
GRID    194     0.      10.0000 0.50000
GRID    195     3.21429 0.      0.51500
GRID    196     3.21429 0.      0.50000
GRID    197     0.      0.      0.51500
GRID    198     0.      0.      0.50000
GRID    199     3.21429 7.50000 0.51500
GRID    200     3.21429 5.00000 0.51500
GRID    201     3.21429 2.50000 0.51500
GRID    202     3.21429 7.50000 0.50000
GRID    203     3.21429 5.00000 0.50000
GRID    204     3.21429 2.50000 0.50000
GRID    205     0.      7.50000 0.51500
GRID    206     0.      5.00000 0.51500
GRID    207     0.      2.50000 0.51500
GRID    208     0.      7.50000 0.50000
GRID    209     0.      2.50000 0.50000
GRID    210     0.      5.00000 0.50000
```

CQUAD4	1	1	198	196	204	209	-.25
CQUAD4	2	1	196	190	188	204	-.25
CQUAD4	3	1	190	174	172	188	-.25
CQUAD4	4	1	174	154	152	172	-.25
CQUAD4	5	1	154	140	138	152	-.25
CQUAD4	6	1	140	126	124	138	-.25
CQUAD4	7	1	126	112	110	124	-.25
CQUAD4	8	1	112	98	96	110	-.25
CQUAD4	9	1	98	84	82	96	-.25
CQUAD4	10	1	84	70	68	82	-.25
CQUAD4	11	1	70	56	54	68	-.25
CQUAD4	12	1	56	42	40	54	-.25
CQUAD4	13	1	42	28	26	40	-.25
CQUAD4	14	1	28	14	12	26	-.25
CQUAD4	15	1	209	204	203	210	-.25
CQUAD4	16	1	204	188	187	203	-.25
CQUAD4	17	1	188	172	170	187	-.25
CQUAD4	18	1	172	152	150	170	-.25
CQUAD4	19	1	152	138	136	150	-.25
CQUAD4	20	1	138	124	122	136	-.25
CQUAD4	21	1	124	110	108	122	-.25
CQUAD4	22	1	110	96	94	108	-.25
CQUAD4	23	1	96	82	80	94	-.25
CQUAD4	24	1	82	68	66	80	-.25
CQUAD4	25	1	68	54	52	66	-.25
CQUAD4	26	1	54	40	38	52	-.25
CQUAD4	27	1	40	26	24	38	-.25
CQUAD4	28	1	26	12	10	24	-.25
CQUAD4	29	1	210	203	202	208	-.25
CQUAD4	30	1	203	187	184	202	-.25
CQUAD4	31	1	187	170	168	184	-.25
CQUAD4	32	1	170	150	148	168	-.25
CQUAD4	33	1	150	136	134	148	-.25
CQUAD4	34	1	136	122	120	134	-.25
CQUAD4	35	1	122	108	106	120	-.25
CQUAD4	36	1	108	94	92	106	-.25
CQUAD4	37	1	94	80	78	92	-.25
CQUAD4	38	1	80	66	64	78	-.25
CQUAD4	39	1	66	52	50	64	-.25
CQUAD4	40	1	52	38	36	50	-.25
CQUAD4	41	1	38	24	22	36	-.25
CQUAD4	42	1	24	10	8	22	-.25
CQUAD4	43	1	208	202	192	194	-.25
CQUAD4	44	1	202	184	182	192	-.25
CQUAD4	45	1	184	168	166	182	-.25
CQUAD4	46	1	168	148	146	166	-.25
CQUAD4	47	1	148	134	132	146	-.25
CQUAD4	48	1	134	120	118	132	-.25
CQUAD4	49	1	120	106	104	118	-.25
CQUAD4	50	1	106	92	90	104	-.25
CQUAD4	51	1	92	78	76	90	-.25

CQUAD4	52	1	78	64	62	76	-.25
CQUAD4	53	1	64	50	48	62	-.25
CQUAD4	54	1	50	36	34	48	-.25
CQUAD4	55	1	36	22	20	34	-.25
CQUAD4	56	1	22	8	6	20	-.25
CQUAD4	57	1	194	192	178	180	-.25
CQUAD4	58	1	192	182	176	178	-.25
CQUAD4	59	1	182	166	164	176	-.25
CQUAD4	60	1	166	146	144	164	-.25
CQUAD4	61	1	146	132	130	144	-.25
CQUAD4	62	1	132	118	116	130	-.25
CQUAD4	63	1	118	104	102	116	-.25
CQUAD4	64	1	104	90	88	102	-.25
CQUAD4	65	1	90	76	74	88	-.25
CQUAD4	66	1	76	62	60	74	-.25
CQUAD4	67	1	62	48	46	60	-.25
CQUAD4	68	1	48	34	32	46	-.25
CQUAD4	69	1	34	20	18	32	-.25
CQUAD4	70	1	20	6	4	18	-.25
CQUAD4	71	1	180	178	160	162	-.25
CQUAD4	72	1	178	176	158	160	-.25
CQUAD4	73	1	176	164	156	158	-.25
CQUAD4	74	1	164	144	142	156	-.25
CQUAD4	75	1	144	130	128	142	-.25
CQUAD4	76	1	130	116	114	128	-.25
CQUAD4	77	1	116	102	100	114	-.25
CQUAD4	78	1	102	88	86	100	-.25
CQUAD4	79	1	88	74	72	86	-.25
CQUAD4	80	1	74	60	58	72	-.25
CQUAD4	81	1	60	46	44	58	-.25
CQUAD4	82	1	46	32	30	44	-.25
CQUAD4	83	1	32	18	16	30	-.25
CQUAD4	84	1	18	4	2	16	-.25
CQUAD4	85	85	197	195	201	207	.125
CQUAD4	86	85	195	189	186	201	.125
CQUAD4	87	85	189	173	171	186	.125
CQUAD4	88	85	173	153	151	171	.125
CQUAD4	89	85	153	139	137	151	.125
CQUAD4	90	85	139	125	123	137	.125
CQUAD4	91	85	125	111	109	123	.125
CQUAD4	92	85	111	97	95	109	.125
CQUAD4	93	85	97	83	81	95	.125
CQUAD4	94	85	83	69	67	81	.125
CQUAD4	95	85	69	55	53	67	.125
CQUAD4	96	85	55	41	39	53	.125
CQUAD4	97	85	41	27	25	39	.125
CQUAD4	98	85	27	13	11	25	.125
CQUAD4	99	85	207	201	200	206	.125
CQUAD4	100	85	201	186	185	200	.125
CQUAD4	101	85	186	171	169	185	.125
CQUAD4	102	85	171	151	149	169	.125

CQUAD4	103	85	151	137	135	149	.125
CQUAD4	104	85	137	123	121	135	.125
CQUAD4	105	85	123	109	107	121	.125
CQUAD4	106	85	109	95	93	107	.125
CQUAD4	107	85	95	81	79	93	.125
CQUAD4	108	85	81	67	65	79	.125
CQUAD4	109	85	67	53	51	65	.125
CQUAD4	110	85	53	39	37	51	.125
CQUAD4	111	85	39	25	23	37	.125
CQUAD4	112	85	25	11	9	23	.125
CQUAD4	113	85	206	200	199	205	.125
CQUAD4	114	85	200	185	183	199	.125
CQUAD4	115	85	185	169	167	183	.125
CQUAD4	116	85	169	149	147	167	.125
CQUAD4	117	85	149	135	133	147	.125
CQUAD4	118	85	135	121	119	133	.125
CQUAD4	119	85	121	107	105	119	.125
CQUAD4	120	85	107	93	91	105	.125
CQUAD4	121	85	93	79	77	91	.125
CQUAD4	122	85	79	65	63	77	.125
CQUAD4	123	85	65	51	49	63	.125
CQUAD4	124	85	51	37	35	49	.125
CQUAD4	125	85	37	23	21	35	.125
CQUAD4	126	85	23	9	7	21	.125
CQUAD4	127	85	205	199	191	193	.125
CQUAD4	128	85	199	183	181	191	.125
CQUAD4	129	85	183	167	165	181	.125
CQUAD4	130	85	167	147	145	165	.125
CQUAD4	131	85	147	133	131	145	.125
CQUAD4	132	85	133	119	117	131	.125
CQUAD4	133	85	119	105	103	117	.125
CQUAD4	134	85	105	91	89	103	.125
CQUAD4	135	85	91	77	75	89	.125
CQUAD4	136	85	77	63	61	75	.125
CQUAD4	137	85	63	49	47	61	.125
CQUAD4	138	85	49	35	33	47	.125
CQUAD4	139	85	35	21	19	33	.125
CQUAD4	140	85	21	7	5	19	.125
CQUAD4	141	85	193	191	177	179	.125
CQUAD4	142	85	191	181	175	177	.125
CQUAD4	143	85	181	165	163	175	.125
CQUAD4	144	85	165	145	143	163	.125
CQUAD4	145	85	145	131	129	143	.125
CQUAD4	146	85	131	117	115	129	.125
CQUAD4	147	85	117	103	101	115	.125
CQUAD4	148	85	103	89	87	101	.125
CQUAD4	149	85	89	75	73	87	.125
CQUAD4	150	85	75	61	59	73	.125
CQUAD4	151	85	61	47	45	59	.125
CQUAD4	152	85	47	33	31	45	.125
CQUAD4	153	85	33	19	17	31	.125

```
CQUAD4    154     85     19      5      3     17          .125
CQUAD4    155     85    179    177    159    161          .125
CQUAD4    156     85    177    175    157    159          .125
CQUAD4    157     85    175    163    155    157          .125
CQUAD4    158     85    163    143    141    155          .125
CQUAD4    159     85    143    129    127    141          .125
CQUAD4    160     85    129    115    113    127          .125
CQUAD4    161     85    115    101     99    113          .125
CQUAD4    162     85    101     87     85     99          .125
CQUAD4    163     85     87     73     71     85          .125
CQUAD4    164     85     73     59     57     71          .125
CQUAD4    165     85     59     45     43     57          .125
CQUAD4    166     85     45     31     29     43          .125
CQUAD4    167     85     31     17     15     29          .125
CQUAD4    168     85     17      3      1     15          .125
CHEXA     169      2    198    196    204    209    197    195 E  169
+E    169 201  207
CHEXA     170      2    196    190    188    204    195    189 E  170
+E    170 186  201
CHEXA     171      2    190    174    172    188    189    173 E  171
+E    171 171  186
CHEXA     172      2    174    154    152    172    173    153 E  172
+E    172 151  171
CHEXA     173      2    154    140    138    152    153    139 E  173
+E    173 137  151
CHEXA     174      2    140    126    124    138    139    125 E  174
+E    174 123  137
CHEXA     175      2    126    112    110    124    125    111 E  175
+E    175 109  123
CHEXA     176      2    112     98     96    110    111     97 E  176
+E    176  95  109
CHEXA     177      2     98     84     82     96     97     83 E  177
+E    177  81   95
CHEXA     178      2     84     70     68     82     83     69 E  178
+E    178  67   81
CHEXA     179      2     70     56     54     68     69     55 E  179
+E    179  53   67
CHEXA     180      2     56     42     40     54     55     41 E  180
+E    180  39   53
CHEXA     181      2     42     28     26     40     41     27 E  181
+E    181  25   39
CHEXA     182      2     28     14     12     26     27     13 E  182
+E    182  11   25
CHEXA     183      2    209    204    203    210    207    201 E  183
+E    183 200  206
CHEXA     184      2    204    188    187    203    201    186 E  184
+E    184 185  200
CHEXA     185      2    188    172    170    187    186    171 E  185
+E    185 169  185
CHEXA     186      2    172    152    150    170    171    151 E  186
+E    186 149  169
```

```
CHEIA    187    2    152    138    136    150    151    137 E  187
+E  187  135  149
CHEIA    188    2    138    124    122    136    137    123 E  188
+E  188  121  135
CHEIA    189    2    124    110    108    122    123    109 E  189
+E  189  107  121
CHEIA    190    2    110     96     94    108    109     95 E  190
+E  190   93  107
CHEIA    191    2     96     82     80     94     95     81 E  191
+E  191   79   93
CHEIA    192    2     82     68     66     80     81     67 E  192
+E  192   65   79
CHEIA    193    2     68     54     52     66     67     53 E  193
+E  193   51   65
CHEIA    194    2     54     40     38     52     53     39 E  194
+E  194   37   51
CHEIA    195    2     40     26     24     38     39     25 E  195
+E  195   23   37
CHEIA    196    2     26     12     10     24     25     11 E  196
+E  196    9   23
CHEIA    197    2    210    203    202    208    206    200 E  197
+E  197  199  205
CHEIA    198    2    203    187    184    202    200    185 E  198
+E  198  183  199
CHEIA    199    2    187    170    168    184    185    169 E  199
+E  199  167  183
CHEIA    200    2    170    150    148    168    169    149 E  200
+E  200  147  167
CHEIA    201    2    150    136    134    148    149    135 E  201
+E  201  133  147
CHEIA    202    2    136    122    120    134    135    121 E  202
+E  202  119  133
CHEIA    203    2    122    108    106    120    121    107 E  203
+E  203  105  119
CHEIA    204    2    108     94     92    106    107     93 E  204
+E  204   91  105
CHEIA    205    2     94     80     78     92     93     79 E  205
+E  205   77   91
CHEIA    206    2     80     66     64     78     79     65 E  206
+E  206   63   77
CHEIA    207    2     66     52     50     64     65     51 E  207
+E  207   49   63
CHEIA    208    2     52     38     36     50     51     37 E  208
+E  208   35   49
CHEIA    209    2     38     24     22     36     37     23 E  209
+E  209   21   35
CHEIA    210    2     24     10      8     22     23      9 E  210
+E  210    7   21
CHEIA    211    2    208    202    192    194    205    199 E  211
+E  211  191  193
```

CHEIA	212	2	202	184	182	192	199	183 E	212
+E 212	181	191							
CHEIA	213	2	184	168	166	182	183	167 E	213
+E 213	165	181							
CHEIA	214	2	168	148	146	166	167	147 E	214
+E 214	145	165							
CHEIA	215	2	148	134	132	146	147	133 E	215
+E 215	131	145							
CHEIA	216	2	134	120	118	132	133	119 E	216
+E 216	117	131							
CHEIA	217	2	120	106	104	118	119	105 E	217
+E 217	103	117							
CHEIA	218	2	106	92	90	104	105	91 E	218
+E 218	89	103							
CHEIA	219	2	92	78	76	90	91	77 E	219
+E 219	75	89							
CHEIA	220	2	78	64	62	76	77	63 E	220
+E 220	61	75							
CHEIA	221	2	64	50	48	62	63	49 E	221
+E 221	47	61							
CHEIA	222	2	50	36	34	48	49	35 E	222
+E 222	33	47							
CHEIA	223	2	36	22	20	34	35	21 E	223
+E 223	19	33							
CHEIA	224	2	22	8	6	20	21	7 E	224
+E 224	5	19							
CHEIA	225	2	194	192	178	180	193	191 E	225
+E 225	177	179							
CHEIA	226	2	192	182	176	178	191	181 E	226
+E 226	175	177							
CHEIA	227	2	182	166	164	176	181	165 E	227
+E 227	163	175							
CHEIA	228	2	166	146	144	164	165	145 E	228
+E 228	143	163							
CHEIA	229	2	146	132	130	144	145	131 E	229
+E 229	129	143							
CHEIA	230	2	132	118	116	130	131	117 E	230
+E 230	115	129							
CHEIA	231	2	118	104	102	116	117	103 E	231
+E 231	101	115							
CHEIA	232	2	104	90	88	102	103	89 E	232
+E 232	87	101							
CHEIA	233	2	90	76	74	88	89	75 E	233
+E 233	73	87							
CHEIA	234	2	76	62	60	74	75	61 E	234
+E 234	59	73							
CHEIA	235	2	62	48	46	60	61	47 E	235
+E 235	45	59							
CHEIA	236	2	48	34	32	46	47	33 E	236
+E 236	31	45							
CHEIA	237	2	34	20	18	32	33	19 E	237
+E 237	17	31							

```
CHEXA          238       2      20       6       4      18      19       5 E   238
+E   238         3      17
CHEXA          239       2     180     178     160     162     179     177 E   239
+E   239       159     161
CHEXA          240       2     178     176     158     160     177     175 E   240
+E   240       157     159
CHEXA          241       2     176     164     156     158     175     163 E   241
+E   241       155     157
CHEXA          242       2     164     144     142     156     163     143 E   242
+E   242       141     155
CHEXA          243       2     144     130     128     142     143     129 E   243
+E   243       127     141
CHEXA          244       2     130     116     114     128     129     115 E   244
+E   244       113     127
CHEXA          245       2     116     102     100     114     115     101 E   245
+E   245        99     113
CHEXA          246       2     102      88      86     100     101      87 E   246
+E   246        85      99
CHEXA          247       2      88      74      72      86      87      73 E   247
+E   247        71      85
CHEXA          248       2      74      60      58      72      73      59 E   248
+E   248        57      71
CHEXA          249       2      60      46      44      58      59      45 E   249
+E   249        43      57
CHEXA          250       2      46      32      30      44      45      31 E   250
+E   250        29      43
CHEXA          251       2      32      18      16      30      31      17 E   251
+E   251        15      29
CHEXA          252       2      18       4       2      16      17       3 E   252
+E   252         1      15
PSHELL           1       1 0.50000       1 1.12200       1
PSHELL          85       1 0.25000       1 1.12200       1
psolid,2,2
matl,1,1.0e7,,0.33,2.58e-4
matl,2,,251.4,0.49,9.067e-5
eigr,1,mgiv,0.0,5000.0,,30,,,+eigr
+eigr,mass
suport,106,12345
spcl,1,6,1,thru,210
param,autospc,yes
param,asing,1
rloadl,10,2001,,,3001
darea,2001,79,3,1.0
tabledl,3001,,,,,,,,+tal
+tal,0.0,1.0,5000.0,1.0,endt
freql,10,5.0,1.0,1000
tabdmpl,101,,,,,,,,+dmp
+dmp,40.0,0.214,63.0,0.216,95.0,0.218,160.0,0.222,+dmp1
+dmp1,200.0,0.224,285.0,0.225,320.0,0.224,440.0,0.216,+dmp2
+dmp2,460.0,0.215,480.0,0.212,520.0,0.208,580.0,0.197,+dmp3
+dmp3,630.0,0.189,665.0,0.183,715.0,0.171,825.0,0.142,+dmp4
+dmp4,870.0,0.130,885.0,0.125,1000.0,0.085,endt
```

LIST OF REFERENCES

1. Johnson, C.D. and Kienholz, D.A., "Finite Element Prediction of Damping in Structures With Constrained Viscoelastic Layers," AIAA Journal, Vol. 20, No. 9, September 1982.

2. Maurer, G.J., Vibration Response of Constrained Viscoelastically Damped Plates: Analysis and Experiments, M.S. Thesis, U.S. Naval Postgraduate School, Monterey, California, December 1987.

3. Nashif, A.D., Jones, D.I.G., and Henderson, J.P., Vibration Damping, Wiley–Interscience Publications, John Wiley and Sons, 1985.

4. Jones, D.I.G., and Henderson, J.P., "Fundamentals of Damping Materials," Vibration Damping Short Course Notes, Section 2.3, University of Dayton, Dayton, Ohio, June 1987.

5. Rogers, L., "Single Constrained Layer Damping Treatment Analysis," Vibration Damping Short Course Notes, Section 6.3, University of Dayton, Dayton, Ohio, June 1987.

6. Henderson, J.P., and Jones, D.I.G., "Fundamentals of Layered Damping Treatments," Vibration Damping Short Course Notes, Section 6.1, University of Dayton, Dayton, Ohio, June 1987.

7. MacNeal–Schwendler Corporation, MSC/NASTRAN Users Manual, Vol. 1, MacNeal–Schwendler Corporation, November, 1985.

8. Johnson, C.D., and Kienholz, D.A., "Finite Element Design of Viscoelastically Damped Structures," CSA Engineering, Inc., Palo Alto, California, 1984.

9. Nashif, A.D., "Layered Damping Treatment Design, Multiple Layer," Vibration Damping Short Course Notes, Section 6.4, University of Dayton, Dayton, Ohio, June 1987.

10. Ross, D., Ungar, E.E., and Kerwin, E.M., "Damping of Plate Flexural Vibrations by Means of Viscoelastic Laminae," Structural Damping, ASME, 1959.

11. Drake, M.L., "Design Techniques – Fourth Order Beam Theory," Vibration Damping Short Course Notes, Section 7.1, University of Dayton, Dayton, Ohio, 1987.

12. University of Dayton Research Institute, "ISD–112 Material Data Sheet," Vibration Damping Short Course Notes, University of Dayton, Dayton, Ohio, June 1987.

13. Gere, J.M., and Timoshenko, S.P., Mechanics of Materials, 2nd Edition, PWS Publishers, Boston, Massachusetts, 1984.

14. Richardson, N., and Potter, R., "Identification of the Modal Properties of an Elastic Structure From Measured Transfer Function Data," presented at the 20th International Instrumentation Symposium, May 1984, Albuquerque, New Mexico, Instrument Society of America reprint, 1974.

15. PDA Engineering, PAT/MSC Interface Guide, Release 2.1, PDA Engineering, September 1988.

16. Johnson, C.D., and Kienholz, D.A., "Finite Element Prediction of Damping in Structures With Constrained Viscoelastic Layers," Report No. 82.053, Anamet Laboratories, May 1982.

17. MacNeal–Schwendler Corporation, MSC/NASTRAN Handbook for Dynamic Analysis, Section 3.2.3, MacNeal–Schwendler Corporation, 1983.

18. PDA Engineering, PATRAN PLUS Users Manual, Vol. 2, Ch. 21, PDA Engineering, 1987.

INITIAL DISTRIBUTION LIST

1.	Defense Technical Information Center Cameron Statior Alexandria, Virginia 22304–6145	2
2.	Library, Code 0142 Naval Postgraduate School Monterey, California 93943–5002	2
3.	Dean of Science and Engineering, Code 06 Naval Postgraduate School Monterey, California 93943–5004	2
4.	Research Administrations Office, Code 012 Naval Postgraduate School Monterey, California 93943–5004	1
5.	Department Chairman, Code 69 Department of Mechanical Engineering Naval Postgraduate School Monterey, California 93943–5004	1
6.	Curricular Officer, Code 34 Naval Engineering Curriculum Naval Postgraduate School Monterey, California 93943–4004	1
7.	Professor Y.S. Shin, Code 69Sg Department of Mechanical Engineering Naval Postgraduate School Monterey, California 93943–5004	3
8.	Dr. K.S. Kim, Code 69Ki Department of Mechanical Engineering Naval Postgraduate School Monterey, California 93943–5004	1
9.	Dr. Arthur Kilcullen, Code 1941 David Taylor Research Center Bethesda, Maryland 20084	1

10.	Dr. Lawrence Maga, Code 1944 David Taylor Research Center Bethesda, Maryland 20084	2
11.	Mr. Doug Noll, Code 1944 David Taylor Research Center Bethesda, Maryland 20084	1
12.	LT Michael J. Bateman, USN 5306 SE 64th Portland, Oregon 97206	1